

5-2018

## The Role of Merlin and Apicobasal Polarity in Endometrial Development and Homeostasis

Erin Lopez

Follow this and additional works at: [https://digitalcommons.library.tmc.edu/utgsbs\\_dissertations](https://digitalcommons.library.tmc.edu/utgsbs_dissertations)

 Part of the [Biology Commons](#), [Genetics Commons](#), and the [Medicine and Health Sciences Commons](#)

### Recommended Citation

Lopez, Erin, "The Role of Merlin and Apicobasal Polarity in Endometrial Development and Homeostasis" (2018). *The University of Texas MD Anderson Cancer Center UTHealth Graduate School of Biomedical Sciences Dissertations and Theses (Open Access)*. 831.

[https://digitalcommons.library.tmc.edu/utgsbs\\_dissertations/831](https://digitalcommons.library.tmc.edu/utgsbs_dissertations/831)

This Dissertation (PhD) is brought to you for free and open access by the The University of Texas MD Anderson Cancer Center UTHealth Graduate School of Biomedical Sciences at DigitalCommons@TMC. It has been accepted for inclusion in The University of Texas MD Anderson Cancer Center UTHealth Graduate School of Biomedical Sciences Dissertations and Theses (Open Access) by an authorized administrator of DigitalCommons@TMC. For more information, please contact [digitalcommons@library.tmc.edu](mailto:digitalcommons@library.tmc.edu).

**THE ROLE OF MERLIN AND APICOBASAL POLARITY IN ENDOMETRIAL  
DEVELOPMENT AND HOMEOSTASIS**

by

**Erin Williams Lopez, BA**

APPROVED:

---

Andrew B. Gladden, Ph.D.  
Advisory Professor

---

Richard Behringer, Ph.D.

---

Russell Broaddus, MD, Ph.D.

---

David Loose, Ph.D.

---

Rachel Miller, Ph.D.

---

APPROVED:

---

Dean, The University of Texas  
MD Anderson Cancer Center UTHealth Graduate School of Biomedical Sciences

**THE ROLE OF MERLIN AND APICOBASAL POLARITY IN ENDOMETRIAL  
DEVELOPMENT AND HOMEOSTASIS**

A

**DISSERTATION**

Presented to the Faculty of

The University of Texas

MD Anderson Cancer Center UTHealth

Graduate School of Biomedical Sciences

in Partial Fulfillment

of the Requirements

for the Degree of

**DOCTOR OF PHILOSOPHY**

by

Erin Williams Lopez, B.A.

Houston, Texas

May, 2018

## Acknowledgements

I would like to thank my advisor, Dr. Andrew B. Gladden, for mentoring and guiding me through my graduate career. You are an excellent scientist who has taught me how to think critically about scientific questions and determine methods to solve them; you also showed me how to evaluate a study and write scientific literature. I appreciate all the support you have given me over the years, you have gone above and beyond as a mentor and helped me even through the most challenging times. I would like to thank the past members of the Gladden lab who helped troubleshoot experiments and made my time as a graduate student more enjoyable. I especially want to thank Frank (Xuebo) Chen who assisted me with the majority of my mouse work over the course of my dissertation. I'd also like to thank Alejandro Villar-Prados who was not only a lab member that would work through experiments with me, but a friend who helped guide me through my graduate career.

I would like to thank both past and present members of the Broaddus and Behringer labs who allowed me to work with them as a lab member throughout my time at the graduate school. Dr. Jessica Bowser taught me about endometrial cancer and different techniques she utilized to study it. She has always been willing to help with my scholarship/fellowship applications and is always willing to provide career advice. Dr. Rachel Mullen frequently would troubleshoot issues with me related to mouse work and endometrial work. Her knowledge on Mullerian duct and endometrial development were invaluable, she also gave me advice and guidance on my scientific writing. Dr. Alejandra Elder has been wonderful to work with in the past year and was always willing to help. She frequently would allow me to bounce

ideas off of her, helped me with experiments, and gave me constructive feedback. I also would like to thank Zer Vue for frequently introducing me to new papers and assisting me with endometrial gland work.

A great amount of appreciation goes to my advisory and examination committee members. I especially want to thank, Dr. Richard Behringer, Dr. David Loose, and Dr. Rachel Miller who had countless ideas and mentored me through my dissertation project. A special thank you to Dr. Russell Broaddus who mentored me and frequently invited me to seminars he thought I would enjoy and learn from. I appreciate that Dr. Broaddus always treated me as if I was in his lab.

I am indebted to Dr.'s David Hong and Jordi Rodon Ahnert for allowing me to shadow them in the clinic. I appreciate Dr. Hong's willingness to teach me about clinical trials, discuss treatment plans, and adverse events related to different drugs.

I am so grateful for the time that many Genetics Department faculty members spent discussing my research and giving me suggestions, especially Dr. Swathi Arur who gave excellent research and career advice. I would like to thank the Genes and Development (now Genetics and Epigenetics) program for an excellent learning environment. I always was given helpful advice by students, post-doctoral fellows, and faculty who consulted me on my research. I would also like to thank the Genetics Microscopy Core, Adriana Paulucci, and Hank Adams, without whom I would not have all the beautiful images in my dissertation.

Thank you to all the staff and faculty that run the graduate school (GSBS). Brenda, Karen, Lily, Michael, and everyone at the GSBS office who has always made GSBS feel like a family. I will miss getting to talk to everyone throughout the

week. A special thank you to Elisabeth Lindheim who is the reason G&D had such a great and welcoming community. She was a great friend through my entire graduate career. Thank you Dr. Bill Mattox for always helping me with fellowships, scholarships, and graduation questions. I want to thank the deans for continuing to work to make our school better, and I'm excited to see where you take GSBS in the future. Thank you Dr. Shelley Barton for giving me the opportunity to learn about leadership within the MD Anderson community.

To my amazing husband, Dallas Lopez, thank you so much for supporting me through this entire process; for everything from moving to Houston, to writing this dissertation. You have kept me going through the rough times, accompanied me for late night time points, and you are the reason I was able to finish graduate school. I cannot imagine life without you and am excited for the next chapter of our lives with our beautiful boys, BoJangles and Bernie.

Thank you to my family, new and old. I appreciate all the support and help you gave me through this process. Thank you to my Mom and Dad, Matt and Patty Williams for supporting my dreams and always believing in me. Thank you to my mother-in-law, Deneen Lopez, who has been incredibly supportive and always willing to roll up her sleeves and help our household in any way that we needed. Finally, thank you to all my friends who have been supportive throughout this endeavor. Whether it was listening to me discuss my science and life, or understanding when I had to cancel plans to work on my dissertation. I am so grateful for each of you in Houston and on the West Coast. Thank you for all your support.

# THE ROLE OF MERLIN AND APICOBASAL POLARITY IN ENDOMETRIAL DEVELOPMENT AND HOMEOSTASIS

Erin Williams Lopez, B.A.

Advisory Professor: Andrew B. Gladden, Ph.D.

Apicobasal polarity and cell adhesion are necessary for the proper formation and organization of epithelial tissues. Merlin couples cell polarity and adhesion through correct localization of the polarity protein Par3 and maturation of apical junctions. Merlin and Par3 are necessary for the development and homeostasis of highly regenerative tissues like the epidermis. The continual repopulation of the endometrium after each menstrual cycle requires a constant reorganization of cell polarity and adhesion. The endometrium consists of a luminal epithelium that postnatally gives rise to the distinct glandular epithelium. Endometrial glands are necessary to secrete nutrients for the pre-implantation embryo. In addition, the endometrial gland is thought to be where endometrial cancer originates. While the endometrium is important for female fertility, relatively little is understood about how glands develop or how endometrial cancer forms. We examine the role of Merlin and apicobasal polarity in endometrial development and homeostasis. We determine that Merlin regulation of apicobasal polarity is necessary for proper endometrial gland formation. Apicobasal polarity is disrupted in low-grade endometrial cancer and mediates Notch regulated proliferation and migration in endometrial cancer cells. This dissertation reveals a critical role for Merlin and cell polarity in endometrial gland development, mammalian fertility, and endometrial cancer.

## Table of Contents

Signature Page.....	i
Title Page .....	ii
Acknowledgements .....	iii
Abstract.....	vi
Table of Contents.....	vii
List of Figures.....	x
List of Tables .....	xii
List of Abbreviations .....	xiii
<b>Chapter 1: Introduction .....</b>	<b>1</b>
1.1 Female Reproductive Tract Development.....	1
1.2 Endometrial Gland Development .....	7
1.3 Wnt signaling.....	8
1.4 Endometrial Cancer.....	16
1.5 Notch signaling .....	19
1.6 Apicobasal Polarity .....	21
1.7 Apicobasal Polarity in Cancer .....	30
1.8 Apicobasal Polarity in the Endometrium .....	36
1.9 Cell Adhesion .....	39
1.10 Merlin .....	43
1.11 Dissertation Summary .....	47
<b>Chapter 2: Materials &amp; Methods.....</b>	<b>49</b>
2.1 Mouse Strains.....	49
2.11 Fecundity Study .....	49
2.2 Immunohistochemistry .....	50
2.3 Cell culture and reagents .....	53
2.31 3D culture assay.....	54
2.33 Generation of primary knockout endometrial cell lines.....	55



2.34 Generation of overexpression endometrial cancer cell lines.....	55
2.4 Quantitative RT-PCR .....	55
2.5 Cell extract preparation and Western blotting .....	57
2.6 Image processing, analysis, and densitometry .....	61
2.7 Statistics.....	61
<b>Chapter 3: Merlin regulates endometrial gland development through polarized signals.....</b>	<b>62</b>
3.1 Introduction .....	62
3.2 Results.....	64
3.21 Merlin deletion causes loss of gland formation and female infertility.....	64
3.22 Apicobasal polarity and junction condensation is lost in Merlin-deficient tissue .....	71
3.23 Proliferation decreases and tension increases in Merlin-deficient tissue .....	75
3.24 Wnt signaling is downregulated in Merlin mutants.....	82
3.3 Summary .....	86
<b>Chapter 4: The Role of Merlin in Endometrial Homeostasis .....</b>	<b>89</b>
4.1 Introduction .....	89
4.2 Results.....	90
4.21 Endometrial epithelium becomes a squamous, stratified epithelium in Merlin mutant mice.....	90
4.22 Changes in endometrial epithelium coincide with changes in Wnt signaling .....	94
4.3 Summary .....	97
<b>Chapter 5: Loss of polarity alters proliferation and differentiation in low-grade endometrial cancers by disrupting Notch signaling .....</b>	<b>99</b>
5.1 Introduction .....	99
5.2 Results.....	102
5.21 Loss of polarity, but not E-cadherin localization, in low-grade endometrial cancer .....	102
5.22 Disruption of polarity in a 3D cell model phenocopies changes in cellular differentiation observed in low-grade endometrial tumors.....	108

5.23 Disruption of apicobasal polarity decreases Notch signaling in epithelial cells and in low-grade endometrial cancer.....	111
5.24 Expression of Par3 in endometrial cancer cells promotes differentiation and decreased proliferation.....	117
5.25 Decreases in proliferation and migration observed in Par3 overexpressing cells is due to Notch signaling.....	120
5.26 PTEN loss decreases the effectiveness of Par3 expression in endometrial cancer cells .....	123
5.3 Summary .....	129
<b>Chapter 6: Conclusions, Discussion, and Future Directions.....</b>	<b>131</b>
6.1 Conclusions and Discussion .....	131
6.11 Overall Conclusions.....	144
6.2 Future Directions .....	147
<b>Chapter 6: Appendix.....</b>	<b>151</b>
<b>Chapter 7: References.....</b>	<b>155</b>
<b>Vita .....</b>	<b>212</b>

## List of Figures

Figure 1 Development of the Uterus.....	3
Figure 2 Wnt, Notch, and Hippo signaling pathways.....	13
Figure 3 Apicobasal Polarity and Cell adhesion. ....	23
Figure 4 Merlin loss in the endometrium causes a loss of glands.....	66
Figure 5 Endometrial Gland Markers within the Nf2eeKO and Nf2seeKO mice at P21. ....	69
Figure 6 Merlin loss causes disruption of apicobasal polarity without altering apical junctions. ....	73
Figure 7 Proliferation and Apoptosis within the developing endometrium.....	78
Figure 8 Increases in tension at the basal membrane corresponds to an increase in F-actin at the apical membrane in Nf2eeKO mice. ....	81
Figure 9 Hippo and Wnt signaling in Nf2eeKO Mice.....	85
Figure 10 Nf2seeKO mice uteri change after puberty to resemble a decidualized uterus. ....	92
Figure 11 Expression of Hippo and Wnt signaling in Nf2eeKO, Nf2seeKO, and Merlin-deficient primary cells.....	96
Figure 12 Loss of apicobasal polarity occurs in low-grade endometrial cancer. ....	104
Figure 13 E-cadherin localization and cilia presence in endometrial cancer with disrupted polarity. ....	107

<b>Figure 14 Depletion of apical polarity proteins cause an increase in multiple lumen structures and a decrease in differentiation markers in epithelial 3D cell culture.....</b>	<b>110</b>
<b>Figure 15 Notch signaling decreases in Par3, Ezrin, and Merlin depleted epithelial cells.....</b>	<b>114</b>
<b>Figure 16 Notch downstream signaling and receptor localization is disrupted in low-grade endometrial cancer. ....</b>	<b>116</b>
<b>Figure 17 Expressing Par3 in endometrial cancer cell lines cause differentiation phenotypes. ....</b>	<b>119</b>
<b>Figure 18 Expressing Par3 in endometrial cancer cell lines blocks proliferation.....</b>	<b>122</b>
<b>Figure 19 Inhibiting Notch signaling rescues Par3 mediated changes in migration and proliferation.....</b>	<b>125</b>
<b>Figure 20 The role of tumor suppressor PTEN in Par3-depletion phenotypes. ....</b>	<b>128</b>
<b>Figure 21 Nf2eeKO mice has a double endometrium phenotype that Nf2seeKO mice do not. ....</b>	<b>138</b>
<b>Figure 22 Summary of Dissertation Findings.....</b>	<b>146</b>

## List of Tables

<b>Table 1 Genes involved with Uterus Development and Homeostasis .....</b>	<b>10</b>
<b>Table 2 Downstream Targets of Notch and Wnt Signaling .....</b>	<b>15</b>
<b>Table 3 Cell Polarity Proteins involvement in Cancer and the Uterus .....</b>	<b>34</b>
<b>Table 4 Functions of Merlin.....</b>	<b>45</b>
<b>Table 5 shRNA oligos for MDCK cells and endometrial cancer cell lines. ....</b>	<b>56</b>
<b>Table 6 qRT-PCR primers for MDCK cells, endometrial cancer cells, and isolated endometriums .....</b>	<b>60</b>
<b>Table 7 Mouse models discussed within the dissertation. ....</b>	<b>154</b>

## List of Abbreviations

ADAM	A desintegrin and metallopeptidase
AKT	Protein Kinase B
APC	Adenomatous polyposis coli
aPKC	atypical Protein Kinase C
BIRC3	Baculoviral IAP repeat containing 3
BMP2	Bone morphogenetic protein 2
Ccnd1	Cyclin D1
CD10	Membrane Metalloendopeptidase
Cdc42	Cell division control protein 42
CK1 $\alpha$	Casein kinase 1 $\alpha$
COUP-TFII	COUP transcription factor 2
CRB3	Crumbs3
CSL	CBF1, Suppressor of Hairless, Lag1
CTGF	Connective tissue growth factor
DLG/Dlgh	Disc Large
DPC	days post coitus
DVL	Disheveled
ECC/EC	Endometrial Cancer
ECM	Extracellular Matrix
EGFR	Epidermal Growth Factor Receptor
EMT	epithelial-mesenchymal transition
ERM	Ezrin-Radixin-Moesin
FAK	Focal Adhesion Kinase
FAs	Focal Adhesions
FOXM1	Forkhead box protein M1
FRT	Female Reproductive Tract
GSK-3 $\beta$	Glycogen synthase kinase 3 $\beta$
Hox	Homeodomain transcription factors
HPV	Human Papillomavirus
IBD	Inflammatory Bowel Disease
JAMs	Junctional adhesion molecules
JNK	Jun Kinase
K14	Keratin 14
Lats1/2	Large Tumor Suppressor 1/2
LEF/TCF	Lymphoid enhancer factor/T-cell factor
LGL	Lethal Giant Larvae
LPT	Looptail Mice ( <i>Vangl2</i> <sup>Lp/wt</sup> )

LRP5/6	Low density lipoprotein receptor related protein 5/6
MOBK1 A/B	Mps One Binder Kinase activator-like A/B
MST1/2	Mammalian Ste20 Kinase 1/2
myoIIB	Myosin IIB
Nf2	Neurofibromatosis Type 2
Nf2eeKO	<i>Nf2<sup>lox/lox</sup>; Wnt7a-Cre</i>
Nf2seeKO	<i>Nf2<sup>lox/lox</sup>; PR-Cre</i>
NHE-RF	Na <sup>+</sup> /H <sup>+</sup> Exchanger Regulatory Factor
NICD	Notch Intracellular Domain
NLK	Nemo Like Kinase
NSCLC	non-small-cell lung cancer
OCs	oval cells
P	Postnatal Day
PALS1	Protein associated with Lin-17
Par3	Partitioning defective 3 homolog
Par6	Partitioning defective 6 homolog
PATJ	PALS-1 associated tight junction protein
PCP	Planar Cell Polarity
PI3K	Phosphoinositide 3-Kinase
PIP <sub>2</sub>	Phosphatidylinositol (3,4,5)-diphosphate
PIP <sub>3</sub>	Phosphatidylinositol (3,4,5)-triphosphate
PKC	Protein Kinase C
PLC	Phospholipase C
pMLC	phospho-Myosin Light Chain
PR	Progesterone Receptor
PTEN	Phosphatase and tensin homolog
RAC	Ras-related C3 botulinum toxin substrate
RhoA	Ras homolog gene family member A
ROCK	Rho-associated kinase
ROR	Retinoid-related orphan receptors
Sav	Salvador
SMA	smooth muscle actin
STAT3	Signal Transducer and Activator of Transcription 3
TAK1	Transforming growth factor beta-activated kinase 1
TAZ	Transcriptional co-Activator with PDZ-binding motif
TCGA	The Cancer Genome Atlas
TEAD	TEA domain-containing transcription factor family
TGFβ	Transforming Growth factor beta
YAP	Yes-associated protein
ZO	Zonula Occludens

## Chapter 1: Introduction

### 1.1 Female Reproductive Tract Development

The Female Reproductive Tract (FRT) consists of the vagina, cervix, uterus, oviducts, and ovaries(1). The FRT originates from the intermediate mesoderm which differentiates into the urogenital system,(2) containing the kidneys, urinary system, and FRT in females. The embryonic mesoderm proliferates and goes through a cell fate change creating two epithelial tubes, the Wolffian duct and the Mullerian duct. The Wolffian duct initially forms transient segments that eventually create one continuous tube. The Mullerian duct is formed when mesonephric epithelial cells invaginate and lengthen adjacent to the Wolffian duct. FRT development requires Wnt-mediated signals stimulated by the Wnt4, Wnt5a, and Wnt9b ligands to regulate Mullerian duct formation and elongation(3–5).

The symmetric Mullerian ducts fuse after elongation, forming the complete FRT (Figure 1a). Mammalian species differ in the degree of fusion, generating different types of uteri with duplex, bipartite, or simplex forms (Figure 1b). A duplex uterus, observed in monotremes and marsupials, results when the uterine horns never fuse and each has an individual cervix. Duplex uteri are split into three sub-categories: without a vagina, with two lateral vaginae and central birth canal, or with a single vagina. Mice have a bipartite uterus (sometimes described as a bicornuate uterus) that has two separate



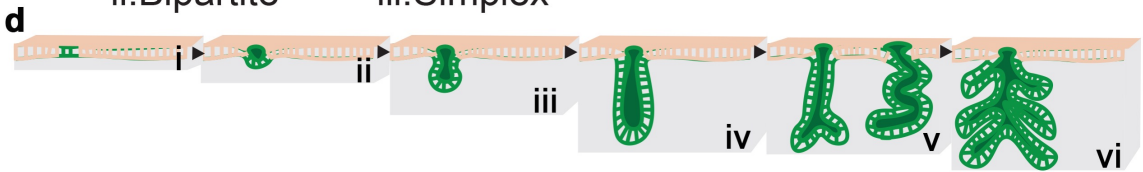
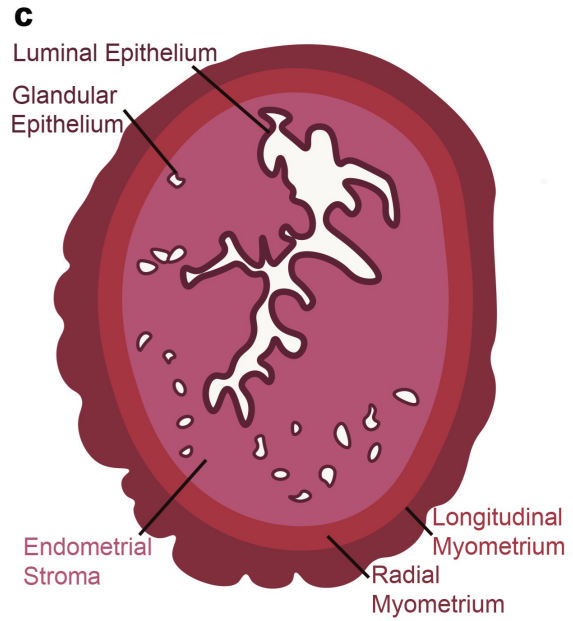
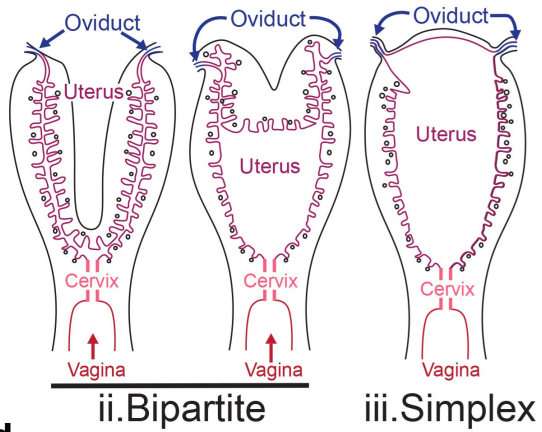
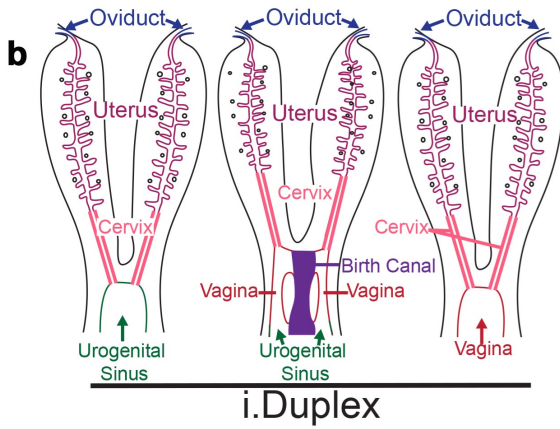
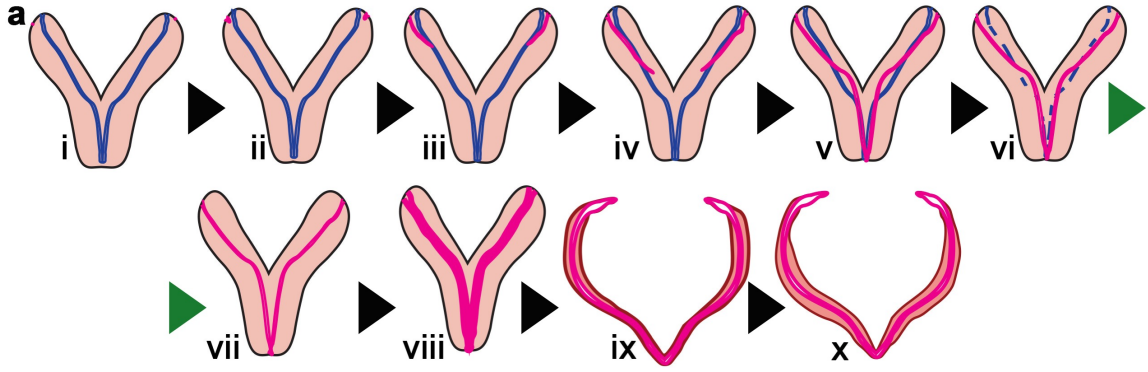


## Figure 1 Development of the Uterus.

The Mullerian duct (red line) migrates adjacent to the Wolffian duct (blue line) to form the primordial FRT(a, i-v). Once the Mullerian duct is fully formed, the Wolffian duct will begin to disintegrate in genetic females (a, v-vii). During disintegration of the Wolffian duct, the Mullerian duct will also differentiate into the Female reproductive tract (FRT) (a, vii-x). There are three types of FRT: (i) duplex, (ii) bipartite, and (iii) simplex. There are three subcategories of duplex FRTs do not have a vagina, have two vaginae, and one that has one vagina. There are a wide variety of bipartite FRTs including the two examples provided. Both exhibit two uterine horns with varying levels of connection and one cervix. A simplex FRT has two oviducts that connect to a single uterus (b). A diagram of a uterus cross-section (c). The outer layers of the uterus include two different myometrial layers. The innermost layer is the luminal epithelium with glandular epithelium strewn throughout the endometrial stroma surrounding the luminal epithelium (c). Endometrial gland development does not begin in most mammals until after birth (d). The luminal epithelium of the endometrium (tan) will begin to bud (i) off the main lumen (green). These buds will (ii) form teardrops, (iii) create elongated tubules, (iv) and eventually form sinuous and branched tubules. After puberty, the tubules will form an extensive secondary branching off the main glandular trunk (d).

uterine horns connected by a central cervix. In some species with a bipartite uterus, the uterine body is fused but still exhibits separate horns (Figure 1b). Finally, a few bat species and some primates like the human have a simplex uterus where the fusion of the Mullerian duct is more extensive, creating one central uterus with two separate oviducts and ovaries. Mice are commonly utilized to investigate mammalian FRT development, as it closely represents human FRT development(6, 7).

Following the completion of Mullerian duct fusion, the Wolffian duct will regress in females (Figure 1a, blue). The differentiation of the Mullerian duct is driven by both repression or absence of signals like androgens and the activation of other signals like COUP-TFII (COUP transcription factor 2)(8). Mullerian differentiation leads to the formation of the oviduct, uterus, cervix, and upper vagina. This differentiation is regulated by a large number of proteins including multiple homeodomain transcription factors (Hox). There are specific Hox genes that pattern the different regions of the FRT. Hoxa9 is expressed during oviduct formation, Hoxa10 and Hoxa11 are required for uterine differentiation, and Hoxa13 promotes cervical and vaginal differentiation(9). Disruption of the Hox patterning, by loss of Hoxa10 and Hoxa11 in mice, for example, causes a portion of the uterus to differentiate into oviduct(10). Similarly, Hoxa13 loss in mice causes the cervix to differentiate into uterus(11). Interestingly, in addition to development driven by Hox expression, the Wnt ligand, Wnt7a, also causes aberrant differentiation of the oviduct into uterus and the uterus into vagina(12).

The differentiation of the fused Mullerian duct structure results in numerous, morphologically diverse tissues. The upper vagina has a stratified squamous epithelium surrounded by a double layer of smooth muscle. The cervix has two distinct areas. One has a stratified squamous epithelium that is encased in a stromal layer, while the other area is a folded simple columnar epithelium that creates mucosal glands. The oviducts have three different portions: the infundibulum (close to the ovary), the ampulla, and the isthmus (closest to the uterus). The infundibulum actively helps move the egg released from the ovary into the oviduct. The ampulla is commonly where an egg is fertilized. The isthmus is a small portion of the oviduct that is connected to the uterus. The uterus is made up of the exterior layer, perimetrium, the myometrium, and the endometrium, the innermost layer (Figure 1c). The perimetrium is a thin membrane with a layer of connective tissue underneath that is the exterior of the uterus. The myometrium, derived from the Mullerian duct mesenchyme, is divided into two histologically distinct sets of smooth muscle (Figure 1c). The longitudinal myometrium is the outermost layer, while the radial myometrium is the inner layer. The endometrium consists of stroma, vasculature, and a simple columnar epithelium. The simple columnar epithelium develops after birth into two distinct populations: luminal epithelium and glandular epithelium (Figure 1c). The luminal epithelium is found on the main central lumen in the uterus and the glandular epithelium extends from the main lumen (Figure 1c). At birth, mice have formed a bipartite uterus, but lack the endometrial glands necessary for reproduction.

After puberty, a mammal will start ovulation through menstruation or estrous. The menstrual cycle length is determined by the first day of menses to the day before the menses of the next cycle begins. In humans the cycle is between 25-30 days in length(13). During this time a group of ovarian follicles will mature with one eventually dominating the other follicles until the oocyte is released in ovulation(13). Meanwhile, the endometrium is primed by estrogen to proliferate and form a proper environment for an embryo(13). Once the egg is released, the follicular cells that have not been released secrete progesterone to prepare the uterus for implantation of the zygote(13). If implantation does not occur, then the follicular cells degrade and menstruation begins when progesterone and estrogen levels are at their lowest point(13). The estrous cycle is divided into four stages: diestrus, proestrus, estrus, and metestrus(14). During diestrus, small follicles are present that begin to grow in proestrus(14). At the same time, the uterus begins to vascularize, endometrial glands grow, and the epithelium increases so that by estrus, there is a maximum amount of growth in the uterus. Estrus is when ovulation begins, where 10-20 eggs are released in mice from the ovarian follicles. Metestrus is similar to the beginning of menses. However, the tissue is not shed but rather reabsorbed into the uterus(14).

This cycling is utilized to prime the female uterus for reproduction. Once an oocyte is fertilized the endometrial glands play a critical role in readying the uterine environment for the embryo. During the fertilization process the endometrial glands secrete proteins which (1) makes the uterus receptive to the blastocyst when it implants, (2) differentiates the endometrial stroma into decidua

and (3) nurtures the embryo during the generation of a placenta(15–18). The endometrial gland is a necessary part of female fertility that begins developing postnatally.

## 1.2 Endometrial Gland Development

Endometrial glands begin to bud in mice (*Mus musculus*) between postnatal day 5 (P5) and P7 from the luminal epithelium. Gland development does not happen as a synchronous event and each gland may be at a different stage of development. Around P7 endometrial glands begin to form teardrop-like structures(19) which then elongate into tubes around P11 that begin to branch by P21(19). After puberty, the glands look similar to a multi-branched tree, with the top of the tree connected to the central lumen (Figure 1d)(20). The endometrial gland epithelium can be distinguished from the luminal epithelium by expression of *Foxa2* and increased *Sox9* nuclear expression(21, 22).

Gland development is a complex and dynamic process that takes the coordination of the luminal epithelium, the differentiating glandular epithelium, the endometrial stroma and the two layers of myometrium in order to form properly. Over the past two decades, scientists have been working to understand the complex molecular mechanism of this glandular development. There are a large number of genes that are involved in endometrial gland development (Table 1, Function: Gland Development). Utilizing a uterine specific Cre driven by the progesterone receptor (*PR-Cre*), it was found that *Ctnnb1<sup>lox/lox</sup>; PR-Cre*, *Wnt7a<sup>lox/lox</sup>; PR-Cre*, and *Wnt5a<sup>lox/lox</sup>; PR-Cre* mice do not form endometrial

glands. *Wnt4*<sup>-/-</sup> mice have a decrease in the number of glands compared to wild-type endometrium when examined in kidney capsule grafting experiments(23). In addition, exposing postnatal mice from P3-P11 to high levels of progesterone causes a loss of gland formation that corresponds to a decrease in canonical Wnt signaling(24). Similar to Wnt signaling mutants, *Sox17*<sup>lox/lox</sup>; *PR-Cre* mice have an aglandular phenotype but curiously Sox17 is known as a negative regulator of Wnt signaling(25). Mice with increased Notch signaling in the uterus, *Rosa26*<sup>N1ICD/N1ICD</sup>; *PR-Cre*, do not form endometrial glands. This implicates numerous membrane receptor signaling pathways in endometrial adenogenesis, especially Wnt signaling(26).

### 1.3 Wnt signaling

Wnt signaling is associated with three different pathways, canonical, non-canonical planar cell polarity, and the non-canonical calcium pathway (Figure 2a). In planar cell polarity (PCP), Wnt ligands bind with Frizzled receptors leading to the recruitment of PCP protein DVL (dishevelled) which activates RAC (Ras-related C3 botulinum toxin substrate), Cdc42 (cell division control protein 42), and RhoA (Ras homolog gene family member A) to affect actin organization (Figure 2a). The calcium/Wnt signaling begins with Wnt ligands binding to Frizzled receptors and ROR (retinoid-related orphan receptors) activating an assortment of kinases like JNK (Jun Kinase) and Protein Kinase C (PKC) (Figure 2a). The most widely studied pathway however is the canonical Wnt signaling pathway. In canonical Wnt signaling, the Frizzled receptors bind with the LRP5/6

Gene Name	Function	Genetic Manipulation	Female Reproductive-tract phenotype	References
Aromatase	Development	Null	Underdeveloped uteri	(27)
Hoxa11	Development	Null	Excessive narrowing of the uterus	(10)
Vangl2	Development	Spontaneous mutation; Grafting Experiments	Septate vagina; Heterozygous mice have reduced gland formation; Mislocalization of E-cadherin; Disruption of planar cell polarity; Loss of actin polarization; Infertile	(28)
Follistatin	Development; Differentiation	Conditional Knockout	Subfertile; poor decidualization; Abnormal endometrial luminal epithelium receptivity	(29)
Hoxa10/Hoxa11	Development; Differentiation	Transheterozygotes	Partial transformation of uterus to oviduct; Excessive narrowing of the uterus	(10)
Activin-like Kinase 2 (ALK2)	Differentiation	Conditional Knockout	Subfertile; poor decidualization	(30)
Estrogen receptor $\alpha$	Differentiation	Null	Sterile; hypoplastic; does not go through estrous cycle	(31)
Estrogen receptor $\alpha/\beta$	Differentiation	Null	Extreme hypoplastic uterus; abnormal uterine architecture; sterile	(31)
Hoxa10	Differentiation	Null	Partial transformation of uterus to oviduct	(10)
Hoxa13	Differentiation	Hypodactyly mutation	Cervical tissue transformed into uterus; hypoplasia of the vagina	(32)
IGF-1	Differentiation	Null	Underdeveloped uteri especially in myometrium	(33)
Ovo1	Differentiation	Null	Dilated uterus; Loss of luminal epithelium	(34)
Wnt7a	Differentiation ; Gland Development	Null; Conditional Knockout	Uterine tissue transformed into vagina and oviduct transformed into uterus; Loss of uterine glands, Abnormal mesenchyme differentiation	(35)
PTEN	Differentiation ; homeostasis	Conditional Knockout	At 1 month had endometrial cancer; 3 months endometrial cancer with myometrial invasion	(36)
Dicer	Gland Development	Stroma Conditional Knockout	Reduced gland formation with few aberrantly in myometrium; decreased endometrial size; dysfunction of the uterotubal junction; reduced oviducts and uterine horns	(37)
Dlx5/6	Gland Development	Conditional Knockout	Reduced gland formation; large lumen with deep invaginations	(38)
Foxa2	Gland Development	Conditional Knockout	Reduced gland formation; subfertile	(21)
Lef1	Gland Development	Null	Loss of uterine glands	(39)
Notch1	Gland Development	Overactivation	Loss of uterine glands; infertile; misregulation of hormone signaling	(26)
PR-Set7	Gland Development	Conditional Knockout	Loss of uterine glands; infertile; increased endometrial epithelial cell death	(40)



Progesterone	Gland Development	Increased amount at early postnatal days	Loss of uterine glands; Infertile; impaired decidualization; no implantation and decreased implantation factors	(41)
Sox17	Gland Development	Conditional Knockout-stroma	Loss of uterine glands; infertile	(25)
Sox9	Gland Development	Overactivation	Increase in uterine gland formation; uterine cysts	(22)
Timp1	Gland Development	Null	Late onset Increase in uterine gland formation; Abnormal endometrial luminal epithelium and shape	(42)
Wnt11	Gland Development	Conditional Knockout	Early increases in gland numbers	(43)
Wnt5a	Gland Development, Differentiation	Null	Short & coiled uterine horns, lack of cervical/vaginal structures; loss of uterine glands	(4)
Wnt4	Gland Development, Homeostasis	Conditional Knockout	Reduced gland formation, abnormal luminal epithelium	(23)
Lgr4	Gland Development, Pregnancy	Conditional Knockout	Reduced gland formation; decreased LIF secretion; subfertile; impaired decidualization	(44)
Cdh1	Gland Development; Homeostasis	Conditional Knockout	Loss of uterine glands; Loss of epithelial markers; Loss of endometrial stroma markers; Increased apoptosis and proliferation; Decreased Wnt and Hox expression	(45)
Ctnb1	Gland Development; Homeostasis	Conditional Knockout	Loss of uterine glands, later k14 positive stratified squamous epithelium; unable to go through decidualization reaction	(46)
Smo	Gland Development; Homeostasis; Stromal Development	Overactivation	Infertile; No decidualization; Uterine hypertrophy; reduced gland formation; stratified squamous luminal epithelium; Uterine stroma change extracellular matrix	(47)
Ctnb1	Homeostasis	Overactivation	Hyperplasia of the gland	(46)
Estrogen receptor $\beta$	Pregnancy	Null	Subfertile (smaller litters)	(48)
Kiss1	Pregnancy	Null	Decreased Lif1 secretion levels	(49)
Lif	Pregnancy	Null	Inability of blastocyst to implant; No decidualization	(15, 16)
Notch1	Pregnancy	Conditional Knockout	Reduced decidualization	(50)

**Table 1 Genes involved with Uterus Development and Homeostasis**

(low density lipoprotein receptor related protein 5/6) co-receptors causing DVL to be phosphorylated which recruits a scaffolding protein, Axin. Axin in complex with APC (adenomatous polyposis coli), CK1 $\alpha$  (Casein kinase 1 $\alpha$ ) and GSK-3 $\beta$  (glycogen synthase kinase 3 $\beta$ ) create the destruction complex. This complex targets  $\beta$ -catenin for multiple phosphorylation events leading to recruitment of the ubiquitin ligase complex which ubiquitinates  $\beta$ -catenin and leads to proteasomal degradation. Thus, when Axin is recruited away from this complex,  $\beta$ -catenin is able to translocate into the nucleus and bind with the LEF/TCF (Lymphoid enhancer factor/T-cell factor) family of proteins derepressing downstream Wnt target genes (Table 2). Interestingly, while  $\beta$ -catenin is a key component of canonical Wnt signaling, the majority of  $\beta$ -catenin is found at adherens junctions. There is a debate on whether junctional  $\beta$ -catenin and cytoplasmic  $\beta$ -catenin pools mix. Another adherens junction protein was also recently found to play a role in Wnt signaling,  $\alpha$ -catenin.  $\alpha$ -catenin increases APC binding to  $\beta$ -catenin allowing for increased degradation of  $\beta$ -catenin and in theory a decrease in canonical Wnt signaling(51). Wnt signaling is thought to be a major pathway in endometrial development. As was previously discussed Wnt ligands and  $\beta$ -catenin were found to affect both Mullerian duct formation and endometrial adenogenesis. Since the loss of  $\beta$ -catenin disrupts endometrial adenogenesis, we can postulate that canonical Wnt signaling is necessary during endometrial gland development. Many of the Wnt ligands, mentioned in section 1.1 Female Reproductive Tract Development, that are associated with endometrial gland

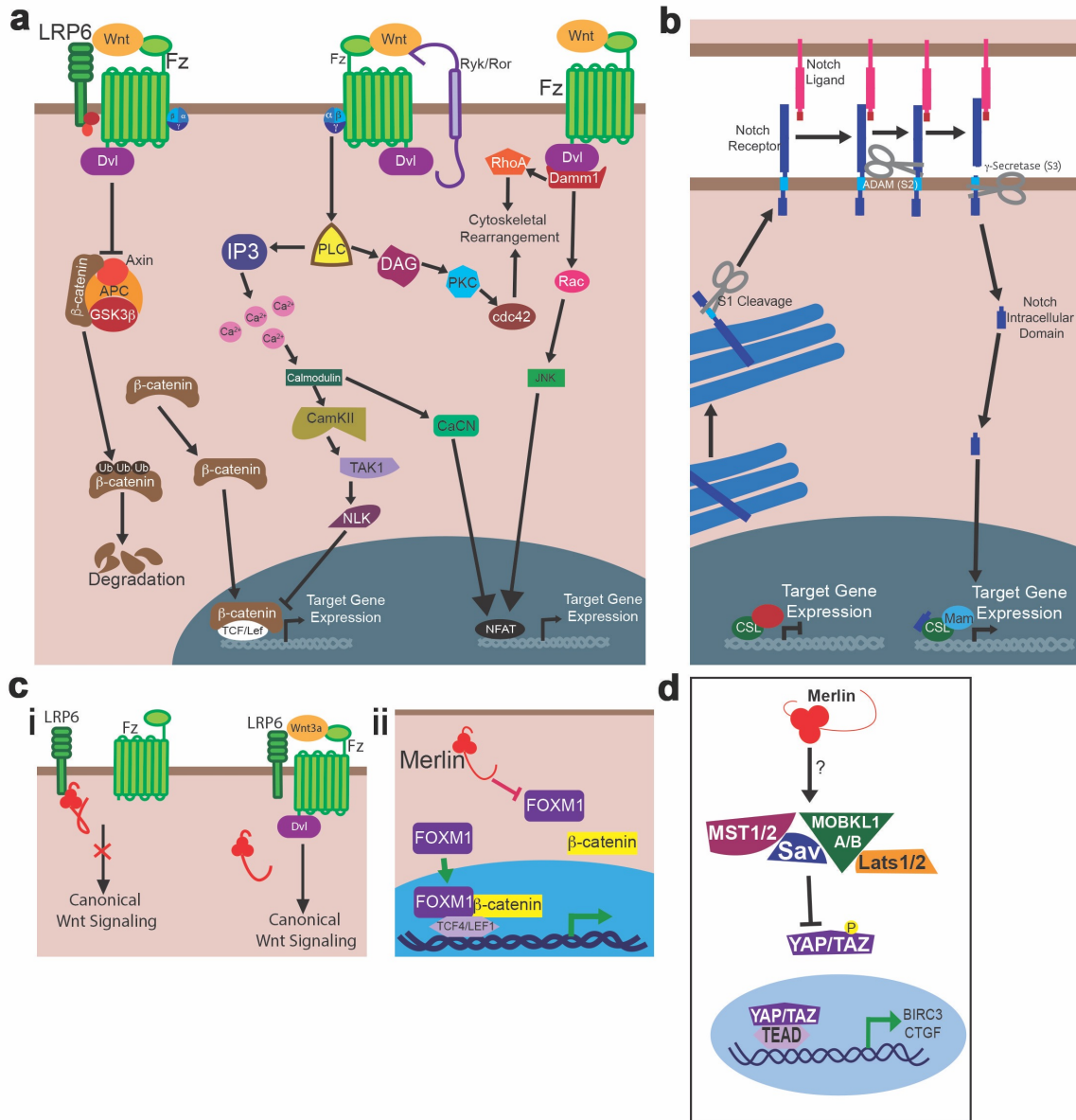


## Figure 2 Wnt, Notch, and Hippo signaling pathways.

There are three main types of Wnt signaling (i) canonical signaling, (ii) non-canonical calcium signaling, (iii) planar cell polarity (**a**). (i) When Frizzled receptors are activated by LRP in canonical Wnt signaling it inhibits the destruction complex (Axin/APC/GSK3 $\beta$ ) from phosphorylating  $\beta$ -catenin.  $\beta$ -catenin is then able to translocate to the nucleus where it increases canonical Wnt target genes. (ii) Frizzled receptors and retinoid-related orphan receptors (RORs) bind to the Wnt ligand activating Phospholipase C (PLC) which in turn activates many different proteins including Inositol trisphosphate (IP3) that utilizes calcium Ca<sup>2+</sup> to activate calmodulin. Activation of Calmodulin causes Transforming growth factor beta-activated kinase 1 (TAK1) to activate Nemo Like Kinase (NLK) which inhibits target genes. (iii) In Planar cell polarity, when Frizzled is activated by the Wnt ligand it binds to intracellular protein, Disheveled (Dvl) which recruits and activates Daam1. Daam1 then activates RhoA which through Rho-associated kinases (ROCK) manipulates and rearranges the cytoskeleton (**a**). Notch signaling has a membrane-bound ligand and receptor that must interact for proper cleavage of the receptor (**b**). The Notch receptor is enzymatically cut in the Golgi apparatus (S1 Cleavage), this is necessary for the Notch receptor to be activated. Once the Notch ligand binds to the Notch receptor, the ADAM (a disintegrin and metalloprotease domain) proteins cleave the extracellular matrix of the Notch receptor (S2 cleavage). This allows for the  $\gamma$ -secretase complex to cleave the transmembrane domain (S3 cleavage) generating the Notch Intracellular Domain (NICD). The NICD is translocated to the nucleus where it interacts with TCF/Lef family members to increase transcription of Notch downstream targets (**b**). Wnt signaling has been shown to be manipulated by the tumor suppressor Merlin in different contexts (**c**). One example is Merlin has been found to inhibit canonical Wnt signaling within Schwannoma cell lines. Kim *et al.* showed that unphosphorylated Merlin inhibits the ability of Frizzled and LRP6 to interact while phosphorylated Merlin no longer binds LRP6 allowing it to interact with Frizzled (i)(52). Merlin blocks FOXM1 (forkhead box protein M1) from Wnt signaling in pancreatic cancer cell lines(53). Loss of Merlin stabilizes FOXM1 protein and increases the amount of FOXM1 that can increase canonical Wnt signaling (ii)(53). The Hippo signaling pathway is active when YAP/TAZ (Yes associated protein/Transcriptional coactivator with a PDZ-binding domain) are not active (translocated to the nucleus and increasing target transcription) (**d**). Merlin activates the MST1/2 (mammalian ste20 homologs 1/2), Sav (Salvador), MOBKL A/B (Mps one binder kinase activator-like A/B), and Lats1/2 (Large tumor suppressor 1/2) group of proteins which inhibit YAP/TAZ nuclear translocation by phosphorylation (**d**)(54). Targets of YAP/TAZ include BIRC3 and CTGF (**d**).

development are utilized more in planar cell polarity (PCP), however whether ligands are canonical or non-canonical is tissue specific. The Lpt mouse, is a PCP mutant mouse model that does form endometrial glands, suggesting that PCP is not necessary for proper endometrial adenogenesis(28).

Apicobasal polarity has also been shown to be important in Wnt signaling. In *Drosophila*, Wnt forms a gradient with a majority of the dWnt localizing to the apical membrane. Interestingly, if dWnt is mutated, basally localized dWnt does not rescue the phenotype(55). Also, proper localization of the Frizzled receptor to the apical or basal membrane was shown to determine whether the receptor activated canonical Wnt signaling or planar cell polarity(56). Understanding the role apicobasal polarity plays in Wnt signaling may contribute to understanding the role of Wnt in endometrial development and homeostasis.

Curiously, a constitutively active  $\beta$ -catenin mouse model (*Ctnnb1*<sup>f(ex3)/+</sup>; *PR-Cre*), exhibits endometrial gland hyperplasia(46). The endometrial gland is hypothesized to be where endometrial cancer originates. Thus, the phenotype in *Ctnnb1*<sup>f(ex3)/+</sup>; *PR-Cre* mouse models may represent an early form of endometrial cancer. In fact, a recent study showed that  $\beta$ -catenin mutations in low-grade and early stage endometrial cancer patients correlated with an increased risk for recurrence and metastasis. This is fascinating because this is a population of patients that have a low risk of recurrence(57). This implies that Wnt signaling is critical within the uterus and an important factor to consider in endometrial cancer.

Gene Name	Canonical Pathway	Located in Endometrium?	Reference
HEYL	Notch	Medium mRNA and low protein diffuse in tissue	(58)
HES1	Notch	Low mRNA levels	(59)
HEY1	Notch	Low mRNA levels	(58)
HEY2	Notch	Low mRNA and medium protein in tissue	(58)
p21	Notch	Medium RNA and medium protein in glands	(60)
Axin2	Wnt	Medium protein levels in glands	(61)
c-Myc	Wnt	Medium protein levels in glands; mutant mice have decreased fertility	(62)
Sox9	Wnt	High protein levels in glands	(63)
Ccnd1	Wnt	Low protein levels in glands	(64)

**Table 2 Downstream Targets of Notch and Wnt Signaling**

\*This is not a comprehensive list just those examined within this study.

## 1.4 Endometrial Cancer

Endometrial cancer is the fourth most common female cancer within the United States and the fifth most common in the world(65, 66). The highest incidences of endometrial cancer are observed in the United States, Canada, and Europe. There are an estimated 10,920 American deaths attributed to endometrial cancer, making it the sixth most deadly female cancer in the US(66). Unlike most other cancer types, the rate of endometrial cancer incidence is increasing and is projected to rise to the third most common female cancer in the United States within the next 25 years(67). In fact, there has been a 2.3% rise in the rate of endometrial cancer from 2008-2012 with a portion of that increase coming from premenopausal women and a 2% increase in the number of deaths related to the disease. There are some disparities within races with endometrial cancer, for instance while there was an 84% survival rate in Caucasian women between 2006-2012, black women saw more than a 20% decrease in survival within the United States. These differences may be caused by disparities in socioeconomic situations. Approximately 95-98% of all endometrial cancers arise in epithelial cells of the endometrium. Traditional classification of endometrial carcinomas is based on clinical and endocrine features as well as histopathological characteristics. Within the last two decades, molecular classification has served as an important advancement to further organize these tumors(68–70).

Pathologically, there are several different histotypes of endometrial cancer, such as clear cell, serous and endometrioid, the most common histotype

(~80%). Standard of care for endometrial cancer generally consists of removing the ovaries (bilateral salpingo-oophorectomy) and a hysterectomy. Depending on the stage of the disease, lymph nodes may also be removed. Women still in their reproductive years may retain their ovaries, preventing early menopause. Surgery is normally followed by adjuvant chemotherapy in cases determined to have high risk of recurrence by the histology (serous) and in cases where cancer is discovered in resected lymph nodes or non-uterine sites.

Clinically, the aggressiveness of the disease is determined during surgical staging and by histological grade. Staging and tumor grade have a fundamental importance in treatment decisions. The Federation of Gynecology and Obstetrics (FIGO) staging used by gynecological oncologists world-wide, place endometrial cancers in one of four stages. Stage I is when the tumor has not spread outside of the uterus and is separated into two subcategories: tumors that have invaded 50% or less into the myometrium (Stage IA) and tumors that have invaded more than 50% of the myometrium (Stage IB). Stage II is defined as when the tumor has spread into the cervix. Stage III is when the tumor has spread from the endometrium, cervix, and into other parts of the female reproductive tract (FRT) and/or lymph nodes. Finally, Stage IV is separated into two subcategories: when the tumor has invaded into the bladder area (Stage IVA) or cells have metastasized into distant organs or lymph nodes (Stage IVB). Tumor grade identifies at what level tumor cells resemble normal endometrial epithelium. Grade 1 is when the endometrial tumor cells are well-differentiated and are predominantly comprised of glandular growth with 5% or less of abnormal tissue.



Grade 2 tumors are moderately-differentiated with between 6-50% of the tissue considered cancerous. Grade 3 tumors are considered poorly-differentiated tumors, with a majority of the tissue maintaining very little to no recognizable epithelial growth patterns. Patients having grade 3 endometrioid tumors have a poor prognosis, similar to non-endometrioid tumors (serous and clear cell).

Endometrial cancers are also classified more broadly to simplify the disease into two categories, Type I and Type II, based on histology, molecular characteristics, and clinical diagnosis of the tumors. It should be noted that this simplified classification is not utilized in the clinic to determine treatment plans. Type I tumors include grade 1 and grade 2 endometrioid tumors. These tumors are less likely to metastasize and have a relatively good prognosis. These tumors are also highly correlated with obesity and excess estrogen. Type I tumors usually have mutations within the AKT/PI3K pathway. Grade 3 tumors are considered Type II along with other non-endometrioid cancers. These tumors are seen at an older age and are more aggressive with a poor prognosis. Type II tumors frequently have p53 mutations estimated in some studies to be present in 90% of cases. Type II tumors also have mutations in other genes including E-cadherin (80-90%), p16 (40%), or Her2 (45-80%) and not always independent of one another(71). It is commonly thought within the field that Type I and Type II tumors form independently and do not progress from one type to another. While a majority of Type I and Type II tumors are separated by specific pathway mutations, there is some overlap.

My work focuses on Type I endometrioid tumors where the epithelium is still identifiable with key epithelial markers. Type I endometrial cancers commonly have PTEN (Phosphatase and Tensin homolog) inactivation (50-80%), microsatellite instability (20-45%), K-ras mutations (10-30%), or  $\beta$ -catenin mutations (20%) though not always separately(57, 71). Since endometrial hyperplasia has PTEN inactivation in about 50% of cases, it is hypothesized that Type I tumors may be progression of hyperplasia. There is a small subset of Type I tumors that have p53 mutations, Her2 overexpression, p16 inactivation, or E-cadherin alterations(71).

Recently, Notch signaling has also been found to be downregulated in early stage and low-grade endometrial cancer cases(72, 73). Multiple Notch receptor activation mouse models have shown that Notch is necessary for proper FRT development(26, 74). Notch signaling is involved in both endometrial development and tumorigenesis, however no one has examined how Notch may be important in uterine homeostasis.

### **1.5 Notch signaling**

Notch signaling consists of a single pass transmembrane receptor that binds to an adjacent single pass transmembrane ligand. This interaction opens up the S2 cleavage site that ADAM (A Desintegrin And Metalloproteinase) family secretases severs (Figure 2b). This is followed by cleavage at two intramembrane sites (S3) by  $\gamma$ -secretase, an enzymatic protein complex, generating the Notch Intracellular Domain (NICD). It is not clear how NICD

localizes to the nucleus from the cell membrane but once present at the nucleus, the NICD is imported into the nucleus via importin  $\alpha/\beta$ 1 signaling(75). NICD interacts with CSL (CBF1, Suppressor of Hairless, Lag-1) to increase downstream target gene expression (Table 2, Figure 2b)(76). Mammals have four Notch receptors (Notch1-4) and five canonical Notch ligands (Jag1-2, Delta-like [Dll]1, 3, 4). While there are differences between the intracellular domains of Notch1-4, data has shown that the intracellular domains are interchangeable(77). Previous work has demonstrated that overall levels of active NICD determine how Notch signaling is functioning within the cell(77, 78). Notch signaling has a wide variety of downstream targets and cellular functions depending on spatiotemporal context.

Notch signaling is necessary for proper fate determination in the glandular and luminal epithelium of the stomach in chicken(79). Specifically, overactivation of Notch signaling promoted glandular epithelium, while inhibition of Notch led to luminal epithelium within the stomach in chicken(79). A uterine conditional overactivation of Notch ( $Rosa26^{N1ICD/N1ICD}$ ; PR-Cre) in mice caused a loss of endometrial glands as previously discussed(26). Interestingly, while histologically there are no endometrial glands, glandular specific markers were found to express throughout the luminal epithelium(26). Given that in the chicken stomach, overactivation of Notch signaling causes glandular epithelium differentiation, potentially these mice have no luminal epithelium present and the entire endometrium is glandular epithelium(26, 79).

Apicobasal polarity is important for proper Notch signaling. The apicobasal polarity regulator, Merlin, is necessary for correct localization of the Notch receptor in *Drosophila*(80). In addition, Par3, an apicobasal polarity protein, causes asymmetric localization of Notch signaling in radial glial cells during asymmetric division(81). In fact, asymmetric divisions, usually governed by polarity proteins, promotes Notch signaling during epidermal development in the mouse as well(82). Understanding apicobasal polarity and the role it plays in cell signaling may help determine how it is involved in endometrial development and homeostasis.

### **1.6 Apicobasal Polarity**

Each cell in an organism has an intricate spatial patterning of proteins and organelles within the membrane and cytoplasm. This patterning is necessary for proper functioning of the cells. The composition of cells and tissues are also specifically organized at either a tissue or organ level, respectively. For example, the uterus is organized (from outermost to inner layers) with the smooth muscle layers surrounding the endometrial stroma with vasculature and glands intertwined. The stroma encases the highly polarized, simple epithelium that surrounds the lumen of the uterus.

At a cellular level, apicobasal polarity determines the side of the cell that faces the extracellular matrix and the membrane that faces into the lumen of the tissue. Polarity is initially established through external cues in the extracellular matrix and cell:cell contacts. There are three major complexes necessary for

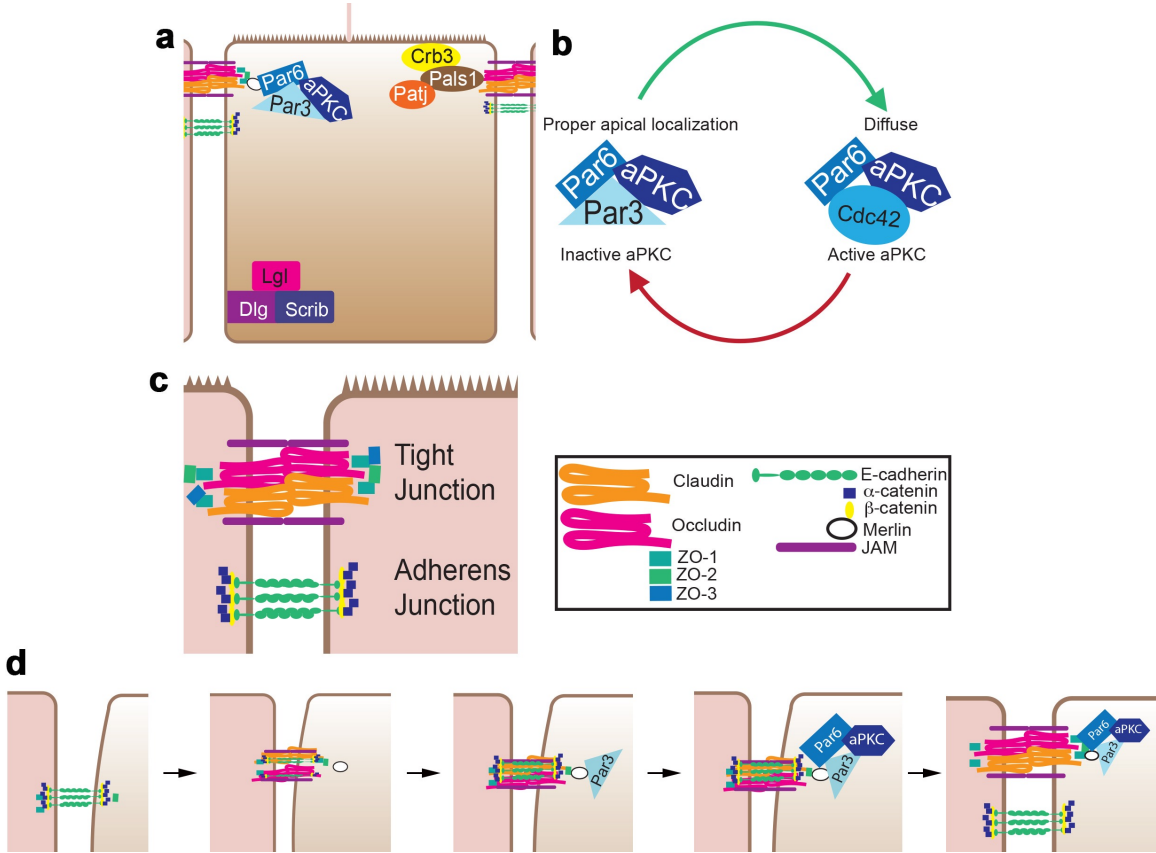


### Figure 3 Apicobasal Polarity and Cell adhesion.

Within a single epithelial cell, there is a gradient of apicobasal polarity proteins with a majority of basal polarity proteins localized on the basal membrane (**a**). The basal complex is the Scrib/Lgl/Dlg. The majority of apical proteins are localized on the apical membrane including two apical complexes. The two apical complexes include the Crb3/Pals1/Patj complex and Par3/aPKC/Par6 complex (**a**). The Par complex switches between Par3 and Cdc42 (**b**). When aPKC/Par6 is in complex within Par3 it causes proper apical localization but aPKC is inactive(83). When Cdc42 is in complex with aPKC/Par6, aPKC is active but the complex is more diffuse within the cell(83) (**b**). The apical junctions in epithelial cells include the tight junction and the adherens junction (**c**). The tight junction consists of transmembrane proteins: occludin, claudin, and JAMs (junction adhesion molecules). In addition, there are the scaffolding proteins Zonula Occludens (ZO) 1-3. The adherens junction consists of cadherin (E-cadherin) molecules that bind extracellularly to other cadherin proteins. The cadherins bind to  $\beta$ -catenin and  $\alpha$ -catenin (**c**). Proper establishment of apicobasal polarity is intertwined with apical junction formation (**d**). When two cells come into contact, primordial adherens junctions form. Par3 is recruited to the primordial junction, followed by the aPKC/Par6 complex. Once Par3/Par6/aPKC are recruited to the primordial junction, junctional maturation occurs forming adherens junctions and tight junctions (**d**).

apicobasal polarity establishment: the Par complex, the Crumbs complex, and the Scribble complex (Figure 3a). These complexes have been found to work in conjunction with each other to form a protein based gradient in the cell. Specific apical and basal kinases oppose each other within the complexes to place apical proteins on the apical perimeter and basal proteins on the basal side(84–87).

The Crumbs complex is localized to the apical tight junctions and was initially discovered to cause a dispersed epithelial cuticle when disrupted in *Drosophila melanogaster*(88). Mammals have three major isoforms of Crumbs (CRB1-CRB3)(89–91). The CRB3 isoform is in a complex with PALS1 (Protein associated with Lin-17) and PATJ (PALS-1 associated tight junction protein) creating the Crumbs polarity complex(90). Crb3 is expressed in many of the tissues in the human body including in the endometrial glandular epithelium(92, 93). Interestingly, the *Crb3*<sup>-/-</sup> mouse does not show apicobasal disruption in any of the examined epithelial tissues(94). This is vastly different than what is observed in three-dimensional (3D) cell culture where cells with Crb3 knockdown are unable to form proper lumens(95, 96). The *Crb3*<sup>-/-</sup> mice do show a decrease in Patj and Pals1 showing that Crb3 is involved in Pals1/Patj expression(94). Patj knockdown and Crb3 overexpression in epithelial cells also causes defects in tight junction formation, however, *Patj* has not been mutated in mice(97–101). *Pals1*<sup>-/-</sup> mice do have a loss of adherens junctions in select epithelium including neural tube epithelium(102). The role the Crumbs complex plays in cell polarity is specific to the cell type and relates to the other polarity complexes.

The Scribble complex localizes to the basal surface, the membrane touching the extracellular matrix, and is necessary to define the basolateral membrane(103). The complex contains Scribble, Discs Large (Dlg) and Lethal Giant Larvae (Lgl) proteins(103, 104). There are four major homologues of Dlg in mammals (Dlg1-4) and two homologues of Lgl in mammals (Llgl1-2). Tissue specific knockout of Scribble in the mammary gland disrupts apicobasal polarity resulting in loss of tissue architecture(105). However, homozygous Scribble mutants, like the spontaneous circletail (*Scrib<sup>Crc/Crc</sup>*) mutant, have severe neural tube closure defects and stereociliary bundle disorganization in the cochlea similar to Planar Cell Polarity (PCP) mouse mutants(106, 107). *Drosophila dlg* mutants have loss of apicobasal polarity of epithelial cells(108). Interestingly, *Dlgh3* mutant (*Dlgh3<sup>tP038A02/Y</sup>*) mice exhibit low penetrance of embryonic lethality and mislocalization of aPKC and apical junction markers at E8.5(109). *Dlgh2-4* knockout mice are viable and have behavioral defects, similar to humans with DLG2-4 mutations that have schizophrenia or mental retardation(110–114). *Dlgh1<sup>-/-</sup>* mice have perinatal lethality and urogenital defects as well(115, 116). Apicobasal polarity has not been examined in depth in the *Dlgh1*, 2, or 4 null mice. *Llgl1<sup>-/-</sup>* mice die at birth from hydrocephalus and *Llgl2<sup>-/-</sup>* mice have placental development defects(117, 118). *Llgl1<sup>-/-</sup>* and *Llgl2<sup>-/-</sup>* mice do not exhibit disruption in apicobasal polarity in the organs examined(117, 118). However, *in vitro* studies showed that when Llgl1-2 were knocked down in combination, apicobasal polarity is disrupted(87). In *Drosophila*, Lgl regulates Notch intracellular domain (NICD) through endosomal trafficking where there is an increase in vesicles and



an upregulation of Notch target genes(119). This is mirrored in Lgl1 depletion in Zebrafish (*Danio rerio*) where Notch signaling increases(120). The Scribble complex is involved in many functions including planar cell polarity, actin cytoskeleton regulation, and vesicular trafficking(105, 106, 119), but is most known for the role it plays in apicobasal polarity.

The Scribble complex is involved in apicobasal polarity through an antagonistic relationship with the Par complex(87). The Par complex is composed of Par3 (Partitioning defective 3 homolog), aPKC (atypical protein kinase c), Cdc42 (cell division protein 42 homolog), and Par6 (Partitioning defective 6 homolog). aPKC phosphorylates Lgl, which prevents apical localization of Lgl and the entire Scribble complex in the *Drosophila* ectoderm(121). In mammalian cell lines, it was shown that Lgl competitively binds to aPKC in place of Par3 or Cdc42 allowing the phosphorylation of aPKC(85). When aPKC is at the basolateral membrane this leads to an overabundance of Lgl binding and an inactivation of the Par complex since neither Par3 or Cdc42 can bind. aPKC is a Serine/Threonine protein kinase that is necessary to maintain the antagonistic relationship with the Scribble complex.

The proteins that compose the Par complex are involved in multiple functions, not just apicobasal polarity. Par3 is a scaffolding protein that has three PDZ domains that bind proteins including PTEN, cell junction proteins, and Par6. In addition, Par3 directly interacts with aPKC. Interestingly, aPKC can phosphorylate Par3 causing dissociation of Par3 from the Par6/aPKC complex. Par3 binding to aPKC/Par6 is necessary for proper apical localization (Figure

3b)(83). Cdc42 is in complex with activated aPKC and is thought to be necessary for activation (Figure 3b)(83).

In epithelial cells, cell polarity proteins act in tandem with specific cell:cell or cell:matrix complexes. The Par complex is established through cellular contact (Figure 3d). In cell culture when two cells make contact, the adherens junction protein, E-cadherin is recruited to the site of contact. This initiates the formation of primordial apical adherens junctions. Par3 is recruited to the primordial junction through the tumor suppressor protein Merlin and junctional adhesion molecules (JAMs)(122, 123). Par6/aPKC subsequently localize to the junction where Par3 binds to the complex (Figure 3d).

Par3 was initially found in *C. elegans* in 1988 when Kemphues *et al.* showed it was necessary for asymmetric division of the one-cell *C. elegans* embryo(124). Par3 has three major isoforms(125). The 180kD and 150kD isoforms both have the aPKC binding domain, while the 100kD isoform does not bind to aPKC(125). Since the 100kD isoform does not bind to aPKC it is thought to not play a role in apicobasal polarity. My dissertation work focuses on the isoforms that bind aPKC and are involved in apicobasal polarity. Par3 has multiple functions within the cell including the regulation of primary ciliogenesis, PI3K/AKT signaling, and apicobasal polarity(124, 126–129). The ability of Par3 to bind to Kif3a, a microtubule motor protein for cilia, is necessary for proper primary cilia formation in cell culture(126). Par3 also binds PTEN and is required for proper localization of PTEN in *Drosophila* and cell culture(130, 131). It was determined that PTEN also played a role in proper Par3 localization and tight

junction function, thus both are necessary for proper apical membrane establishment(127, 131, 132).

Par3 is necessary for the proper establishment of the apical cell membrane in model organisms and mammalian cell culture(128, 129). Par3 was found to be critical for correct asymmetric division of radial glial cells into a daughter radial glial cell and a neuron. This was found to be mediated through asymmetric division of Notch signaling(81). Studies of the *Par3* knockout mouse (*Par3*<sup>ΔE3/ΔE3</sup>) showed a failure of epicardial development leading to embryonic lethality between embryonic day 12.5-14.5 (E12.5-E14.5)(133). The epicardial progenitors are unable to form cysts that are necessary for proper formation of the epicardium(133). This inability to bud into cysts is hypothesized to be from mislocalization of polarity proteins(133). Defective epithelial cyst formation has also been observed in *Par3* knockdown cells(72, 134). Besides aberrant heart development, the *Par3*<sup>ΔE3/ΔE3</sup> mice also exhibit some amount of stunted growth at E9.5 and a shortened tail(133). It is suggested the reason there are not more evident issues with other epithelial organs at earlier embryonic stages is because other proteins like Par3L or Par3β compensate for the loss of Par3. Conditional *Par3* knockout (*Par3*<sup>lox/lox</sup>; *K14-Cre* hereafter referred to as *Par3eKO*) within the skin causes an inside-out barrier defect in newborn pups with mislocalization of tight junction proteins, ZO-1 and claudin-1(135). An inside-out barrier defect is when the barrier that holds moisture and other substances in the body is defective, thus a severe barrier defect would cause lethal dehydration. A similar phenotype is observed in Claudin-1 null mice(136). Except for the mislocalization

of Claudin-1, the tight junction loss reverts back to wild-type by P58 in Par3eKO mice(135). This may be attributable to a compensatory mechanism. As the Par3eKO mice age there is an increase in hypertrophic and multilobular sebaceous glands(135). In addition, there is an increase in overall epidermal thickness in Par3eKO mice at birth(135). Further phenotypes related to cancer have been identified in *Par3* knockout mice that will be discussed in 1.7 Apicobasal Polarity in Cancer(137, 138). Par3 has also been found to be critical in mammary gland development(139). Par3 knockdown caused a 44% decrease in growth of mammary glands across the fat pad when transplanted compared to wild-type control cells(139). In addition, the Par3 knockdown glands were unorganized, multilayered, and small(139). It was found that the aPKC binding domain of Par3 was necessary to rescue the growth of the mammary gland(139).

Atypical Protein Kinase C (aPKC) is one of three subfamilies of PKCs (novel PKC and classical PKC) that contains two proteins PKC $\zeta$  and PKC $\lambda/\iota$ . aPKC proteins have various roles through tissue development that have been observed in mouse models. *Pkc $\zeta$*  null mice are viable but show abnormalities in the ratio of B:T cells caused by NF- $\kappa$ B signaling(140). The important role of aPKC proteins in the immune system was confirmed when both *Pkc $\lambda/\iota$*  and *Pkc $\zeta$*  affect the ability of T lymphocytes to properly go through asymmetric division(141). This disruption of asymmetric division is also observed with other polarity mutants in different cell types(81). *Pkc $\lambda/\iota$*  has been implicated in the development and maintenance of many organs including the kidney and the hair follicle(142–147). When *Pkc $\lambda/\iota$*  is deleted in the developing kidney nephrons

(*aPkcλ<sup>lox/lox</sup>; Nphs1-Cre*) it causes renal dysfunction by 4 weeks of age leading to death by about 6 weeks of age. The renal dysfunction is due to mislocalization of nephrin and podicin proteins which are necessary for proper formation of the podocyte tight junction(145), similar to polarity proteins in other epithelium. Loss of *Pkcλ* in the epidermis (*aPkcλ<sup>lox/lox</sup>; K5-Cre*) causes progressive hair loss due to a slow regression of the bulge stem cell niche through an increase in asymmetric cell divisions and a decrease in symmetric cell divisions(147).

While Par6 has not been thoroughly studied *in vivo*, there is a Par6 $\alpha$  mutant (*PARD6 $\alpha$ <sup>tm1.1(KOMP)Vlcg/tm1.1(KOMP)Vlcg</sup>*) generated by the International Knockout Mouse Consortium with a few noted phenotypes including changes in T-cell numbers, aberrant bone mineral content and changes in body fat(148). There has been some work that links Par6 to cancer. Par6 was found to promote proliferation of breast cancer cells and epithelial-mesenchymal transition (EMT) through TGF $\beta$  in non-small-cell lung cancer (NSCLC) cell lines(149, 150). High levels of Par6 have also been correlated with aggressive prostate cancers and EMT in breast cancer indicating the Par complex may be involved and promote tumorigenesis.

### 1.7 Apicobasal Polarity in Cancer

Apicobasal polarity is a characteristic of all epithelial tissues. A majority of solid tumors lose apicobasal polarity, however in the past it was thought to be a secondary effect of the driver mutations and cancer hallmarks, such as EMT that are necessary for cancer metastasis(151). Recently, evidence has been

mounting that implicates a major role of polarity in the progression of cancers (Table 3). The Crumbs3 protein from the Crumbs complex has been shown to suppress features of tumorigenesis (metastasis, pluripotency) in normal kidney and breast cell lines(152, 153). The Scribble complex proteins, Scribble and Dlg, are targeted by the Human Papillomavirus (HPV) for degradation and this decrease of protein at the membrane is correlated with higher grade and more invasive cervical malignancies(154–156). Scribble deficiency in mice predisposes them to prostate cancer(157). Interestingly, Scribble is mislocalized in prostate cancer and basal breast cancer patients and correlate with a poor prognosis(157, 158). While there are some excellent reviews on both the involvement of the Crumbs and Scribble complexes in cancer(159, 160), my dissertation work focuses on the Par complex.

The Par complex has been found to be lost in a variety of cancers including breast, colon, and gastric cancer(92, 93, 161). Par6 has been shown to be necessary for EMT in a breast cancer cell line when TGF $\beta$  (transforming growth factor  $\beta$ ) signaling is disrupted however no *in vivo* studies have confirmed this(149). There is a decrease in Par6 protein levels in stomach and colon cancer however this has not been examined in detail(92, 93). Pkc $\zeta$  has been found to act as a tumor suppressor while Pkc $\iota$  acts as an oncogene in some mouse models. Pkc $\zeta$ <sup>-/-</sup> lungs that were stimulated by the oncogene, Ras, had a 20% increase in tumor burden compared to wild-type Ras-stimulated lungs(162). Galvez *et al.* determined that Pkc $\zeta$  suppresses Interleukin-6 (IL6)(162), an inflammatory signal that is increased in cancer patients(163).

Gene (Protein)	Uterine Phenotype	Experimental Cancer-related Data	Human Cancer Data	References
Crb3 ( <b>Crumbs3</b> )	Not known	Loss contributes to tumorigenesis; targeted by viral oncoproteins for degradation	Amplification in sarcoma, neuroendocrine prostate, breast cancer, paraganglioma; deletion in uterine, stomach and lung adenocarcinoma	(152, 164–166)
Dlg1 ( <b>Dlg1</b> )	Absent vagina, No lateral fusion of the Mullerian ducts	Directly interacts with APC and PTEN; with Dlg3 and Dlg4 interacts with oncoprotein Net1; DLG paralogs targeted by human virus oncoproteins;	Dlg1 somatic mutations in breast cancer	(116, 166–168)
Dlg2 ( <b>Dlg2</b> )	Not known	Not known	Amplification in breast, prostate, ovarian, and lung cancer; mutations in melanoma, uterine, stomach, lung, stomach, colorectal, cholangiocarcinoma, bladder cancer	(164, 165)
Dlg3 ( <b>Dlg3</b> )	Not known	Associates with APC; cancer cell lines overexpression results in suppression of cell growth, cell migration, and invasion; interacts with oncoprotein Net1	Dlg3 is downregulated in gastric, esophageal, and glioblastoma; upregulated in serous ovarian carcinoma and breast cancer	(169–171)
Dlg4 ( <b>Dlg4</b> )	Not known	Interacts with oncoprotein Net1; degradation of Dlg4 by HPV	Deletion in prostate, pancreas, bladder, liver, colon, and lymphoma	(164, 165, 171, 172)
Dlg5 ( <b>Dlg5</b> )	Not known	Loss induces breast cancer cell migration and disruption of apicobasal polarity; Loss shows increases in Hippo signaling in breast cell lines	Genetic variant (R30Q) associated with inflammatory bowel disease and Crohn's disease; Dlg5 loss in prostate cancer; Dlg5 upregulated in gastric and pancreatic cancers	(164, 165, 173–175)
Lgl1 ( <b>Lgl1</b> )	Not known	Lgl1 KO mice have brain dysplasia and invasion	Loss of copy number correlates GBM poor survival; lost/downregulated in melanoma, prostate, breast, and colon cancers; Lgl1 loss correlates with	(117, 164, 165, 169)(117)

			advanced staging of colorectal cancer and melanoma	
Lig2 ( <b>LgI2</b> )	Not known	Mutations in zebrafish causes epidermal hyperproliferation	Decreased expression/mislocalization in gastric cancers; low levels correlated with colorectal cancer aggressiveness	(169, 176, 177)
Mpp5 ( <b>Pals1</b> )	Not known	Pals1 is necessary for cerebellar progenitor cell proliferation; Important for E-cadherin membrane trafficking in MDCK cells	Mutations in bladder, uterine, cholangiocarcinoma, colorectal, adenoid cystic carcinoma, melanoma; amplification of prostate esophagus, stomach, head & neck, ovarian, and sarcoma; deletions in adenoid cystic carcinoma	(164, 165, 178, 179)
Pard3 ( <b>Par3</b> )	Not known	Par3 KO in skin delays Ras-induced papillomas but predisposes skin to keratoacanthoma; Par3 KD increases metastasis in breast cancer	Downregulated in breast cancer and improper localization in metastatic disease; proper localization decreased in metastatic disease; Downregulated in ESCC & correlated with metastasis; Deletion in HNSCC and glioblastoma; Upregulated and associated with poor prognosis in hepatocellular carcinoma	(137, 180–183)
Pard6a/Pard6b/Pard6g ( <b>Par6</b> )	Not known	Par6 promoted proliferation of breast cancer cells; Establishes front to rear polarity; necessary for cancer cell invasion and cell:cell adhesion; Par6 phosphorylation induces E-cadherin reduction and TGF $\beta$ EMT in NSCLC cells	Par6 thought to be pro-tumorigenic in breast cancer; Par6 $\beta$ upregulated in breast cancer and associated with EMT characteristics; high Par6 in stromal cells correlates with better prognosis in NSCLC; high levels correlated with aggressive prostate cancers	(149, 150, 164, 165)
Patj ( <b>Patj</b> )	Not known	Targeted by viral oncoproteins for degradation	Mutations in melanoma, lung adenocarcinoma, head & neck cancer, cholangiocarcinoma	(164–166)
PRKCI ( <b>PKC<math>\iota</math></b> )	Not known	Promotes breast cancer cell metastasis; promotes tumor growth for glioblastoma cells; promotes Cholangiocarcinoma cell migration, metastasis and proliferation	Upregulated in NSCLC, colon cancer, ovarian cancer, esophageal squamous cell carcinoma (ESCC), breast cancer, hepatocellular carcinoma, basal cell skin cancer; correlated with poor survival in patients	(164, 165, 184–187)



PRKCZ ( <b>PKCζ</b> )	Not known	Suppresses IL6 decreasing cell proliferation in lung cancer model	Higher levels of PRCKZ or PRCKI correlate with delayed tumor recurrence in bladder cancer; Upregulated in hepatocellular carcinoma prostate cancer, bladder transition cell carcinoma, pancreatic ductal cancer, head and neck squamous cell carcinoma, and breast cancer; Correlates with poor survival in patients with non-GIST STSs; May play a role in breast cancer metastasis; Higher levels correlates with a better prognosis in colorectal cancer patients	(162, 164, 165, 185)
PTEN ( <b>PTEN</b> )	PTEN <sup>+/-</sup> mice have endometrial neoplasia; Conditional PTEN knockout in the endometrium causes endometrial cancer	PTEN <sup>+/-</sup> mice have neoplasia in many organs	Commonly lost tumor suppressor	(164, 165, 188)
Scrib ( <b>Scribble</b> )	Not known	Loss promotes prostate and lung cancer formation & progression; increased Scribble increases AKT signaling in breast cancer models	Reduced Scribble correlates with invasiveness in cervical cancer; increased Scribble increases; tumor suppressor in human cancers; amplified in many human cancers	(105, 164, 165)
Stk11 ( <b>Par4/Lkbi</b> )	LKB1 <sup>+/-</sup> mice develop endometrial adenocarcinomas; Conditional deletion of LKB1 in the uterus caused completion transformation of the endometrium and highly invasive and deadly endometrial cancer	LKB1 deficiency promotes breast cancer cell invasion; LKB1 loss activates TGF-β signaling angiogenesis; Loss of LKB1 expression and K-Ras activation resulted in melanoma formation; LKB1 loss increases CSCs; LKB1 tumor suppressor gene mutations cause autosomal dominant condition, Peutz-Jeghers	Implications in NSCLC, ovarian, uterine; amplified in pancreatic, NEPC, sarcoma, cholangiocarcinoma, ACC, MBL, Glioma, and GBM; mutated in lung, LUAD, cholangiocarcinoma, esophagus, bladder, HNC, pancreas, and stomach	(164, 165, 188–190)

**Table 3 Involvement of Cell Polarity Proteins in Cancer and the Uterus**

Par3 suppresses breast tumorigenesis through aPKC(138, 185). When Par3 is depleted *in vivo* with a mutated oncogene, such as Notch or Ras<sup>61L</sup>, there is an increase in metastatic disease caused by an increase in matrix metalloproteinase 9 (MMP9) which is important for degrading the extracellular matrix (ECM)(138). MMP expression has been associated with increased migration and invasion. MMP9 was upregulated through an increase in IL6 production stimulating Stat3 (Signal Transducer and Activator of Transcription 3) signaling(138). This was found to be caused by an overactivation of Pkcι that is normally controlled by Par3(185). Similarly in skin, Par3 loss (Par3eKO) caused a 70% increase in the number of mice with keratoacanthoma, a relatively rare tumor in mice(137). Intriguingly, in oncogenic Ras skin cancer mouse models, Par3eKO caused a delay in papilloma development and a reduction in tumor growth but caused a 12% increase in metastasis of the tumors that were observed(137). Since papilloma tumors originate from oncogenic Ras expression in keratinocytes while keratoacanthomas are thought to come from the basal and suprabasal layers of the epidermis, this study may show a tissue specific function of Par3 as either an oncogene or a tumor suppressor(137). In both cases, loss of Par3 seemed to stimulate invasion or migration of the cancer cells(137). In addition, clear cell renal cell carcinomas with overexpression of Par3 have been correlated with a lower survival rate, insinuating that Par3 may be an oncogene in renal carcinomas(191). Par3 has been directly tied to tumor progression which may be because Par3 interacts with many known tumor suppressors, such as PTEN (Phosphatase and Tensin homolog), as well as oncogenes(192, 193).

PTEN is most well-known for blocking PI3K (Phosphoinositide 3-Kinase) signaling by converting PIP<sub>3</sub> (Phosphatidylinositol (3,4,5)-triphosphate) to PIP<sub>2</sub> (Phosphatidylinositol (3,4,5)-diphosphate). PIP<sub>3</sub> is necessary for proper phosphorylation of AKT (Protein Kinase B), which leads to activation of the PI3K pathway. PTEN is a tumor suppressor that is deleted or mutated in a large number of cancer types including glioblastomas, breast, prostate, and endometrial(194–196). PTEN is also involved in cell polarity through the Par complex. A few studies have shown that PTEN and Par3 bind to each other and that PTEN can affect proper polarization of mammalian epithelium(130, 131). About 43% of all endometrial malignancies have PTEN mutations with more than 50% of the epithelial-specific tumors being mutated(196). Surprisingly though, 64% of all endometrial malignancies (75% of epithelial tumors) have PTEN protein loss indicating control of PTEN could be through post-translational mechanisms(196). While PTEN is mutated in a majority of endometrial cancer cases, polarity has not been thoroughly examined within the endometrium.

### **1.8 Apicobasal Polarity in the Endometrium**

The dynamic nature of the endometrium along with the two forms of tubulogenesis (Mullerian duct and endometrial gland), that occurs in uterine development imply that cell polarity is highly regulated within the endometrium. While, apicobasal polarity has not been examined in cycling mice, glycoproteins like Muc1 have been examined in great detail. Muc1 and other mucins are found at only the apical lumen of the luminal and glandular epithelium(197). This

insinuates some level of apicobasal polarity within the endometrial epithelium. During the estrous cycle, Muc1 heavily stains the apical lumen at the highest points of estrogen (estrus and proestrus) while the diestrus and metestrus stages have decreased staining corresponding with high levels of progesterone(197). It appears that proestrus has the most discrete apically localized Muc1(197). Since proestrus and estrus represent the most differentiated state, we can postulate that these states are when apicobasal polarity and cell adhesion are fully established. In addition, endometrial integrins are upregulated during the menstrual cycle in humans, where different phases show differing levels of integrins(198). This may suggest that different phases of the menstrual cycle require a more polarized endometrial epithelium. Since the endometrium is being shed (and reabsorbed during estrous), this may be from the reorganization of the polarity and adhesion complexes. Interestingly, integrins and Muc1 change expression and localization during blastocyst implantation as well(197). Implantation is where a majority of polarity related studies have been performed in the uterus. In general, to increase uterine receptivity there is a reduction in glycoproteins. This reduction in glycoproteins along with an increase in select integrins show that polarity is dynamically regulated within the endometrium(199).

Disrupting homeostasis in the endometrium is known for causing diseases like endometriosis or endometrial cancer. Homeostasis can be affected by disruptions in polarity or polarity regulating proteins like Ezrin(200). Ezrin is an ERM (Ezrin-Radixin-Moesin) family member that marks the apical surface and is

involved in cortical actin stability(201). An increase in Ezrin expression is observed in endometriosis, a disease in which endometrial tissue grows in aberrant locations throughout the body, including the ovaries, oviducts, and lining of the pelvis(202).

While no one has looked in depth at how apicobasal polarity affects endometrial gland development, *DLGH1*<sup>-/-</sup> mice were found to have aberrant Mullerian duct development that caused a loss of vaginal tissue and an endometrium that is more caudal within the uterus(116). Unfortunately, postnatal development of the uterus has not been examined in these mice. Scribble, the basal polarity protein, has also been shown to affect Mullerian duct formation including a loss of Sox9 expression and thinning of the Mullerian duct compared to wild-type mice at E13.5(157). A planar cell polarity protein, Vangl2, can also affect the localization of Scribble within the FRT(107). Planar cell polarity is the organization of specialized apical structures on cells across the tissue. The *Vangl2*<sup>lp</sup> mouse exhibits both a mislocalization of Scribble from the basolateral membrane but also shortened uterine horns(28). Interestingly, mice heterozygous for *Vangl2*<sup>lp</sup> generate a significantly reduced number of glands(28). Many of the secreted Wnt proteins that cause aglandular phenotypes when mutated are thought to be involved in planar cell polarity as well as canonical Wnt signaling. These studies with the *Vangl2*<sup>lp</sup> PCP mutant mice show that not all planar cell polarity proteins are involved in gland development similar to Wnt7a(35).

Since cell adhesion and cell polarity are intertwined analyzing the data from conditional deletion of cell adhesion genes in the uterus may hint at how apicobasal will affect endometrial gland development. When E-cadherin (*Cdh1<sup>lox/lox</sup>; PR-Cre*) or  $\beta$ -catenin (*Ctnnb1<sup>lox/lox</sup>; PR-Cre*), adherens junction proteins, are deleted in the mouse endometrium, an aglandular phenotype is observed(45, 46). However, in E-cadherin null endometrium, the luminal epithelium also looks abnormal and no longer is positive for the common luminal epithelium marker, cytokeratin 8(45). This suggests the possibility that glands are unable to form because the precursor luminal epithelium does not develop properly(45). In addition, the aglandular phenotype observed in  $\beta$ -catenin null mice suggests it is more likely canonical Wnt signaling that drives the aglandular phenotype(46). Understanding how cell adhesion and cell polarity are involved in endometrial development may aid us in determining how the different signaling pathways are utilized.

### 1.9 Cell Adhesion

Every tissue in the body utilizes cell adhesion in order to properly function and communicate with the neighboring cells and environment. Cell adhesion is especially well characterized in epithelium, however, it has also been examined in cardiomyocytes, endothelial, and Schwann cells(203–205). Epithelial cells have junctions at the interface with the extracellular matrix (ECM) and between neighboring cells. The adhesions that anchor the cell to the ECM include the focal adhesions and the hemidesmosomes. Focal adhesions are regulated by

Rho activity and contain numerous proteins including Focal Adhesion Kinase (FAK) and Vinculin(206, 207). Hemidesmosomes mediate the attachment of intermediate filaments to the cell membrane and are attached to the ECM through integrins. Hemidesmosomes are found in a selective number of tissues, specifically epithelial tissues, such as the mammary gland or skin.

On the lateral cell membrane, there are cellular junctions that attach the epithelial cells together. This includes tight junctions and adherens junctions in the apical domain as well as desmosomes. The desmosomes are similar to hemidesmosomes in that they anchor intracellular intermediate filaments to the membrane, however the proteins that compose the junctions are different. Desmosomes are made of desmogleins, desmocollins, and desmoplakins, while hemidesmosomes are composed of integrins(208). The adherens junction utilizes two cadherin molecules, one anchored to each cell, that can have either homophilic or heterophilic adhesion in the extracellular domain.  $\beta$ -catenin and p120 bind directly to the cadherins.  $\beta$ -catenin binding is necessary for proper actin binding through  $\alpha$ -catenin. These junctions are necessary for the initial cell:cell contact and play a role in stabilizing junctions (Figure 3d). There is a hierarchy to junction formation. Initially, adherens junctions are formed at the point of contact, then desmosomes, and finally tight junctions. Issues with proper ordering of junctions has been associated with different diseases like inflammatory bowel disease (IBD)(209–211). In addition, there is some evidence that adherens junctions have a role in different signaling pathways, which may contribute to diseases like IBD. The tight junctions are electrically resistant

junctions and necessary for proper barrier formation in most epithelium. Tight junctions are composed of multiple transmembrane and scaffolding proteins including claudins, occludin, and the zonula occludens (ZO) 1-3.

My work focuses on the apical junctions consisting of adherens junctions and tight junctions (Figure 3c). The apical junctions form as the epithelial cells organize and differentiate. Junctional maturation will then occur when the tight and adherens junction proteins form discrete and functional junctions (Figure 3d). These junctions are necessary for organs to properly work. Deletion of numerous genes encoding tight junction proteins exhibit surprising phenotypes. For example, ZO-1 deficiency is embryonic lethal for mice by E11.5 and was shown to have an angiogenesis defect that leads to an immature yolk sac(212). Interestingly, when ZO-1 is lost in the renal podocytes (*Tjp1<sup>lox/lox</sup>, Nphs1-Cre*) similar to the aPKC mutant mouse, podocyte tight junctions were unable to form properly(145, 213). Occludin null mice have normal tight junctions in both structure and function in the kidney. Thus we can conclude that Occludin (gene: OCLN) is not required for proper tight junction function in the kidney(214). *OCLN<sup>-/-</sup>* mice do exhibit aberrant branching of the gastric glands and male mutants were infertile(214). Interestingly, female Occludin null mice were fertile but could not suckle their pups(214). Claudins (gene: CLDN) are necessary for proper tight junction formation and when specific Claudins are overexpressed in fibroblasts, cells that normally do not have tight junctions, they form tight junction-like structures. *CLDN11<sup>-/-</sup>* mice no longer have tight junctions in multiple tissues, remarkably these mice are still viable(215). Similar to *OCLN<sup>-/-</sup>* mice the *CLDN11<sup>-/-</sup>*



males are sterile but the females breed similar to wild-type mice(215). *CLDN1*<sup>-/-</sup> mice have an inside-out barrier defect in the epidermis similar to the Par3eKO mice(135, 136).

Adherens junction proteins have been examined a with uterine specific Cre. A conditional  $\beta$ -catenin knockout mouse (*Ctnnb1*<sup>lox/lox</sup>; *PR-Cre*) has an endometrial aglandular phenotype that was previously discussed in section 1.8 Apicobasal Polarity in the Endometrium. *Ctnnb1*<sup>-/-</sup> mice are embryonic lethal during gastrulation where the ectodermal cell layer is unable to develop(216). *Cdh1*<sup>-/-</sup> mice are also embryonic lethal due to an inability to form a trophectodermal epithelium(217). In addition, a mutation in E-cadherin that disrupts Ca<sup>2+</sup> binding (*Cdh1*<sup>tm1Cbm/tm1Cbm</sup>) are embryonic lethal at a similar stage as the *Cdh1*<sup>-/-</sup>, potentially showing the lethality is due to loss of adherens junctions(218). Conditional loss of E-cadherin in the uterus (*Cdh1*<sup>lox/lox</sup>; *PR-Cre*) causes an aglandular phenotype that was previously mentioned in section 1.8 Apicobasal Polarity in the Endometrium(45). *Cdh1*<sup>lox/lox</sup>; *PR-Cre* mice do not show histological signs of columnar epithelium by P10(45). In addition, these mutants showed a loss of  $\beta$ -catenin,  $\alpha$ -catenin, and tight junction proteins(45). This loss of normal adhesion structures within the epithelium is hypothesized to be the cause of the abnormal epithelial architecture(45). The inherent connection between cell polarity and cell:cell adhesion in regulating uterine development and disease would indicate that how this connection is modulated would be important in the uterus. Curiously, female mice heterozygous for the tumor suppressor Merlin, which has been shown to coordinate apicobasal polarity and adhesion, have

small litters, but why these mice have reduced litter sizes is not known(219).

Understanding the role of Merlin in the uterus will help to comprehend how polarity and adhesion coordinate regulation of uterine homeostasis.

### 1.10 Merlin

Merlin is a tumor suppressor protein that was originally discovered as the gene (*NF2*) mutated in Neurofibromatosis Type 2(220, 221). Merlin is a scaffolding protein that links a multitude of other proteins causing it to have a wide-variety of functions (Table 4). It is well known for being a negative regulator of Hippo signaling in the mammalian brain and liver (Figure 2d)(222, 223). In addition, Merlin is necessary for proper junctional maturation and apicobasal polarity establishment in epithelial tissues(122). Merlin is a member of the Ezrin-Radixin-Moesin (ERM) family, but unlike the other ERM family members, Merlin is missing the C-terminal actin binding site. Ezrin, Radixin, and Moesin are hypothesized to have overlapping functions in different epithelial tissues. However, Merlin has been shown to have distinct roles. While initially discovered in *NF2*-associated central nervous system tumors, Merlin has been found to affect the development and homeostasis of different mammalian epithelial tissues(122, 224, 225). Merlin has a such a wide-variety of functions (Table 4), it is pertinent to understand how it affects the female uteri.

*Nf2*<sup>-/-</sup> mice are embryonic lethal by E8.0 because they are unable to induce mesodermal differentiation during gastrulation(226). In addition, conditionally knocking out Merlin in specific tissues causes aberrant tissue

Phenotype	Model	Reference
Hyperproliferation of the eye epithelial cells	<i>Drosophila</i> Mer	(227)
Embryonic lethality caused by loss of extraembryonic structures	Mouse Model ( <i>Nf2</i> <sup>-/-</sup> )	(226)
Increased metastatic disease; Decreased female fertility	Mouse Model ( <i>Nf2</i> <sup>+/-</sup> )	(219)
Loss of contact inhibition and mislocalization of β-catenin; Unstable adherens junctions; increased pEGFR; inability for Merlin to associate with EGFR through NHE-RF1 (normally confluency dependent)	<i>Nf2</i> <sup>-/-</sup> MEFs	(228, 229)
Both: Loss of sperm; Testicular atrophy; Increase in Lymphomas, chronic hepatitis, and invasive kidney adenocarcinoma; <i>Nf2</i> -isoform 2 <sup>-/-</sup> specifically caused delayed sensory reactions, signs of axonal neuropathy, irregularly shaped axons	Mouse models <i>Nf2</i> -isoform 1 <sup>-/-</sup> ; <i>Nf2</i> -isoform 2 <sup>-/-</sup>	(230, 231)
Increased internalization of EGFR at confluence; Increased mechanical tension and myosin II activity	Liver-derived epithelial cells from <i>Nf2</i> <sup>-/-</sup> livers; Caco2 cells with shNf2	(232)
Expansion of liver progenitor cells; increased risk of cholangiocellular & hepatocellular carcinoma	Mouse Model ( <i>Nf2</i> <sup>lox/lox</sup> ; <i>Alb-Cre</i> )	(224)
Fiber cells overproliferate and do not differentiate properly; Mislocalization of ZO-1; Multilayering of lens cells with an extracellular matrix.	Mouse Model ( <i>Nf2</i> <sup>lox/lox</sup> ; <i>Le-Cre</i> )	(233)
Decrease in nerve regeneration; Delayed motor and sensory recovery	Mouse Model ( <i>Nf2</i> <sup>lox/lox</sup> ; <i>Nefh-Cre</i> )	(234)
Schwann cell hyperplasia and tumors; cataracts and cerebral calcifications	Mouse Model ( <i>Nf2</i> <sup>lox/lox</sup> ; <i>PO-Cre</i> )	(235)
Schwann cell hyperplasia and tumors; cataracts and cerebral calcifications	Mouse Model (P0-Sch-Δ(39-121), overexpression)	(236)
Renal intratubular neoplasia at 3 months, hyperproliferative and invasive renal carcinoma by 10 months induced by aberrant EGFR signaling, inability to stabilize apical junctions	Mouse Model ( <i>Nf2</i> <sup>lox/lox</sup> ; <i>Vil-Cre</i> ) ( <i>Nf2</i> <sup>lox/lox</sup> ; <i>Mx1-Cre</i> )	(225)
Required for proper apical junction maturation; Necessary for proper apicobasal polarity establishment; Inside-out barrier defect; Disorganization and stratification defects of epidermis	Mouse Model and Primary Keratinocytes ( <i>Nf2</i> <sup>lox/lox</sup> ; <i>K14-Cre</i> )	(122)
Mislocalization of Ezrin; misoriented spindles; Multi-lumen 3D cultures; aberrant centrosome localization	shRNA-Nf2 in Caco2 cells; Mouse models ( <i>Nf2</i> <sup>lox/lox</sup> ; <i>K14-Cre</i> , <i>Nf2</i> <sup>lox/lox</sup> ; <i>Vil-CreERT2</i> ,	(237)

Loss of hair follicle planar cell polarity; Improper development of the bulge stem cell; Decrease in Sox9 expression	Mouse Model ( <i>Nf2<sup>lox/lox</sup></i> ; <i>K14-Cre</i> )	(238)
--	--	-------

**Table 4 Functions of Merlin in different tissues**

morphogenesis and homeostasis. In the liver, when Merlin is lost (*Nf2<sup>lox/lox</sup>; Alb-Cre* hereafter referred to as Nf2LKO), it causes an overgrowth of the liver oval cells (OCs), without causing any phenotypes in the hepatocytes and this was shown to be caused by an overactivation of EGFR signaling(224). Nf2LKO mice also exhibit hepatocellular carcinoma and cholangiocarcinoma if they survive to adulthood(224). Interestingly, while OCs were determined to be the source of the tumors, different labs observe EGFR or Hippo signaling as the main cause of tumorigenesis(223, 224). The tumorigenic properties of Merlin have been observed in other mutants as well. *Nf2<sup>+/-</sup>* mice have a high frequency of osteosarcomas as well as a higher number of hepatocellular carcinomas that metastasize(219). This was different than humans, who are hemizygous for Nf2, that commonly get vestibular schwannomas(239). Merlin loss in the kidney (*Nf2<sup>lox/lox</sup>; Vil-Cre*) causes invasive renal carcinomas by 6 months of age(225). These tumors had a decrease in junction and polarity markers similar to affects observed in the skin(122, 225). In the skin, Merlin was determined to be necessary for proper recruitment of Par3 to the primitive apical junction before junctional maturation(122). Loss of Merlin in the basal cells of the epidermis (*Nf2<sup>lox/lox</sup>; K14-Cre* hereafter referred to as Nf2skinKO) causes an inside-out barrier defect like other cell adhesion and polarity mutant mice(122, 135, 136). Nf2skinKO mice also exhibit abnormal skin morphology from aberrant asymmetric divisions of the basal cells(122). Merlin deficiency in Schwann cells produces a loss of contact inhibition which is instigated by increases in canonical Wnt signaling(240). Merlin inhibition of canonical Wnt signaling is also observed

in pancreatic cancer cell lines(53). However, it appears that how Merlin affects Wnt signaling is tissue dependent (Figure 2c)(53, 241–243). Merlin is involved in many signaling pathways because of the proteins it is able to bind to and indirectly regulate. A Merlin binding partner, NHE-RF (Na<sup>+</sup>/H<sup>+</sup> Exchanger Regulatory Factor), is found to localize to the apical lumen of the endometrium at specific times during the menstrual cycle and is hypothesized to be important in estrogen signaling and proliferation(244). Merlin has been found to affect the localization of the membrane-bound receptor, Notch, in *Drosophila*(80). In addition, Notch signaling has been shown to be regulated during the menstrual cycle(245). Merlin may play an important role in endometrial development and homeostasis through the different proteins and pathways it interacts with(80, 122, 246, 247).

### 1.11 Dissertation Summary

This dissertation examines how Merlin and apicobasal polarity affect endometrial development and endometrial cancer. We find that Merlin is necessary for proper endometrial gland formation. In addition, Merlin may be important in Mullerian duct polarized migration. We determined that conditional loss of Merlin within the endometrium causes a mislocalization of polarity proteins and infertility through changes in F-actin that may facilitate the decrease observed in Wnt signaling. Furthermore, Merlin is necessary for proper endometrial homeostasis during aging. In addition, we have established that apicobasal polarity is lost in endometrial cancer and polarity loss causes changes

in compartmentalization of the membrane-receptor, Notch. Finally, we observed that Notch signaling plays a role in polarity induced proliferation and migration changes in endometrial cancer cell lines.

## Chapter 2: Materials & Methods

This chapter is modified from Williams, E., Villar-Prados, A., Broaddus, R., Gladden, A. (2017) Loss of polarity alters proliferation and differentiation in low-grade endometrial cancers by disrupting Notch signaling. PLoS ONE 12 (12): e0189081. <https://doi.org/10.1371/journal.pone.0189081> is licensed under CC BY (Creative Commons Attribution license) by PLoS One.

### 2.1 Mouse Strains

We generated both the  $Nf2^{lox/lox}; Wnt7a-Cre$  and the  $Nf2^{lox/lox}; PR-Cre$  mouse lines by crossing the previously generated  $Nf2^{lox/lox}$  mice with either  $Wnt7a-Cre$  mice or  $PR-Cre$  mice(248–250). When crossing, Cre was paternally contributed and control mice were either  $Nf2^{lox/lox}$ ,  $Nf2^{lox/wt}$ ; -Cre as heterozygous deletion showed no phenotype in the uterus. Mice were maintained on a mixed FVB, C57BL/6 background. The MD Anderson Cancer Center Institutional Animal Care and Use Committee (IACUC) approved all animal procedures. Mice were bred to generate homozygous female mutants.

#### 2.11 Fecundity Study

Six wild-type ( $Nf2^{lox/lox}$ ,  $Nf2^{lox/wt}$ ;  $PR-Cre$ ,  $Nf2^{lox/wt}$ ;  $Wnt7a-Cre$ ) and 6  $Nf2^{lox/lox}$ ;  $PR-Cre$  mice were mated for 3 months. Mice were examined for plugs every morning. After mice were plugged, weight was taken at E0.5 and then again at E7.5 until mice were at E14.5.  $Nf2^{lox/lox}$ ;  $PR-Cre$  mice did plug but did not gain weight while wild-type mice would start to increase in weight around E7.5. Females were left with males during the entire 3 months and litters were counted



for number of pups. 3.5 DPC uteri were obtained from mice, 3 days after vaginal plugs were observed.

## 2.2 Immunohistochemistry

Use of human tissues was approved by the IRB of the University of Texas MD Anderson Cancer Center (LAB1-718) (PI: Broaddus). Informed written consent was obtained through the MD Anderson Cancer Center “Front Door” tissue banking consent policy (LAB03-0320). All authors received training on working with and the ethics of human specimen research from MD Anderson Cancer Center. De-identified primary human endometrial tissue samples were obtained from the tissue bio-specimen and pathology core facility at MD Anderson Cancer Center. Frozen endometrial tissue sections were immediately fixed in 4% paraformaldehyde/PBS for 20 minutes at room temperature. Samples were permeabilized using 0.5% Triton in PBS for 15 minutes at room temperature and then blocked for 30 minutes in blocking buffer containing 10% fetal bovine serum (FBS) and 1% bovine serum albumin (BSA) diluted in PBS-0.01% Tween 20 (PBST). Sections were subsequently incubated with the following primary antibodies: Par3 (1:500, rabbit, Millipore, 07-330), Ezrin (1:500, mouse, Invitrogen, 3C12), E-cadherin (1:1000, mouse, BD, 610182), Acetylated Tubulin (1:1000, mouse, Sigma, T6793), ZO-1 (1:500, rabbit, Invitrogen, 61-7300), Notch1 (1:500, rabbit, Cell signaling, D1E11), Notch2 (1:750, rabbit, Cell signaling, D76A6), Pan Cytokeratin (1:500, rabbit, Abcam, PA5-21985), c-Myc (1:250, mouse, Santa Cruz, sc-40), and Pericentrin (1:1000, rabbit, Abcam,

ab4448) overnight at 4°C. Slides were then washed three times in PBST and incubated with secondary antibodies CY3 Rabbit (1:200, Jackson ImmunoResearch), Alexa 488 Mouse (1:200, Jackson ImmunoResearch), Phalloidin CY5 (1:250, Invitrogen), and 4'6'-diamidino-2-phenylindole (DAPI, 1:1000). Slides were washed two times in PBST, one time in PBS and mounted with Vectashield (Vector Laboratories).

Staining of MDCK 3D cultures was adapted from previous descriptions (237, 251), briefly, cultures were fixed in 3.7% Formalin in cytoskeletal buffer (10mM 2-(N-morpholino)-ethanesulfonic acid sodium salt (MES) pH 6.1, 138 mM KCl, 3mM MgCl<sub>2</sub>, 2mM EGTA) for 20 minutes at room temperature. Washed in PBS and then permeabilized in 0.5% Triton/PBS for 20 minutes at room temperature. Cultures were then washed in PBS and subsequently washed with 100mM Glycine/PBS for 15 minutes, 3 times. Cultures were blocked for 1 hour in PBST/0.2% Triton/1% BSA/10% FBS and then left overnight at room temperature with primary antibodies in blocking buffer. The MDCK cell culture was washed in PBST 3 times for 20 minutes and then incubated in blocking buffer with secondary antibodies for 1 hour at room temperature.

All mouse tissue was fixed in either 3.7% Formalin or 4% PFA in PBS. Tissue was then either processed for paraffin-embedding (McCormick Scientific) or OCT-embedding (Fischer Healthcare). H&E staining: Paraffin-embedded samples were heated to 55°C for 20 minutes. Samples were incubated in histoclear (3x) for 10 minutes each. Samples were progressively hydrated in (100% (x2), 95% (x2), and 70% EtOH) ethanol and then deionized water for 22

minutes. Samples were stained with Harris Hematoxylin modified (StatLab) for 7 minutes followed by washing in EtOH Acid (1% HCl in 70% EtOH) and bluing in 0.1% Sodium Bicarbonate. Samples were stained with 0.5% eosin Y (Sigma Aldrich) for 5 seconds before being washed in 4x 100% EtOH. Samples were incubated in Hlستoclear (3x, 10 minutes) before being mounted with Permount (Fischer). BrdU and Foxa2 staining: All mice were pulsed with BrdU (100 $\mu$ g per gram of body weight) for 2 hours before being sacrificed. OCT-embedded samples were thawed and dried for 10 minutes. Samples were then washed in PBS 2x for 30 minutes each and permeabilized in 0.5% Triton/PBS for 20 minutes at room temperature. Samples were then washed in PBS, 3 times before incubated in 1.5N HCl in PBS for 10 minutes. Slides were washed three times in PBS. Samples were blocked for 1 hour in PBST/10% FBS and then left overnight at room temperature with primary antibodies (BrdU [1:200, mouse, abcam, ab6326]; Cleaved Caspase 3 [1:400, rabbit, Cell Signaling, Asp175] or Par3 [1:500, rabbit, Millipore, 07-330], FoxA2 [1:2000, rat, Seven Hills BioReagents, WRAB-1200],  $\beta$ -catenin [1:1000, mouse, BD, 610153]) in blocking buffer. The mouse tissue samples were washed in PBST 3 times for 20 minutes and then incubated in blocking buffer with secondary antibodies for 1 hour at room temperature. Other immunofluorescent stainings: OCT-embedded samples were thawed and dried for 10 minutes. Samples were then hydrated in PBS 2x for 30 minutes each and permeabilized in 0.5% Triton/PBS for 20 minutes at room temperature. Samples were then washed in PBS. Samples were blocked for 1 hour in PBST/10% FBS/1% BSA and then left overnight at room

temperature with primary antibodies (Sox9 [1:250, rabbit, Santa Cruz, sc-20095]; E-cadherin [1:1000, mouse, BD, 610182], Par3 [1:500, rabbit, Millipore, 07-330], ZO-1 [1:500, rabbit, Invitrogen, 61-7300], Muc1 [1:100, rabbit, Dan Carson's Laboratory(252)], Foxa2 [1:2000, rat, Seven Hills BioReagents, WRAB-1200], Vinculin [1:300, mouse, Millipore, MAB3574], Myosin IIB [1:500, rabbit, Biologend, 909901], Rho [1:100, mouse, Santa Cruz, sc-418], pMLC [1:500, rabbit, abcam, ab2480],  $\beta$ -catenin [1:1000, mouse, BD, 610153], Merlin [1:100, rabbit, Santa Cruz, sc-331], P-cadherin [1:200, rat, Takara, M109], Yap [1:300, mouse, Cell Signaling, 4912]) in blocking buffer. The mouse tissue samples were washed in PBST 3 times for 20 minutes and then incubated in blocking buffer with secondary antibodies, smooth muscle actin-Cy3 (1:200, mouse, Sigma, C6198, SMA), or Phalloidin Cy3 (1:200, Invitrogen, A12380) for 1 hour at room temperature. All samples were mounted with Fluoromount-G (Southern Biotech, 0100-01). All tissue samples and cells labeled were visualized using a Nikon A1 laser scanning confocal microscope.

### 2.3 Cell culture and reagents

Madin-Darby Canine Kidney (MDCK) cell lines and endometrial cancer cell lines were cultured in Dulbecco's Modified Eagle's Medium (DMEM) with 10% fetal bovine serum (FBS). Generation of knockdown MDCK cell lines is described below. Knockdown MDCK cells were selected for with puromycin (0.7 $\mu$ g/mL). Re-expression cell lines were selected for with hygromycin (3 $\mu$ g/mL). The  $\gamma$ -secretase inhibitor DAPT (Sigma) was placed on cells at a concentration

of 1 µg/ml in new media added with fresh DAPT every 24 hours for 48 hours for BRDU and expression experiments and up to 72 hours for migration experiments. Primary endometrial epithelial cells was isolated by a protocol adapted from *Eritja et al*(253). Cells were isolated at P60 from *Nf2<sup>lox/lox</sup>* females and kept in DMEM/F12 (Sigma, D8062) supplemented with 1% antibiotics/antimycotics (Sigma, A5965) and 1mmol/L HEPES (Corning cellgro, 25-060-CI). Ad5CMVCre-eGFP (Adenovirus cre) was added at 80-90% confluency at a concentration of 100 MOI/cell. Cells were incubated for 24 hours in adenovirus cre before media was changed. Cells were fixed within 72 hours.

### **2.31 3D culture assay**

MDCK 3D cyst formation was modified from previously described work(254). In short, an 8-well chamber slide was pre-coated with a collagen mixture (24µM Glutamine, 2.35mg/mL NaHCO<sub>3</sub>, 1x MEM, 20mM HEPES, 2mg/mL Collagen I). MDCK cells were suspended in the same collagen mixture at a concentration of 3x10<sup>4</sup>. DMEM with 10% FBS was added 45 minutes after placing the chamber slide in the 37°C incubator. The DMEM media was changed every 2-3 days without disturbing the matrix/cell layer.

### **2.32 Generation of knockdown MDCK cell lines**

Virus was produced by transfecting HEK293T cells at 80-90% confluency with the pLK0.1 lentiviral expression vector obtained from Open biosystems (Par3 kd clone ID: TRCN0000118134 and Ezrin kd clone ID: TRCN0000062462, Table 5), Scr-shRNA and Nf2 kd shRNA in the pLK0.1 vector obtained from the McClatchey lab (Table 5)(255). In addition, packaging vectors (VSVG and ΔVPR)

were utilized. MDCK cells were infected with the virus and polybrene (1µg/mL) in DMEM with 10% FBS. The following day, new media was added with puromycin (0.7µg/mL) for selection. Knockdown was verified by Western blots.

### 2.33 Generation of primary knockout endometrial cell lines

Adenovirus cre was utilized to infect *Nf2<sup>lox/lox</sup>* endometrial epithelium. Endometrial cells were infected with the virus in DMEM with 10% FBS. The following day, new media was added. Knockout was verified by PCR.

### 2.34 Generation of overexpression endometrial cancer cell lines

The day before the transfection, cells were plated at  $2 \times 10^5$  on each well of a 6-well dish. Par3-myc was transfected in when the cells reached 50-70% confluency using Lipofectamine LTX (Invitrogen) and Plus Reagent (Invitrogen). The Par3-myc construct was a gift from Iam Macara (Addgene plasmid #19388) and has been previously described(256). 24 hours post-transfection, fresh media was put on cells. Cells were fixed 48 hours after original transfection.

## 2.4 Quantitative RT-PCR

For Human Endometrial Tissue Samples: The qRT-PCR was performed as indicated by *Schlumbrecht et al*(257). For MDCK cells, endometrial cancer cells, and isolated endometrium: RNA was extracted by treating cells or tissue with Trizol and chloroform. RNA was purified with 100% isopropanol and 75% ethanol. RNA pellets were dissolved in 30-50µL of DEPC water at 55°C. RNA purity was confirmed by nanodrop to have a A260/A280 ratio greater than 1.8. cDNA was synthesized using a SuperScript First-Strand Synthesis kit. The cDNA was analyzed using SYBR green quantification with the 7900HT Sequence

<b>Name</b>	<b>Sequence</b>
Par3 kd 8134	5'-ATCATAAGATTTGTCGATGGC-3'
Par3 kd 8135	5'-TATCATAAGATTTGTCGATGG-3'
Ezrin kd	5'-TTTATTATCCACATAGTGGAG-3'
Nf2 kd	5'-GAGGAAGCAACCCAAGACGTT-3'
Scr-shRNA	5'-CAGTCGCGTTTGCGACTGG-3'

Table 5 shRNA oligos for MDCK cells and endometrial cancer cell lines.

Detection System (Applied Systems). Primers used are found in the table, (Table 6). Samples were assayed in triplicate. Data were normalized to HPRT. Samples below the limit of quantification were not included. The fold change of the  $\Delta\text{CT}$  compared to HPRT was utilized for analysis ( $2^{-\Delta\text{CT}}$ ). For Isolated Endometrium: Uteri were extracted and placed in Trizol. Samples were frozen until genotyping was complete. Tissue was broken up using a cryogenic mortar and pestle. A similar protocol to MDCK cells was utilized to isolate RNA and run qRT-PCR.

## 2.5 Cell extract preparation and Western blotting

For Western blots, cells were scraped off culture dishes and suspended in Triton lysis buffer (1% Triton X-100, 50mM Tris-HCl pH 7.4, 140mM NaCl, 1mM EDTA, 1mM EGTA, 1mM PMSF, 1mM Na<sub>3</sub>VO<sub>4</sub>, 1mM sodium fluoride, 1mM  $\beta$ -glycerophosphate, 10 $\mu$ g/mL aprotinin, 10 $\mu$ g/mL leupeptin) followed by sonication. Cell lysates were then centrifugation and the debris was removed. Bradford assays were used to quantify the amount of proteins. Cell lysates (30 $\mu$ g) were loaded onto SDS-PAGE gels and transferred to a PVDF membrane. Membrane blots blocked for at least 1 hour in 5% milk in TBST. Primary antibody was added overnight at 4°C. Primary antibodies include: (1:500, rabbit, Cell signaling, D1E11), Notch2 (1:750, rabbit, Cell signaling, D76A6), Par3 (1:750, rabbit, Millipore, 07-330), Ezrin (1:1000, mouse, Invitrogen, 3C12), Notch1 PTEN (1:1000, rabbit, Cell Signaling, 138G6), Merlin (1:400, rabbit, Santa Cruz, sc-332) and  $\beta$ -tubulin (1:1000, Sigma/Santa Cruz, T7816/sc-9104). Secondary antibodies



Name	F/R	Sequence
$\beta$ Actin	F R	5'-CTAAGGCCAACCGTGAAAAG-3' 3'-ACCAGAGGCATACAGGGACA-5'
GAPDH	F R	CCCTTCATTGACCTCAACTACA ATGACAAGCTTCCCGTTCTC
HPRT	F R	AGCTTGCTGGTGAAAAGGAC TTATAGTCAAGGGCATATCC
h-HPRT	F R	TTCTGTGGCCATCTGCTTAG GTTTAGGAATGCAGCAACTGAC
Notch1 -1	F R	CAGCCCTTGTCTCCAGAATG TTGGCACCGTTCTTACAGG
Notch1 -2	F R	GGATGGCATCAATAGCTTCATG CCAGGGTCACAGTCACATTTG
Notch2 -1	F R	TCGGGATAGCTATGAGCCCT GGCATGTTGCTTTCCCAAC
Notch2 -2	F R	ATTCATGCAGGTTAGAGAAGGAC CTGTCTGAGAGCTCAGTGACCTTA
Notch3 -1	F R	ATCAACCGCTATGACTGTGTC TCCATTTTCCCATCCACG
Notch3 -2	F R	GCTGCGAAACTGATGTCAAC GCTACTCTGACACTCATCCATG
Notch4 -1	F R	AGTAACCCCTCAAACACAGC ACAAATCCACACCCATCACC
Notch4 -2	F R	GGTAAACCCATGTGAGTCCAG AGTTCTGTCCATTGTAGCCTG
JAG1 -1	F R	GAAAGTGCCCAGAGCCTAAA CAGGACAGCTGAAGAACTGAA
JAG1 -2	F R	GAACCTGATTGCGAGCTACTAC GGTGGACAGATACAGCGATAAC
JAG2 -1	F R	GGACGCCAATGAATGTGAAG CGGGATGCAGAGACAGTAATAG
JAG2 -2	F R	ACCTGATTGGTGGCTATTACTG CTGCCCATGACAGTCGTTTA
DLL1 -1	F	CCGATGACCTCACAAACAGAAA

	R	CACACGAAGCGGTAGGAATAC
DLL1 -2	F	GCAGATCAAGAACACCAACAAG
	R	GTCCAAAGGACAGCAAGA
DLL3 -1	F	GAATCACCTGAAGATGGAGAC
	R	GCTCCAAAGGACAGCAAGA
DLL3 -2	F	CGGATGGACCTTGCTTCAAT
	R	ACAGTTGGAGCCTTGGAAATC
DLL4 -1	F	GCTCAAGAACACAAACCAGAAG
	R	GGCCAGATTATAGTCCAATGT
DLL4 -2	F	TCCACTGGCATCTGTGTTTC
	R	CCTCCTCTCTCCTCTGATTT
P21 -1	F	CATCCTGGCCTGTAAGTT
	R	CTTGCCCTTCAGAGGCTTATAG
P21 -2	F	AGCTGAACAAGGAGTCAGATG
	R	CAGGGCCAGAAGAGACAATAA
HeyL -1	F	AGTTGATCTTGGGTTCACTCTC
	R	ACCAGAAAGGCTTGGGAATAG
HeyL -2	F	GTTCTTCATCCAGGGAGCTCTAAA
	R	GAGGAAGATGCCTTCACAGATAG
Hey1 -1	F	GCTATGGACTATCGGAGTTTGG
	R	CTGGGAGGCGTAGTTGTTAAG
Hey1 -2	F	GCCCGATATCTGAGCATCATT
	R	CGTAGTTGTTAAGGTGGGAGAC
Hey2 -1	F	GCGGCGAGATCGGATAAATAA
	R	TGATCTACCGTCATTTGCAGTAT
Hey2 -2	F	AACATCTCAGATTATGGCAAGAAAG
	R	CCAGTCGTCTCAACTCAGATAAA
Hes6 -1	F	AAAGCGCGCCTAGACAAA
	R	CCGTCTGGTCTTGTAAGTTGAT
Hes6 -2	F	CCAACACCTGTCGCTCTT
	R	CTTGTAAGTTGATGCCCATGAC
Ccnd1 -1	F	GCCCTCCGTATCTTACTTCAAG
	R	GCGGTCCAGGTAGTTCATG
Ccnd1 -2	F	CATCTACACTGACAACTCTATCCG
	R	TCTGGCATTGTTGGAGAGGAAG
Myc -1	F	GCTGTTTGAAGGCTGGATTC

	R	GATGAAATAGGGCTGTACGGAG
Myc -2	F	CGATTCCACGGCCTTCTC
	R	TCTTCCTCATCTTCTTGCTCTTC
Sox9 -1	F	CAAGACTCTGGGCAAGCTC
	R	GGGCTGGTACTTGTAATCGG
Sox9 -2	F	GCCGACTCCCCACATTC
	R	CGCTTCAGATCAACTTTGCC
Sox17 -1	F	CGATGAACGCCTTTATGGTG
	R	TTCTCTGCCAAGGTCAACG
Sox17 -2	F	AATATGGCCCACTCACACTG
	R	TTTCTCTGTCTTCCCTGTCTTG
Wnt7a -1	F	ACGAGTGTGAGTTTCAGTTCC
	R	AATCGCATAGGTGAAGGCAG
Wnt7a -2	F	TTACACAATAACGAGGCGGG
	R	TTGTCCTTGAGCACGTAGC
Hoxa11 -1	F	AGGAGAAGGAGCGACGG
	R	GGTATTTGGTATAAGGGCAGCG
Hoxa11 -2	F	CTAAACTAGCATCCCTACCCTG
	R	ATCAGTTCTTGCCTCTTCCG
Birc2	F	GAAGAAAATGCTGACCCTACAGA
	R	GCTCATCATGACGACATCTTTC
Birc3	F	AGAGAGGAGCAGATGGAGCA
	R	TTTGTTCTTCCGGATTAGTGC
CTGF	F	GGGCCTCTTCTGCGATTC
	R	ATCCAGGCAAGTGCATTGGTA
Merlin -1	F	CTCCTGCATACCTGCATATCTC
	R	CTAAGCCAGTCCCACTTCTAC
Merlin -2	F	CAGGGAAGAGAAGGCTAGAAAG
	R	ATTGGGTTTCATGGGTGGATAG

Table 6 qRT-PCR primers for MDCK cells, endometrial cancer cells, and isolated endometrium

were put on the next day for at least 30 minutes. Protein expression was depicted using enhanced chemiluminescence on a LiCor machine.

## **2.6 Image processing, analysis, and densitometry**

All tissue samples and cells were visualized using a Nikon A1 laser scanning confocal microscope or a Nikon 80i upright Fluorescent Microscope. Images were processed using the Nikon-Elements software (Nikon). Quantitative analysis of endometrial tumor samples was performed blind by an independent investigator. Quantitative analysis of the mouse tissue including myometrium, cell adhesion angles, BrdU, and Cleaved Caspase 3 (CC3) calculations was performed utilizing ImageJ. Line intensity plots (Phalloidin, pMLC, [Vinculin, Myosin IIB], Sox9, [P-cadherin, E-cadherin], Muc1, and FoxA2 were also performed on ImageJ analysis. Densitometry was performed by Image Studios Version 3.1 using the data from the LiCor machine.

## **2.7 Statistics**

The quantitative data in this dissertation was analyzed utilizing either two-tailed Student's t-test or ANOVA. Data that was found to be significant was marked with some form of an asterisk and discussed in figure legends. Data was considered significant if  $P < 0.05$ .

## Chapter 3: Merlin regulates endometrial gland development through polarized signals.

### 3.1 Introduction

Female infertility is a complex problem that is still not well understood. In the United States, 17% of women need infertility assistance(258, 259). In a multitude of animal models the endometrium has been found to be a common cause of impaired fertility, specifically when endometrial glands are lost. The endometrium is composed of stromal cells that surround the luminal and glandular epithelium. The luminal epithelium, the epithelium surrounding the uterine cavity, gives rise to glandular epithelium that invaginates into the stroma after birth. The glandular epithelium is hypothesized to secrete mucins to protect the uterus from infection and histrophs to facilitate proper uterine and blastocyst response during pregnancy(197, 260).

Endometrial glands are observed in mouse models to be necessary for protein secretion correlated with successful implantation as well as a source of nutrients as the placenta is generated(17, 18, 261). Data examining fertile and infertile women demonstrated that increased plasma levels of Interleukin 1 $\beta$  and Tumor Necrosis Factor were predictive of a successful implant in women undergoing *in vitro* fertilization(262, 263). Examining how the endometrial glands form may lead to a better understanding of how female infertility arises and can be potentially treated.

Endometrial glands are formed through a process called tubulogenesis that occurs postnatally in both mice and humans. There are many methods of tubulogenesis that have previously been reviewed but endometrial glands are thought to go through a budding process(264). At postnatal day 0 (P0) in mice the endometrium has only the central lumen of epithelial cells. Beginning at P5, small invaginations begin to form off the main luminal epithelium and buds start to develop at P7(265). At P8 a portion of the buds begin to extend and form structures resembling teardrops(19). At P11, elongation of the initial buds and teardrops begin to rotate forming a more complex, spiral shape gland by P21(19). Following the onset of puberty around P60, a gland will consist of branched structures coming off of a main stem (Figure 1d)(20). Development of the endometrial gland involves both Wnt and Notch signaling, however, what how these pathways regulate elongation or branching is still not known. There are many genes that have been associated with gland formation through information obtained from different mouse models manipulating genes including FoxA2,  $\beta$ -catenin, and Notch1 (Table 1)(21, 26, 46). While the molecular mechanisms underlying endometrial gland development have begun to be examined, there are still many unanswered questions that could help us understand both endometrial gland formation and infertility.

Endometrial gland formation takes a collaboration between cell adhesion and apicobasal polarity to properly form glandular architecture. Without proper cell adhesion, the epithelium would not hold together to form the discrete structures as is shown when E-cadherin is deleted from the endometrium(45).

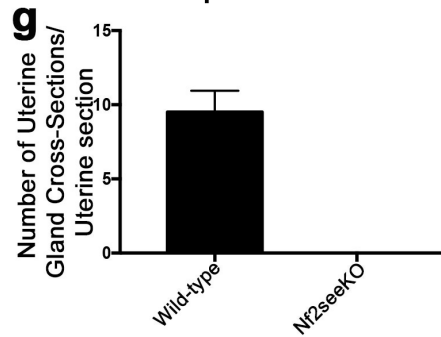
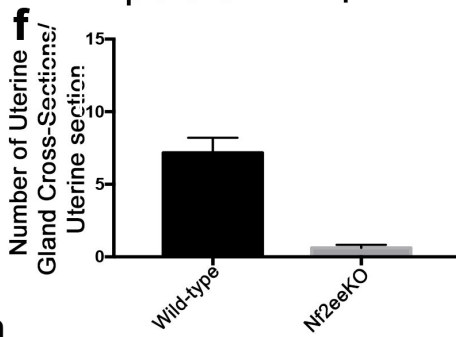
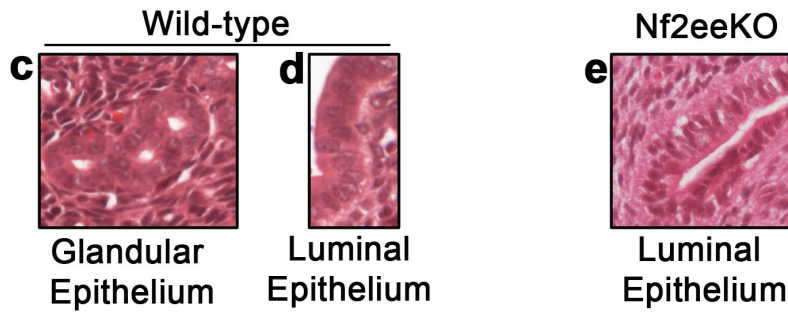
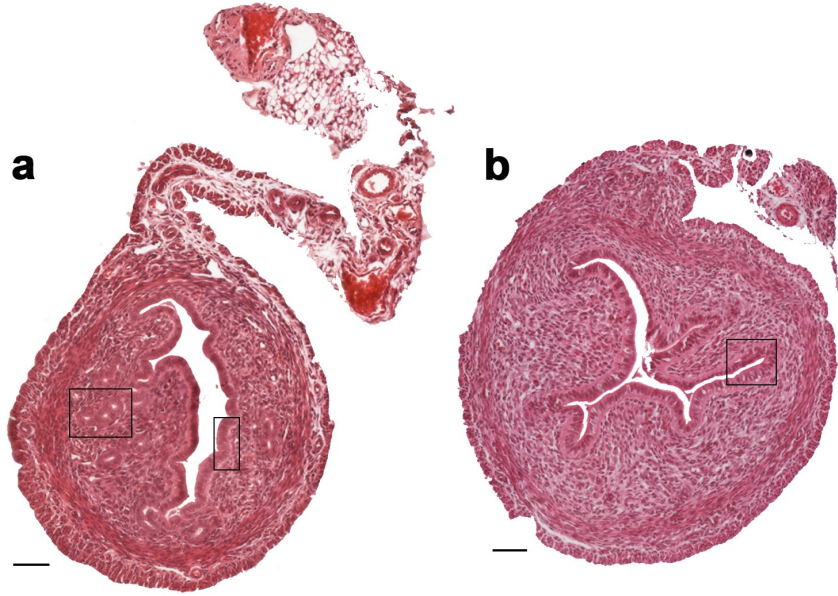
Without cell polarity, polarized migration and cell adhesion do not properly function. In order to understand how apicobasal polarity and cell adhesion are involved in endometrial gland formation, we examine a protein that is known to couple proper apical junction maturation and polarity establishment, Merlin. Originally discovered for its role in Neurofibromatosis Type 2, a benign tumor disease, it has since been shown *in vivo* to be important for the development and homeostasis of epithelial tissues including the skin, kidney, and liver(122, 224, 225). *Nf2*<sup>+/+</sup> mice were found to be sub-fertile however why these mice have reduced fertility is not known(219). Utilizing endometrium specific Merlin knockout mice, we were able to determine the role of Merlin during endometrial development and how it may lead to infertility.

## 3.2 Results

### 3.21 Merlin deletion causes loss of gland formation and female infertility.

Conditional loss of Merlin in endometrial epithelium (*Nf2*<sup>lox/lox</sup>; *Wnt7a*-cre; *Nf2*eeKO) or in the endometrial epithelium and stroma (*Nf2*<sup>lox/lox</sup>; *PR*-cre; *Nf2*seeKO) causes a loss of endometrial glands before puberty at P21 and is not due to a delay in gland formation as no glands are observed during estrus at P60 (Figure 4a-e, not shown). Wild-type mice at P21 have an average of 8-10 endometrial gland cross sections per uterine section, while Merlin null mice have less than one (Figure 4f-g).

Since endometrial glands are necessary for proper female fertility, we examined whether fertility was intact. We performed a fecundity study over 3



**h**

	# of Mice	# of Litters	# of Pups	Mean Litter/Mouse	Mean # of Pups /Litter
Wild-type	6	17	116	3	7
Nf2seeKO	6	0	0	0	NA

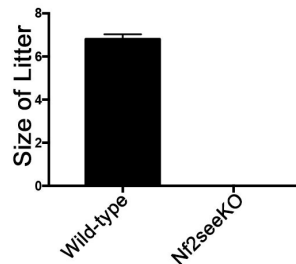
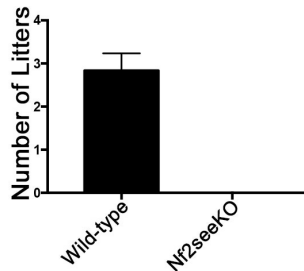




**Figure 4 Merlin loss in the endometrium causes a loss of glands.**

Wild-type (a) and *Nf2<sup>lox/lox</sup>; Wnt7a-Cre* (Nf2eeKO, b) H&E staining show the loss of glands on the Nf2eeKO uteri. Magnification of the wild-type (c) glandular epithelium, (d) luminal epithelium and the Nf2eeKO (e) luminal epithelium. Quantifications of the number of glands observed in a cross-section of wild-type and Nf2eeKO mice (f, n=13) or wild-type and *Nf2<sup>lox/lox</sup>; PR-Cre* mice (Nf2seeKO, g, n=3). A table summarizing the data obtained from a 3-month fecundity study with the Nf2seeKO mice (h). Quantifications of the number of litters a single mouse had (i) or the average number of pups per litter (j) within the fecundity study.

months where 6 *Nf2seeKO* mutants and 6 wild-type female mice were mated to wild-type male mice. The 6 wild-type mice on average had 3 litters with 7 pups per litter, while the *Nf2seeKO* mice did not have any litters (Figure 4h-j).

Vaginal plugs were observed in the *Nf2seeKO* mice similar to wild-type littermates suggesting mating and estrus is normal in the female mice. Weight was examined after plugs were observed. Wild-type mice showed increases in weight around E7.5. *Nf2seeKO* mice never gained weight during the normal gestation period of 19 days. This suggests that the pregnancy is lost before E7.5 and that *Nf2* mutant female mice are infertile.

In addition to fertility, endometrial glands have distinct markers from the luminal epithelium. Previous studies have shown that wild-type endometrial glands have nuclear Sox9 staining and we observe similar results that is quantitated by a line plot (Figure 5a, g, white line denotes line quantitation)(22). We also examined nuclear Sox9 in *Nf2eeKO* and *Nf2seeKO* endometrial epithelium and found the luminal epithelium had a similar intensity of Sox9 as the wild-type luminal epithelium (Figure 5a-c, g). Additionally, another endometrial gland marker, FoxA2(21), was not found in the majority of *Nf2eeKO* or *Nf2seeKO* endometrial epithelium, while the wild-type mice had intense FoxA2 nuclear staining in the glandular epithelium (Figure 5i-m). The *Nf2eeKO* and *Nf2seeKO* luminal epithelium did exhibit some nuclear FoxA2 at discrete locations, specifically near curves in the luminal epithelium (Figure 5k-l) that had a similar intensity to the glandular epithelium of the wild-type tissue (Figure 5i, k, l, n). A

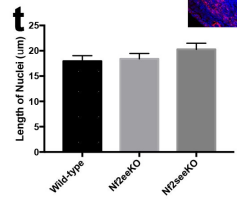
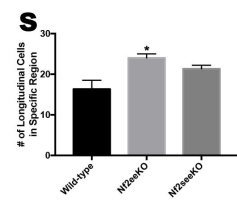
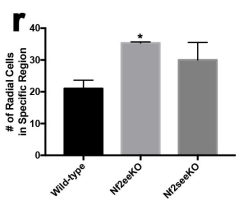
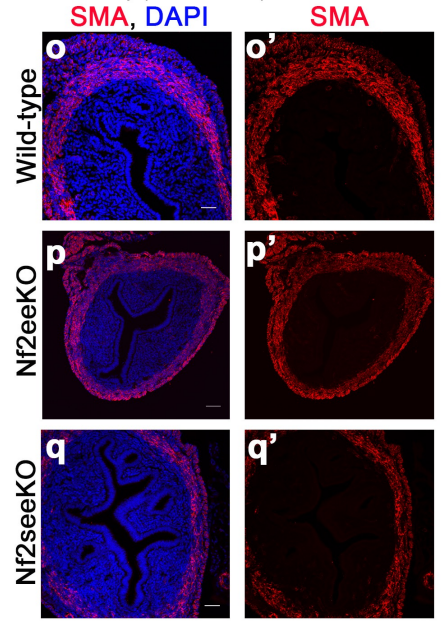
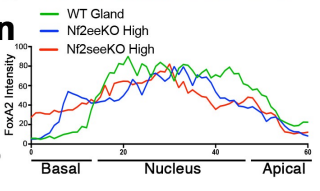
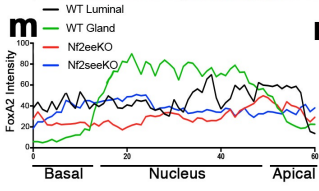
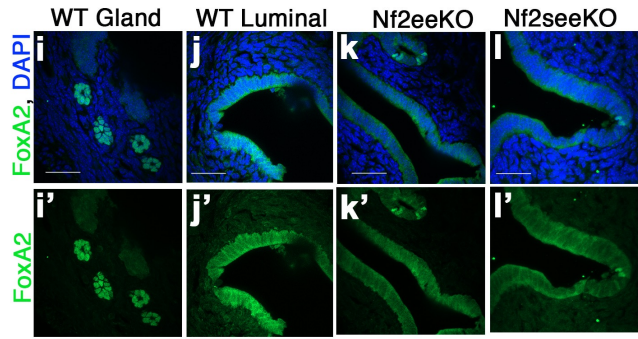
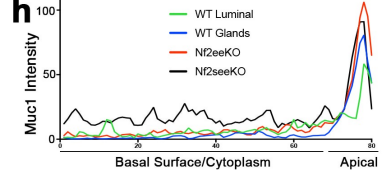
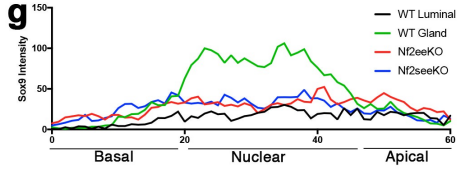
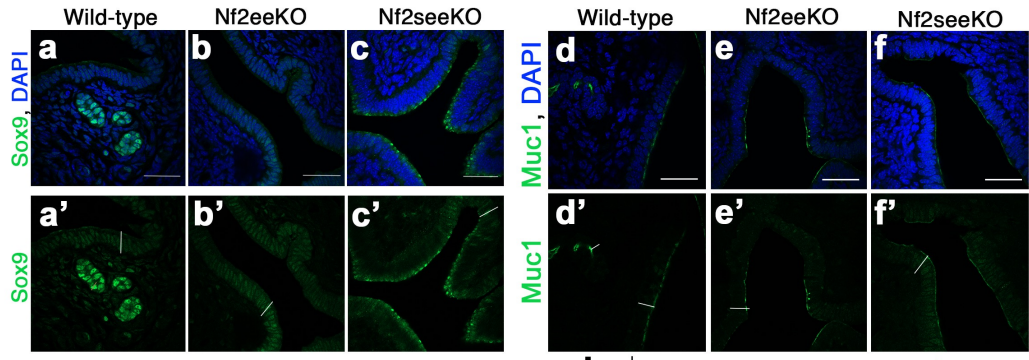


**Figure 5 Endometrial Gland Markers within the Nf2eeKO and Nf2seeKO mice at P21.**

Sox9 was examined in wild-type (**a, a'**), Nf2eeKO (**b, b'**), and Nf2seeKO (**c, c'**) mice. Muc1 was examined in wild-type (**d, d'**), Nf2eeKO (**e, e'**), and Nf2seeKO (**f, f'**) mice. The line intensity of Sox9 in wild-type glandular epithelium, as well as, wild-type, Nf2eeKO, and Nf2seeKO luminal epithelium compared, the left area of the line represents the basal boundary of the cell (**g**). The line intensity of Muc1 staining in wild-type glandular and luminal epithelium compared to Nf2eeKO and Nf2seeKO luminal Muc1 staining (**h**). FoxA2 staining in wild-type endometrial glands (**i, i'**), wild-type (**j, j'**), Nf2eeKO (**k, k'**), and Nf2seeKO (**l, l'**) luminal epithelium. Line plots of FoxA2 intensity in wild-type glandular epithelium compared to wild-type, Nf2eeKO, and Nf2seeKO luminal epithelial cell (**m**), left region of line plot is the basal boundary of the cell. Line intensity of FoxA2 in wild-type endometrial glands compared to Nf2eeKO and Nf2seeKO luminal epithelium (**n**). Immunofluorescence images of SMA (smooth muscle actin) in wild-type (**o, o'**), Nf2eeKO (**p, p'**) and Nf2seeKO (**q, q'**) uteri. Quantification of the density of the outer radial myometrium (n=3, **r**). Quantification of the density of the inner longitudinal myometrium (n=3, **s**). Quantification of the length of longitudinal nuclei (n=3, **t**). \*P<0.05

similar phenotype was observed with Sox9 in some samples of Nf2eeKO and Nf2seeKO luminal epithelium though not as consistent (not shown). Endometrial glands are hypothesized to secrete more mucins than the endometrial luminal epithelium. Thus, we were interested if Muc1 decreased in the endometrium of our Nf2 mutant mice. We observed that the wild-type mice exhibited a higher intensity of Muc1 staining in the glandular epithelium than in the luminal epithelium (Figure 5d, h). Compared to wild-type luminal epithelial cells, Nf2seeKO and Nf2eeKO luminal epithelium showed increased Muc1 staining on portions of the epithelium (Figure 5d-f, h). Interestingly, these Nf2eeKO and Nf2seeKO luminal Muc1 stainings, were a similar intensity as the glandular staining of the wild-type mice (Figure 5h). These increases in glandular markers provide evidence that the mutant luminal epithelium is capable of differentiating into glandular epithelium but is unable to assemble the glandular architecture.

The endometrium is known to be necessary for proper myometrium development(266). Given the alterations in glandular architecture in the Nf2-deficient endometrium, we were interested in how the myometrium was affected in the Nf2eeKO and Nf2seeKO uteri. To examine the myometrium, we stained for smooth muscle using SMA (smooth muscle actin) and found that at P21, the longitudinal and radial SMA populations look relatively similar between the wild-type and mutant mice (Figure 5o-q). When examined closely, we determine the number of nuclei increased in the outer, radial myometrium compared to wild-type mice (Figure 5r). Similarly, the inner, longitudinal cells showed a slight

increase in nuclei density compared to the wild-type myometrium (Figure 5s). In both myometrial cell types the Nf2eeKO mice showed the highest density of cells compared to the wild-type or Nf2seeKO mice. To understand if the change in density was caused by a difference in nuclei size, we measured the length of the longitudinal myometrial nuclei and did not observe a substantial difference (Figure 5t).

### **3.22 Apicobasal polarity and junction condensation is lost in Merlin-deficient tissue**

Since there was an obvious change in histology in the Nf2eeKO and Nf2seeKO mice, we wanted to examine whether cell polarity and cell:cell adhesion were altered. We first verified that Merlin was disrupted in our mutant endometrium (Figure 6a). Endometrial tissue was isolated from wild-type or Nf2-deficient mice and analyzed by PCR to determine if Cre mediated recombination had occurred. Using three separate PCR primer sets we established whether the uterine tissue was heterozygous or homozygous for the Nf2 targeted allele. In addition, we verified the presence of Cre and deletion of Exon 2 following Cre-mediated recombination. We found that Exon 2 had been recombined in tissue expressing Cre indicating deletion of Merlin (Figure 6a). Since Merlin has previously been shown to disrupt apicobasal polarity, specifically the Par complex, we examined the localization of Par3 in Merlin null endometrial tissue(122). While Par3 localizes to the apical surface of the luminal and

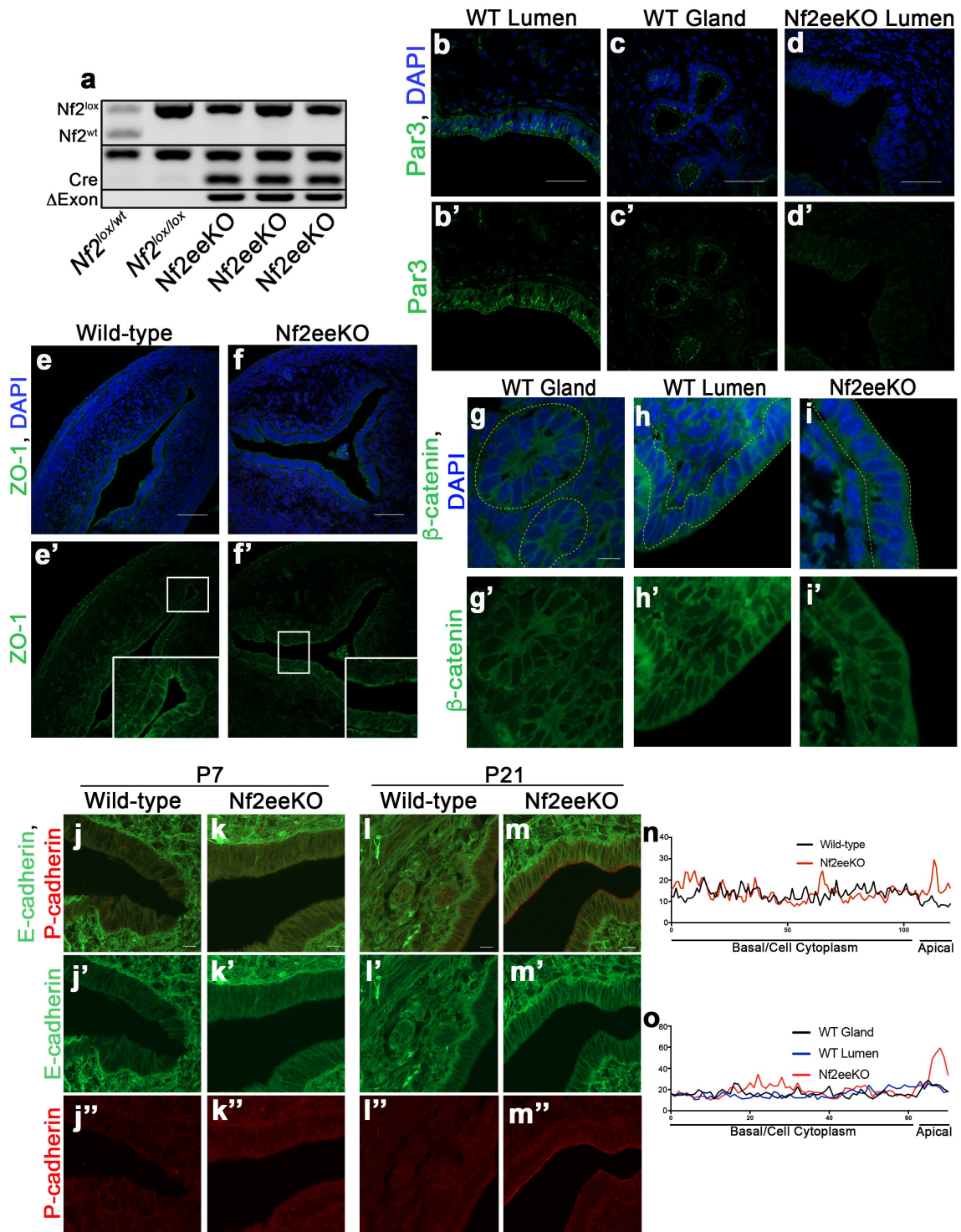


**Figure 6 Merlin loss causes disruption of apicobasal polarity without altering apical junctions.**

Merlin loss was examined by PCR for recombination of the targeted *Nf2* allele (**a**). Par3 staining in wild-type luminal epithelium (**b**) and glandular epithelium (**c**) show apical localization in wild-type, however *Nf2<sup>ee</sup>KO* luminal epithelium (**d**) has diffuse staining. ZO-1 staining in wild-type (**e, e'**) and *Nf2<sup>ee</sup>KO* (**f, f'**) show minimal changes to the apical localization.  $\beta$ -catenin staining in wild-type glands (**g, g'**), wild-type luminal epithelium (**h, h'**), and *Nf2<sup>ee</sup>KO* luminal epithelium (**i, i'**) show no changes. Yellow dotted line signifies the epithelial tissue. Staining of E-cadherin and P-cadherin in wild-type (**j, l**) and *Nf2<sup>ee</sup>KO* (**k, m**) mice at P7 (**j-k**) and P21 (**l-m**) show an increased luminal staining of P-cadherin and minimal changes to E-cadherin at P21. Line intensity graphs of co-localization of wild-type and *Nf2<sup>ee</sup>KO* (**n-o**) show an increase of P-cadherin at the apical lumen at both P7 (**n**) and P21 (**o**).



glandular epithelium in wild-type mice (Figure 6b-c), there is loss of Par3 at the apical surface in the Nf2-deficient luminal epithelium (Figure 6d). This suggests apicobasal polarity is disrupted similar to what has been observed in other epithelial tissues(122).

Additionally, since Merlin is critical in junctional maturation, we were interested in whether apical junction proteins like ZO-1,  $\beta$ -catenin, and E-cadherin were mislocalized. ZO-1 was examined by immunofluorescence and found to still localize to the apical junctions (Figure 6e-f).

This was surprising since in other Merlin-deficient epithelial tissues ZO-1 localizes to the cytoplasm(122). Proper localization of ZO-1 can indicate that tight junctions are able to form, however, it does not address whether the junctions are fully functional. Additionally,  $\beta$ -catenin, an adherens junction protein, was examined for proper localization to the apical junctions. Nf2eeKO mice had similar localization of  $\beta$ -catenin to the luminal epithelial membrane as wild-type littermates on the endometrial luminal and glandular epithelium (Figure 6g-i). E-cadherin was also examined in Nf2eeKO mice compared to wild-type mice. E-cadherin appeared relatively similar between wild-type and mutant mice (Figure 6j'-m'). There was some intense punctate E-Cadherin staining noted in a subset of the Nf2eeKO mice, not observed in wild-type littermates (not shown). Thus, the majority of proteins in adherens junctions appear to localize properly.

Interestingly, P-cadherin is another cadherin that is known to be expressed within the endometrium(267–269). P-cadherin is involved in mammary

tubulogenesis where it is expressed on the cap cells in terminal end buds(270). Bazellières et al. showed that P-cadherin and E-cadherin can play different roles in mechanical stress and cellular tension(271). E-cadherin has been shown to strengthen the cell adhesions, while P-cadherin regulates the intercellular tension(271). Thus, we decided to examine P-cadherin in the pre-cycling uterus. In wild-type uteri, P-cadherin is dispersed throughout the membrane of the epithelium, while in the Nf2eeKO mice, P-cadherin localizes to the apical lumen (Figure 6j"-m"). This P-cadherin apical localization occurs early during gland development at P7 (Figure 1d, Figure 6j"-k") and intensifies over time observable at P21 (Figure 6l"-m").

### **3.23 Proliferation decreases and tension increases in Merlin-deficient tissue**

In order to determine why the correct endometrial gland architecture did not form, endometrial tissue was examined at an earlier stage of gland formation e.g. P7 (Figure 1d). Gland formation has been examined in a multitude of tissues, however the exact mechanism by which the endometrium forms glands is not completely understood. In order for the buds to form and then go through tubulogenesis, any combination of proliferation and apoptosis may cause the cellular changes necessary for gland formation. Additionally, since changes in P-cadherin were observed (Figure 6j"-m"), local changes in cell:cell and cell:matrix tension likely play a role in the elongation of the gland structure. Proliferation was examined following a 2-hour pulse of BrdU. In Nf2eeKO mice, there was a

decrease in BrdU incorporation in both the epithelium and the stroma (Figure 7a-b). The epithelium and the stroma showed about a 5% decrease in BrdU incorporation (Figure 7e-f). This suggests there is a small decrease in cellular proliferation in the endometrium due to Merlin loss in the epithelium. In addition to proliferation, we examined apoptosis using the apoptotic marker cleaved caspase 3 (CC3). CC3 levels were low in both wild-type and Nf2eeKO mice and no significant difference was observed (Figure 7c-d, g).

Besides examining proliferation and apoptosis, we were interested in how tension was affected in the Nf2eeKO endometrium since P-cadherin localization changed. Co-localization of Vinculin and Myosin IIB (myoIIB) indicates an increase in cellular tension. When epithelium have low amounts of tension at cell:cell contacts in particular at the adherens junctions, this causes  $\alpha$ -catenin to form a tertiary structure decreasing the association of actin, myoIIB, and Vinculin to the adherens junction(272). When  $\alpha$ -catenin is under tension then myoIIB and Vinculin are able to associate with the junctional complex(272). In addition, Vinculin is stabilized at Focal Adhesions (FAs) on the basal membrane as actin-myosin related tensionincreases(273, 274). Thus, co-localization of Vinculin and myoIIB can indicate cell:cell and cell:ECM contacts are under tension.

Examination of wild-type endometrium shows little to no co-localization of Vinculin and myoIIB except in small sections at the basal membrane of the luminal epithelium (Figure 8a). The Nf2eeKO mice however, had co-localization of Vinculin and myoIIB across a majority of the basal membrane of the luminal epithelium (Figure 8b). The co-localization was more intense in Nf2eeKO

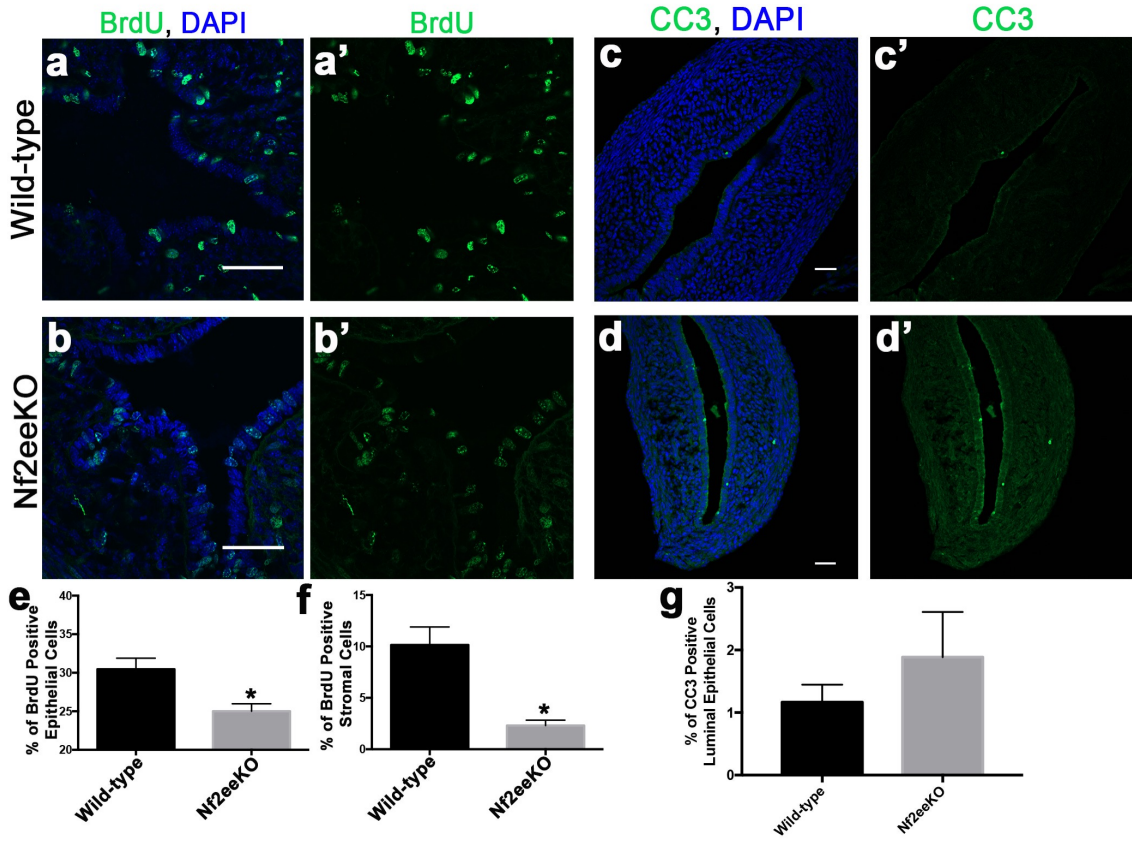


### **Figure 7 Proliferation and Apoptosis within the developing endometrium.**

BrdU staining, signifying the amount of proliferation in wild-type (**a, a'**) and Nf2eeKO (**b, b'**) endometrial epithelium and stroma. Cleaved Caspase 3 (CC3) showing the amount of apoptosis in the wild-type (**c, c'**) and Nf2eeKO (**d, d'**) endometrial epithelium. Quantification of the amount of BrdU positive cells within the luminal epithelium (**e**) and endometrial stroma (**f**). Percent of cells that have CC3 in the luminal epithelium of wild-type versus Nf2eeKO mice (**g**). \*  $P < 0.05$

endometrium compared to any co-localization observed in the wild-type endometrium (Figure 8a-b, e). In addition, pMLC (phospho-Myosin Light Chain) is known to indicate areas of high cellular tension. ROCK (Rho-associated protein kinase) phosphorylates MLC which causes myosin ATPase to activate actin(275). We observed an increase in the intensity of pMLC at the basal membrane in Nf2eeKO mice compared to wild-type mice (Figure 8c-d). A comparison of line plots showed a large increase of pMLC on the basal membrane of Nf2eeKO endometrium compared to wild-type endometrium (Figure 8f).

To examine tissue tension in a morphological manner, we utilized the cellFIT program that generates mathematical equations and common assumptions to map differing areas of tension within a cell sheet(276). Unfortunately, cellFIT was not able to obtain true cell measurements in uterine tissue sections resulting in inconsistent readouts even on the same image. While we continued to examine other mathematical modeling systems, we found a majority of systems are not designed for *in vivo* tissue, but rather cell culture(277). Cell culture based modeling systems have found that utilizing the angle of cell:cell and cell:ECM interactions can help determine where high vs. low tension is located (Figure 8h)(277). Using this strategy, we measured the cell:cell and cell:ECM angles, in wild-type samples (n=3) and determined the wild-type cell:cell: angles are obtuse, while a majority of the mutant (n=3) cell:cell angles are acute suggesting that the mutant cells are compressing their apical surface (Figure 8g). In addition, the cell:ECM interactions showed

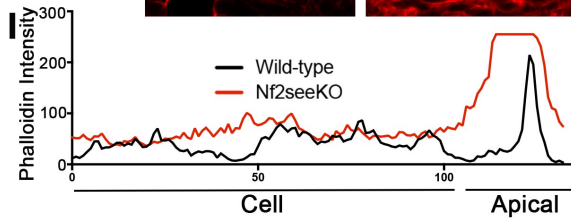
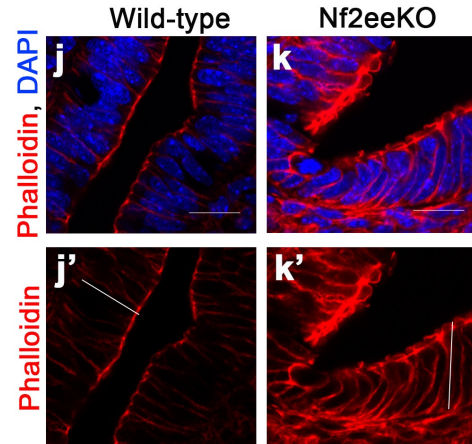
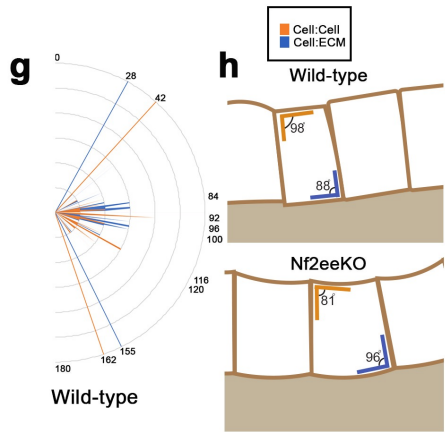
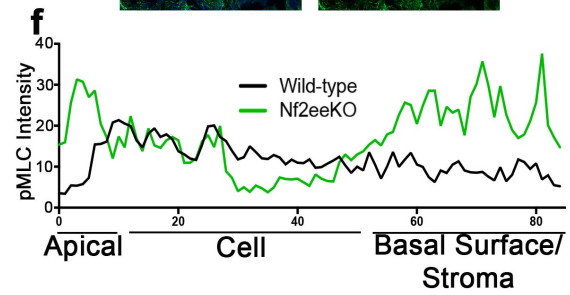
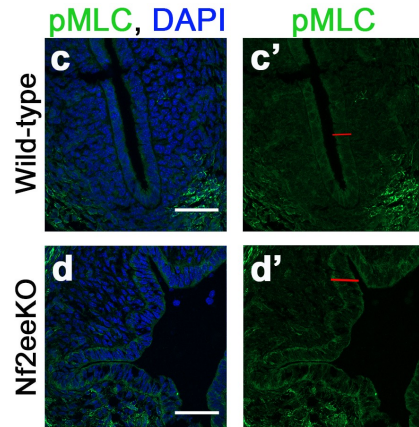
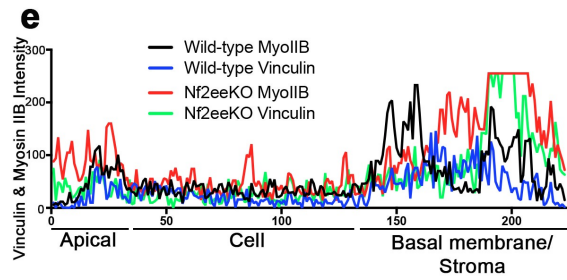
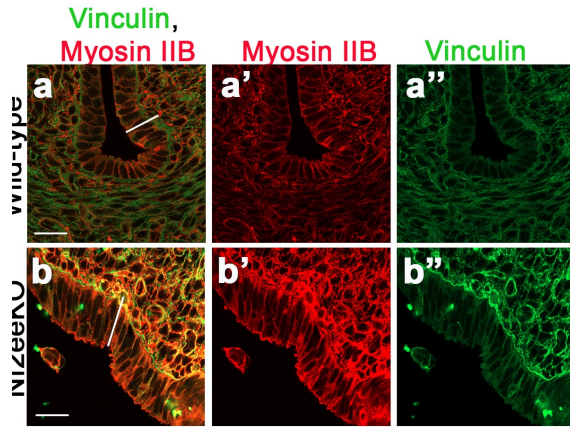


**Figure 8 Increases in tension at the basal membrane corresponds to an increase in F-actin at the apical membrane in Nf2eeKO mice.**

Wild-type (a) and Nf2eeKO (b) endometrium show differing co-localizations of Myosin IIB (a'-b') and Vinculin (a''-b''). pMLC is increased at the basal membrane of Nf2eeKO (d, d') versus wild-type (c, c') luminal epithelium. Comparison of the intensity of Myosin IIB and Vinculin in wild-type and Nf2eeKO uteri (e). Quantification of pMLC intensity in wild-type versus Nf2eeKO uteri (f). Quantification of the angles observed between the extracellular matrix and the basal membrane (Cell:ECM) or apical junctions (Cell:Cell) of the luminal epithelium in wild-type (g-h, Cell:ECM median=88°, Cell:Cell median=98°) and Nf2eeKO (h-l, Cell:ECM median=96°, Cell:Cell median=81°) mice. Phalloidin staining of F-actin in wild-type (j, j') and Nf2eeKO (k, k') endometriums (j-k). Comparison of the line intensity of Phalloidin at the apical surface of wild-type and Nf2eeKO mice from (j-k) images (l). White lines denote where line intensity was measured (j', k').



obtuse angles in the mutant mice compared to acute angles in the wild-type mice (Figure 8g, i).

In order for this switch of cell interaction angles to occur, we hypothesized that mutant endometrium is under increased tension. Additionally, because of the direction of the angle changes, we postulated that this could be from increased apical constriction producing a contractile actin ring on the apical surface of the mutant endometrial epithelium. To examine whether an actin ring was present, we stained endometrial tissue with Phalloidin, an F-actin dye, and found that Nf2eeKO tissue has more intense Phalloidin staining around the apical lumen than the wild-type endometrium (Figure 8j-l). This indicates the potential changes in tension observed at the basal membrane may be from apical constriction pulling the cells in a manner where they are unable to form a glandular structure.

### **3.24 Wnt signaling is downregulated in Merlin mutants**

In order to understand what signaling pathways may be involved in the lack of adenogenesis, we examined pathways known to be regulated by Merlin including the Hippo and  $\beta$ -catenin signaling pathways. Merlin is well known for the tissue specific role it can play as a positive regulator of Hippo signaling in *Drosophila* and in mammalian brain and liver(223, 278). Hippo signaling is inactive when YAP (Yes-associated protein) or Taz (transcriptional co-activator with PDZ-binding motif) translocates into the nucleus and interacts with transcription factors like TEAD (TEA domain-containing transcription factor

family) proteins to increase target gene expression (Figure 2d). A kinase complex made up of MST1/2 (Mammalian Ste20 Kinases 1/2), Sav (Salvador), MOBKL A/B (Mps One Binder Kinase activator-like A/B), and Lats1/2 (Large Tumor Suppressor 1/2) phosphorylate YAP sequestering it to the cytoplasm where it is degraded(54). Wild-type and Nf2eeKO mice at either P7 or P21 showed no nuclear Yap staining, suggesting that Hippo signaling is not increased in the Merlin-knockout uterus (Figure 9b-e). We confirmed the staining with embryonic osteoblasts in cartilage primordium where nuclear YAP staining has been previously shown (Figure 9a)(279). To confirm these results, we examined YAP downstream targets BIRC3 (Baculoviral IAP repeat containing 3) and CTGF (Connective tissue growth factor) by qRT-PCR in uteri isolated from Nf2eeKO female mice at P7. While CTGF did not show a significant change between wild-type and Nf2eeKO mice (Figure 9f), BIRC3 did show an increase in expression suggesting some targets of YAP may be increased (Figure 9f).

Numerous observations indicate that Wnt signaling is involved in endometrial gland development so we also examined Wnt signaling regulators and downstream targets (Figure 9g-l). We noticed a slight increase in Axin1 and Axin2 (Figure 9g). In addition, we observed an increase in Ccnd1 expression, though Ccnd1 is downstream of multiple pathways that may be affected in Nf2eeKO mice (Figure 9l). Furthermore, Wnt7a expression increased in the Nf2eeKO uterus at P7, but Wnt7a has been implicated as a ligand utilized in the planar cell polarity pathway, potentially indicating planar cell polarity is being affected in the Nf2eeKO mice (Figure 9k). Myc, a common Wnt downstream

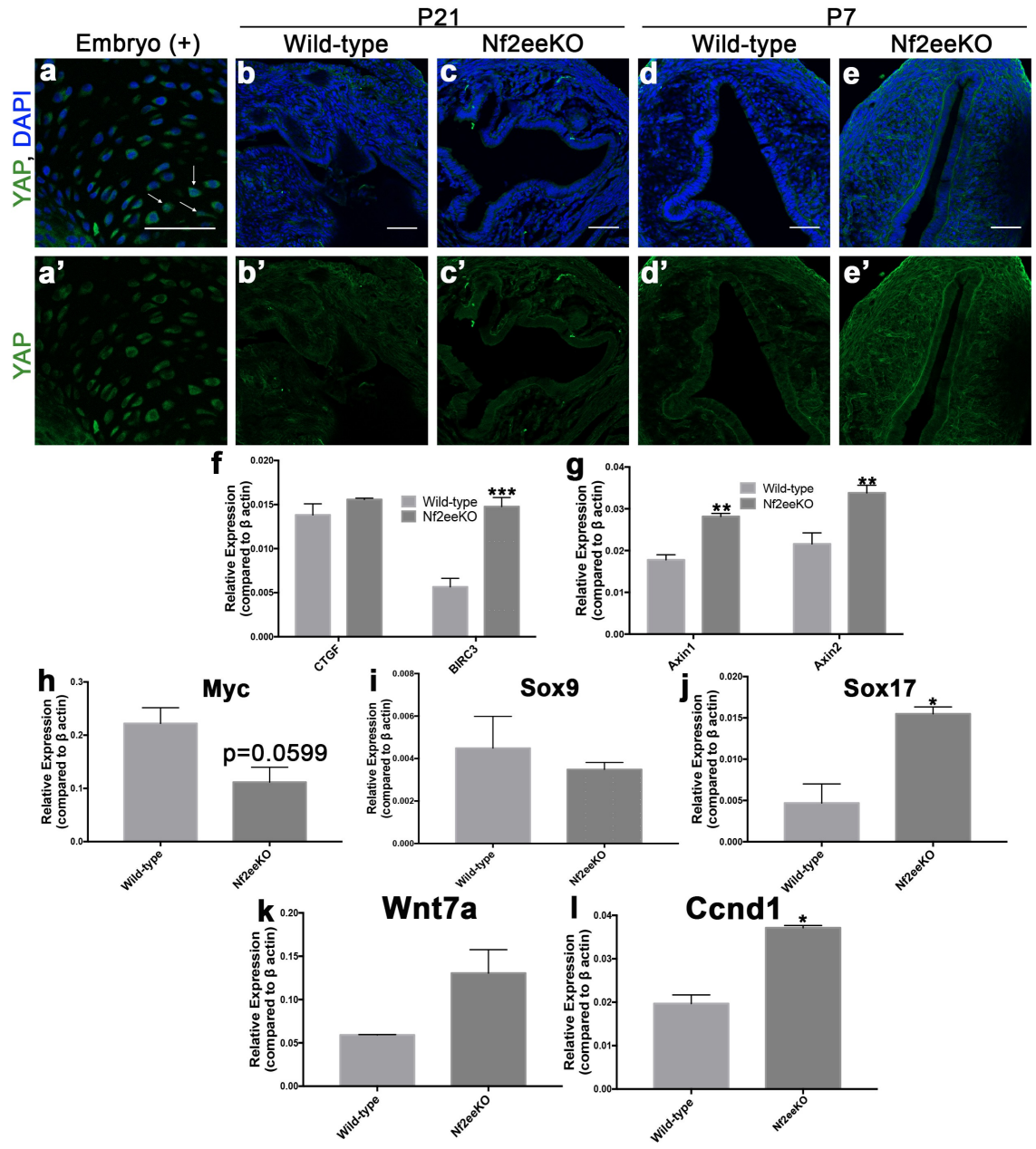


### Figure 9 Hippo and Wnt signaling in Nf2eeKO Mice.

Yap staining in embryonic osteoblasts in cartilage primordium as a positive control (**a, a'**). Yap staining in wild-type (**b, b', d, d'**) and Nf2eeKO (**c, c', e, e'**) endometrium. qRT-PCR of Hippo signaling downstream targets CTGF and BIRC3 in wild-type and Nf2eeKO mice (**f**). Axin1 and Axin2 mRNA expression in wild-type and Nf2eeKO mice (**g**). qRT-PCR of Myc (**h**), Sox9 (**i**), Sox17 (**j**), Wnt7a (**k**), and Cyclin D1 (**l**) in wild-type and Nf2eeKO mice. \*P<0.05, \*\*P<0.01, \*\*\*P<0.005

target was significantly decreased in Merlin-deficient endometrium (Figure 9h). Additionally, another Wnt downstream target, Sox9 was slightly decreased (Figure 9i). Sox17 is known in mouse models of gastric cancer to be involved in a feedback loop with Wnt signaling. When Wnt signaling increasing, it results in an increase in Sox17 that suppresses additional Wnt signals(280). Sox17 expression was shown to increase in Nf2eeKO mice (Figure 9j)(25, 281). This indicates that during initiation of endometrial gland formation, Wnt signaling is decreased in Merlin-deficient endometrium.

### 3.3 Summary

Previous reports show that Nf2 heterozygous mice have decreased fertility, however whether this is due to alterations of the uterus are not known(282). We generated a conditional knockout of Merlin in the uterus utilizing the *Nf2<sup>lox/lox</sup>* mouse crossed to either the *Wnt7a-Cre* or *PR-Cre* mouse to create endometrial epithelial specific mutants (Nf2eeKO) and whole endometrium knockouts (Nf2seeKO) respectively. Both mutants exhibited an aglandular phenotype and Nf2seeKO mice were infertile. Given previous work demonstrating endometrial glands are essential for proper fertility, the infertility in mice lacking Merlin in the uterus could be attributed to decreased or absent gland function. We examined endometrial gland specific transcription factors and Muc1 expression in Nf2eeKO and Nf2seeKO mice. While a majority of the luminal epithelium in Nf2eeKO and Nf2seeKO mice showed similar intensity of Sox9, FoxA2, and Muc1 as the wild-type luminal epithelium, there were distinct

regions that showed increased intensity. Interestingly, the discrete areas of increased Sox9, FoxA2, or Muc1 had similar levels as wild-type glandular epithelium. This suggests that Nf2eeKO and Nf2seeKO luminal epithelium can differentiate in to glandular epithelium correctly but cannot form the proper architecture.

In order to understand why the glandular architecture may not form properly, we examined proliferation, apoptosis, and cellular tension within the tissue. We found there were slight decreases in proliferation in Nf2eeKO mice compared to wild-type mice. Additionally, we determined that cellular tension was increased at the basal membrane of the luminal epithelium in Nf2eeKO mice compared to wild-type mice. We found an increase of F-actin at the apical surface of Nf2eeKO luminal epithelium compared to wild-type mice suggesting an increase in apical constriction. The apical constriction may be pulling on the basal membrane causing the increase in tension at the cell:ECM interface.

Merlin regulates Hippo signaling, cell adhesion, and cell polarity. When examined by immunofluorescence, only apicobasal polarity was significantly affected. However, what signaling pathways may be involved in Nf2eeKO and Nf2seeKO endometrial gland formation were not clear. We found that other Wnt signaling mutant mice have a similar phenotype and a canonical Wnt signaling downstream target was decreased as measured by qRT-PCR. Interestingly, we also examined a Wnt signaling negative regulator, Sox17, measured by qRT-PCR and found Sox17 was increased in the Nf2-deficient mice at P7. Alterations in tension and cadherins can modulate the levels of Sox17(283) and the nuclear

localization of  $\beta$ -catenin(284). This indicates that the observed increase in apical P-cadherin may be causing the decrease in Sox17 expression. Another hypothesis is that the changes in tension in the Nf2eeKO mice cause the decrease in Wnt signaling. This study helps understand the role of polarity, tension, and Merlin within endometrial gland development and female infertility. Since there are 3.53 million women who are unable to become pregnant in the United States, these mouse models will be helpful in understanding female infertility and potential treatments (259).

## Chapter 4: The Role of Merlin in Endometrial Homeostasis

### 4.1 Introduction

Merlin is necessary for proper development of the endometrium (Chapter 3). Merlin has been shown in other epithelial organs to cause both developmental diseases and carcinomas(224, 225). An example is the role Merlin plays in epidermal barrier development, where it regulates establishment of adherens junctions and apicobasal polarity(122). Merlin-deficient skin no longer forms an organized stratified squamous epithelium but rather a disorganized epithelial tissue that loses organ function(122).

Similar to the skin, the uterus is a complex organ that is shed and remodeled frequently through menstruation or estrous. The uterus has a multitude of functions focused around reproduction, including generating a suitable environment for an embryo. The intricacy of the uterus can lead to a variety of FRT diseases that are still not completely understood including endometriosis, uterine fibroids, and endometrial cancer. Menstruation and estrous cause a re-organization of the uterus with each cycle; during this process, both cell adhesion and cell polarity are re-established. Since Merlin connects cell adhesion and apicobasal polarity together(122), Merlin may be necessary for proper homeostasis in the uterus as well. Within this dissertation, homeostasis is defined as the proper maintenance of the mouse or human endometrium and myometrium architecture. Using TCGA (the Cancer Genome Atlas) data we found Merlin is mutated, deleted, or amplified in 5% of human endometrial



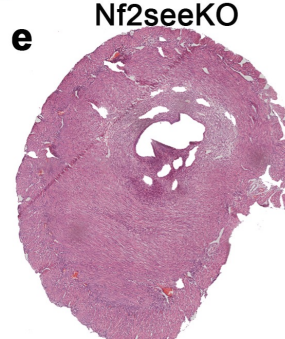
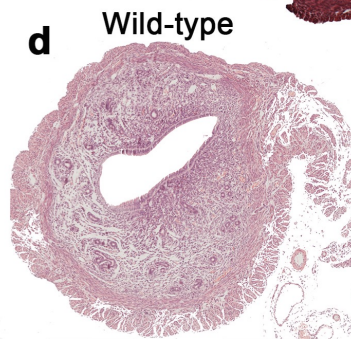
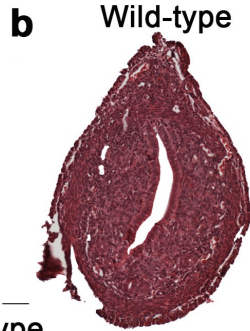
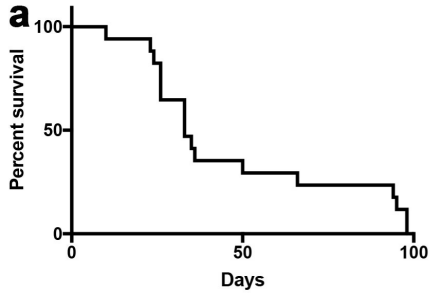
cancers(164, 165). Merlin has also been shown to be regulated post-translationally when homeostasis is disrupted in the breast as well(285). This implies that Merlin may be affected in more cases of endometrial cancer as well.

Merlin (gene name: NF2) was originally found in Neurofibromatosis type 2, a central nervous system tumor disorder, where there was a loss of heterozygosity of Merlin. Interestingly, Merlin has been found to cause carcinomas through a multitude of pathways including EGFR and Wnt signaling(286, 287). How Merlin affects the uterus is not yet well understood, our current knowledge includes the fact that *Nf2*<sup>+/-</sup> mice are subfertile(219) and from Chapter 3 that conditional Merlin knockout causes a loss of endometrial glands and infertility. Understanding how Merlin is involved in homeostasis of the adult mouse uterus may help us learn more about other endometrial diseases like cancer.

## 4.2 Results

### 4.21 Endometrial epithelium becomes a squamous, stratified epithelium in Merlin mutant mice

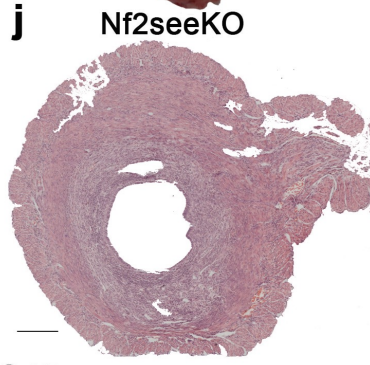
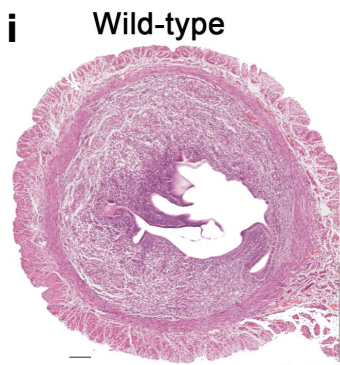
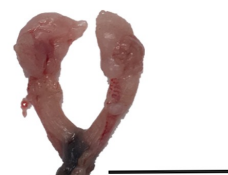
After puberty, the endometrium forms an intricate architecture where tubules branch off the main lumen and secondary branches form glandular epithelium (Figure 1d)(20). *Nf2*eeKO (*Nf2*<sup>lox/lox</sup>; *Wnt7a-Cre*) and *Nf2*seeKO (*Nf2*<sup>lox/lox</sup>; *PR-Cre*) mice do not form glands by P21 (Chapter 3) but how Merlin deficiency affected the post-puberty endometrium is still not understood. Since *Nf2*eeKO mice do not frequently survive past 2 months (Figure 10a), we utilized the *Nf2*seeKO mice to examine how Merlin-deficiency affects endometrial



Nulliparous Cycling Uterus

Wild-type

Nf2seeKO Nf2seeKO  
5 months 2 months



3.5 DPC Uterus

Post-Parous

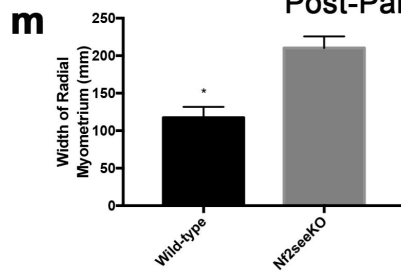
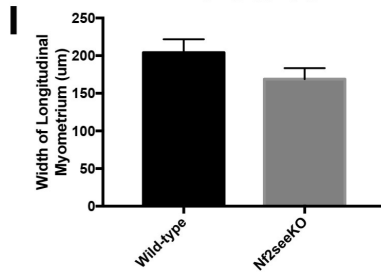


**Figure 10 Nf2seeKO mice uteri change after puberty to resemble a decidualized uterus.**

Survival curve of Nf2seeKO mice until 100 days when 100% of mice were lost (a). Wild-type (b) and Nf2seeKO (c) mice at P21 show a loss of glands in Nf2seeKO but no other visible phenotype. By 3 months of age, virgin Nf2seeKO exhibit an abnormal morphology with a dense myometrium and stroma compared to wild-type mice (d-e). Gross morphology of the uteri shows a thick uterine horn in the Nf2seeKO mice by 5 months compared to wild-type (f-g), however at 2 months the horns look relatively normal (h). Wild-type (i) and Nf2seeKO (j) uteri and 3.5 days post coitus (DPC) look similar to Nf2seeKO uteri at 3 months (e). Interestingly, Nf2seeKO uteri that have been serially mated have an exacerbated morphology compared to Nf2seeKo at 3.5 DPC with a thick longitudinal myometrium and thin radial myometrium (k). Quantification of the thickness of the longitudinal myometrium in  $\mu\text{m}$  (l). Quantification of the thickness of the radial myometrium in  $\mu\text{m}$  (l). \* $p < 0.0033$ .

homeostasis. It should be noted that the reason for death is not known, however, it does not appear to be related to the endometrial phenotype. At P21, wild-type mice have 8-10 endometrial glands on average within the endometrium (Figure 4a, f-g, Figure 10b), while Nf2seeKO mice do not form endometrial glands (Figure 4g, Figure 10c). Interestingly, by 3 months of age the Nf2seeKO uteri significantly changed showing a simpler luminal epithelium with a small ovular lumen compared to wild-type endometrium (Figure 10d-e). Additionally, we saw a denser stroma and a thicker myometrium than wild-type uteri (Figure 10d-e). The gross morphology of mutant uteri show thickened and firm horns compared to wild-type uteri at 5 months of age (Figure 10f-g). Around P60, we began to notice a vagina with a dark brown coloring in the Nf2seeKO FRT that we continued to observe in the older Nf2seeKO females (Figure 10g-h). Interestingly, the Nf2seeKO mouse endometrial luminal epithelium is positive for keratin 14 (K14), a squamous epithelial marker normally contained in the vaginal epithelium. Wild-type endometrial luminal epithelium is not positive for K14, therefore this may indicate a possible cell fate change in the epithelium.

The aberrant histology of the Nf2seeKO aged uterus appeared similar to an early pregnant uterus (3.5-5.5 days post coitus)(288). We became interested in whether this histological phenotype usually observed during normal pregnancy could be exacerbated following breeding. Wild-type female uteri at 3.5 DPC (days post coitus) had a condensed endometrial stroma that looked similar to decidua, the endometrial glands had decreased in size, and the endometrial lumen was condensing into a smaller luminal structure (Figure 10i). Nf2seeKO

female uteri at 3.5 DPC had a similar condensed endometrial stroma, especially around the myometrium with a shrunken endometrial lumen in a circular shape (Figure 10j). In addition, we observed serially mated Nf2seeKO females had an exacerbated phenotype compared to post-puberty mutant or 3.5 DPC uteri (Figure 10e, j, k). In fact, the radial myometrium was significantly thicker in the serially mated Nf2seeKO females compared to the wild-type 3.5 DPC. However, the longitudinal myometrium was not significantly different (Figure 10l-m). Since pregnancy and puberty cause a change in hormonal cycling/changes in the hypothalamic-pituitary-gonadal axis, we postulate that hormones may play a role in this uterine phenotype.

#### **4.22 Changes in endometrial epithelium coincide with changes in Wnt signaling**

In P7 mice, we observed a decrease in proliferation and no increase in apoptosis (Figure 7). Therefore, we were interested to know what caused the observed increase in cell density after puberty. Initially, we examined Hippo signaling since Merlin is a negative regulator of Hippo, and Hippo signaling is known to regulate organ size. We noted increases in both BIRC3 and CTGF in Nf2seeKO mice at P60 (Figure 11a). Nf2seeKO mice after puberty also showed an increase in CTGF but a decrease in BIRC3 (Figure 11e). In addition, since canonical Wnt signaling mutants have previously been shown to affect endometrial gland formation and to cause K14<sup>+</sup> epithelium(46), we examined Wnt signaling downstream targets, Cyclin D1 (Ccnd1) and Myc by qRT-PCR

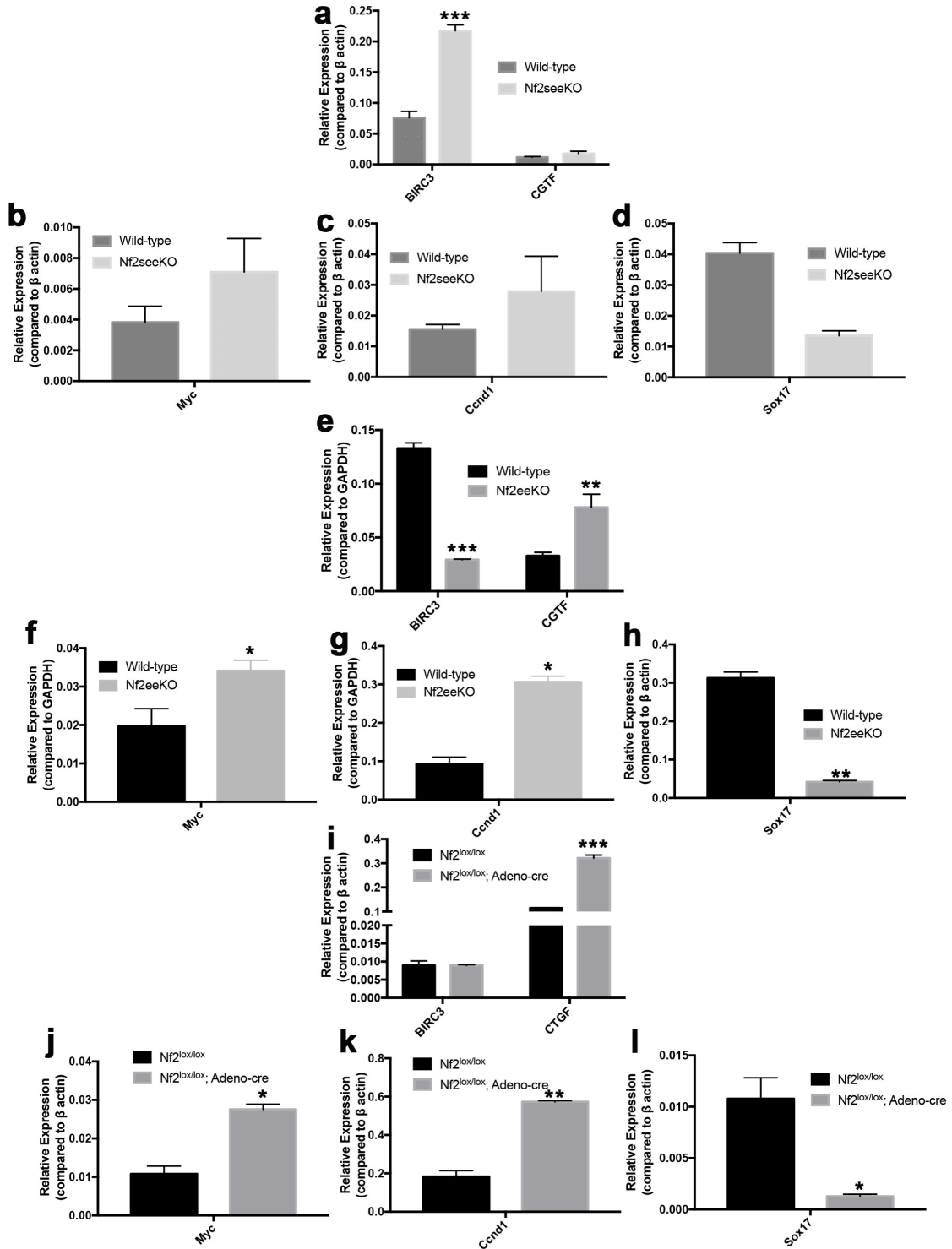


**Figure 11 Expression of Hippo and Wnt signaling in Nf2eeKO, Nf2seeKO, and Merlin-deficient primary cells.**

Expression of the Hippo signaling downstream targets, BIRC3 and CTGF, in Nf2seeKO (a), Nf2eeKO (e), and Merlin-deficient endometrial cells (Nf2KOcells, i). Expression of Myc, a Wnt signaling downstream target, in Nf2seeKO (b), Nf2eeKO (f), and Nf2KOcells (j). Quantification of mRNA expression in Ccnd1 in Nf2seeKO (c), Nf2eeKO (g), and Nf2KOcells (k). Sox17 mRNA expression in Nf2seeKO (d), Nf2eeKO (h), and Nf2KOcells (l). Stable normalized genes were used \*P<0.05, \*\*P<0.01, \*\*\*P<0.005

(Figure 11b-c, f-g). Interestingly, in aged Nf2seeKO and Nf2eeKO mice, we observed an increase in both Ccnd1 and Myc (Figure 11b-c, f-g). We also examined the Wnt signaling negative regulator, Sox17, which was shown to increase in P7 Nf2eeKO mice. In both Nf2eeKO and Nf2seeKO post-puberty mice, we found a substantial decrease in Sox17 mRNA expression (Figure 11d, h). Furthermore, when endometrial epithelium was isolated and put into culture, we observed a similar change in mRNA expression of BIRC3, CTGF, Ccnd1, Myc, and Sox17 (Figure 11i-l). This suggests that after puberty there is a switch in Merlin null mice from loss of Wnt signaling to overexpression of Wnt signaling that may be hormone related.

### 4.3 Summary

Merlin is necessary for fertility (**Figure 4h-j**) in female mice and is also necessary for proper homeostasis of uterine tissues. Loss of Merlin causes an abrupt change to all compartments within the uterus (myometrium, endometrial stroma, and endometrial epithelium). Changes within all the tissues of the uterus on an endometrial specific knockout is not necessarily surprising since past work has shown that the endometrial epithelium communicates with both the stroma and the myometrium(248, 266, 289). However, since a majority of Nf2eeKO mice are not able to survive to 4 months, it is not clear if this is due to the epithelium, or a combination of signaling from the stroma and epithelium.

The endometrial epithelium is fascinating because we observe a cell fate change from K14<sup>-</sup> to K14<sup>+</sup> tissue. This implies that loss of Merlin can cause a cell



fate change within epithelial cells. In addition, Wnt signaling appears to significantly increase in the uterine tissue based on mRNA expression of downstream targets. Both the Wnt7a and  $\beta$ -catenin conditional knockout mice also show a change in endometrial epithelial architecture, however it is not known whether canonical Wnt signaling changes in the older Wnt7a and  $\beta$ -catenin knockout females(46, 290). The increase observed in Ccnd1 and Myc are also observed in primary cells isolated in culture. Since epithelial cells in culture proliferate in order to reach confluency, this increase in Ccnd1 and Myc are not unexpected and correlates with other data that shows mRNA expression is upset quickly when primary endometrial epithelial cells are cultured. Since the histological changes occur after puberty and are more pronounced in parous females versus nulliparous females, we hypothesize that the changes in uterine architecture and potentially the overexpression of Wnt signaling are related to hormonal fluctuations. This study shows that Merlin loss affects both development and homeostasis of the uterus and more work is necessary to understand how Merlin affects the aging uterus.

## **Chapter 5: Loss of polarity alters proliferation and differentiation in low-grade endometrial cancers by disrupting Notch signaling**

This chapter is based upon Williams, E., Villar-Prados, A., Broaddus, R., Gladden, A. (2017) Loss of polarity alters proliferation and differentiation in low-grade endometrial cancers by disrupting Notch signaling. PLoS ONE 12 (12): e0189081. [https://doi.org/ 10.1371/journal.pone.0189081](https://doi.org/10.1371/journal.pone.0189081) is licensed under CC BY (Creative Commons Attribution license) by PLoS One.

### **5.1 Introduction**

Merlin has been shown to affect endometrial homeostasis and proper polarity protein localization in the endometrial epithelium (Chapter 3-4). Polarity genes are shown as being mutated, amplified or deleted in 37% of endometrial adenocarcinomas in the TCGA database(164, 165). Alterations in members of the Par complex accounts for 18% of these cancer cases(164, 165). These members include Par3, aPKC, and Par6. In general, polarity complexes are necessary for proper apical and basal membrane formation; this functionally is dependent on the integrity/completeness of the complex. Accordingly, dysregulation or disruption of any polarity gene or protein members can cause mislocalization and dysfunction of all polarity proteins irrespective of mutation, gene amplification, deletion, or epigenetic changes(103). Apicobasal polarity, specifically the Par complex is known to be affected in a multitude of cancers(138, 166, 184, 291). As previously discussed, Par3 loss causes an increase in metastasis in some breast cancer mouse models(138). Conditional

Par3 knockout in epidermal tissue causes an increase in melanoma and hyperplasia of melanocytes when a skin carcinogen is applied(292). While Par3 has been shown to increase tumor formation and affect tumor progression, there are few studies to understand how Par3 and the Par complex is involved in the formation of tumors.

The Par complex is known to be necessary for proper compartmentalization of membrane receptor signaling. For example, Notch signaling requires Par3 for the asymmetric division of Notch in mouse radial glial cells(81). In addition, Par complex regulators like Merlin are known to affect the proper localization of transmembrane proteins like Notch(80). The correct membrane localization of EGFR (epidermal growth factor receptor), a transmembrane protein has been shown to be necessary for proper vulval development in *C. elegans*(293). Another set of receptor tyrosine kinases, FGFRs (fibroblast growth factor receptors) are known to localize to different compartments within the same cell-type, thus localization of each may be necessary for coordinating different signaling pathways within cells(294). The Frizzled receptors involved in canonical Wnt signaling or planar cell polarity localize to different areas of the membrane in the same cell-type(56). This suggests that correct compartmentalization of receptors is necessary for proper membrane-bound receptor signaling. Interestingly, while it is known that the different Notch receptor extracellular domains determine the capability to localize to the membrane and efficiency to be cleaved, it is not well understood how

specific membrane localization of the receptors plays a role in Notch signaling(77).

As discussed in Chapter 1, the canonical Notch signaling pathway has a membrane-bound receptor and ligand that must interact for increased expression of downstream targets. Notch signaling is hypothesized to function as a switch causing different phenotypes depending on the overall level of NICD (Notch intracellular domain). This feature is not dependent on the specific Notch receptor being utilized(77, 79). While there is a basic understanding of Notch signaling, it's activity in a multitude of diseases like cancer, highlights the need to further understand the Notch pathway.

Previous work has shown that Notch signaling can be tumor suppressive or oncogenic in a cancer dependent manner(295–297). In the cervix, Notch signaling appears to be tumor suppressive(72, 298, 299). In contrast, Notch is upregulated in ovarian cancer, implying it is oncogenic. The role that Notch plays in reproductive cancers is unclear and controversial(300). Interestingly, two different conditional Notch1 activating mutants have been generated in the FRT (*Rosa26<sup>N1ICD/N1ICD</sup>; Amhr2-Cre* [1], *Rosa26<sup>N1ICD/N1ICD</sup>; PR-Cre* [2])(26, 74). The *Amhr2* mutant drives overexpression of Notch1 in areas of the ovary, endometrial stromal cells, and myometrium, while the PR mutant forces overexpression of Notch1 in the entire endometrium, ovary, and oviduct(26, 74). The *Rosa26<sup>N1ICD/N1ICD</sup>; Amhr2-Cre* mouse was found to have defects in the architecture of the oviduct and cause cyst formation at around 3-4 months of age. Similar to *Nf2eeKO* and *Nf2seeKO* mice, *Rosa26<sup>N1ICD/N1ICD</sup>; PR-Cre* mice do not

form endometrial glands(26, 74). Both mutants were determined to be infertile(26, 74). Whether these mice show similar decidual-like abnormalities as the Nf2seeKO mice in the post-puberty uterine tissues is not known. It is possible that the aglandular phenotype seen in both mice may be related to the disruption of apicobasal polarity. Accordingly, we postulate that apicobasal polarity is critical for proper endometrial maintenance, whereby its loss and dysregulation of Notch signaling is involved in endometrial tumorigenesis.

## **5.2 Results**

### **5.21 Loss of polarity, but not E-cadherin localization, in low-grade endometrial cancer**

Normal human endometrium consists of a single layer of polarized glandular epithelium resting on the basement membrane and surrounded by adjacent stromal cells(301). To determine the status of apicobasal polarity in endometrial cancer (EC), we first examined the localization of the apical protein, Ezrin and the apical polarity protein, Par3 in normal endometrium in relation to the localization of adherens junction protein, E-cadherin. Both Par3 and Ezrin localized to the apical side of the polarized glandular epithelium of normal endometrium (Figure 12a, d). We next examined Ezrin and Par3 localization in G1 EC and G2 EC samples. We observed a decreased apical localization of both Par3 and Ezrin in glandular structures of the tumors compared to minimal

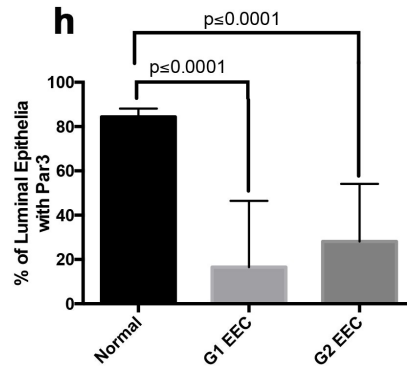
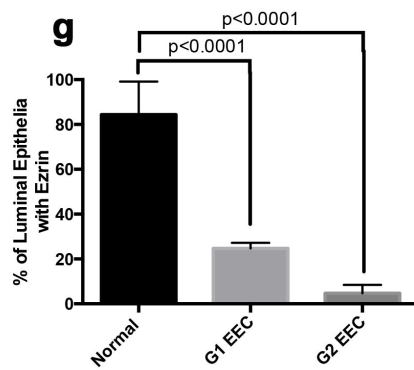
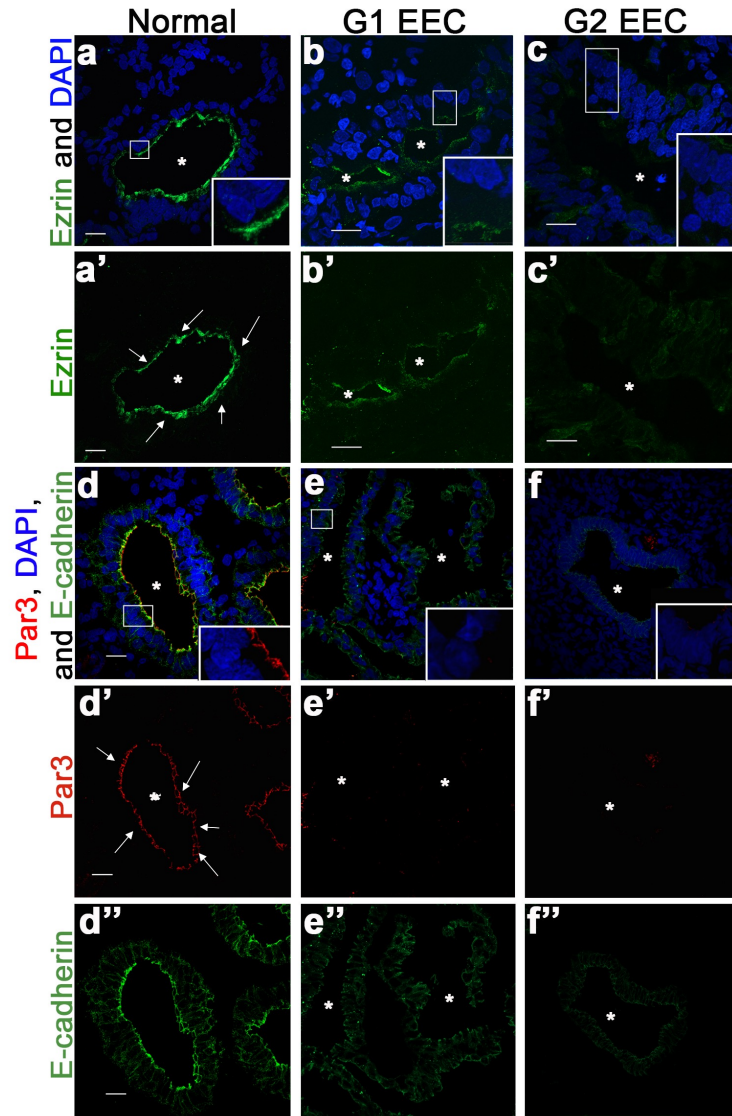


**Figure 12 Loss of apicobasal polarity occurs in low-grade endometrial cancer.**

Human endometrial tissue (**a, a', d, d', d''**), normal; (**b, b', e, e', e''**) grade 1 endometrioid endometrial carcinoma, G1 EEC; and (**c, c', f, f', f''**) grade 2 endometrioid endometrial carcinoma, G2 EEC stained with antibodies for the apical proteins (**a-c**) Ezrin or (**d-f**) Par3, E-cadherin and DAPI. Scale bar, 20  $\mu\text{m}$ . Asterisks indicate glandular lumen and arrows show apical localizing protein (**a'**) Ezrin or (**d'**) Par3. Scale bar, 20  $\mu\text{m}$ . (**g** and **h**) Quantification of (**a-c**) Ezrin or (**d-f**) Par3 apical localization in 10 lumens of each sample (n = 3 normal, n = 2 G1 EEC, n = 2 G2 EEC) showing loss of apical protein localization in low-grade EEC. Error bars represent SEM.

changes in E-cadherin localization (Figure 12a- f, Figure 13a-c, e).

Quantification of the percentage of glandular epithelial cells with apical localization of either Ezrin or Par3 shows nearly a four-fold decrease in ECs compared to normal endometrium (Figure 12g-h). Additionally, the presence of the apically localized differentiation marker acetylated tubulin, which marks cilia(302–304), was decreased in G1 and G2 EC (Figure 13f-i). These data indicate that apicobasal polarity is disrupted in low-grade endometrial tumors.

We previously demonstrated that establishment of apicobasal polarity in developing epithelial tissue requires adherens junction (AJ) formation(122). Loss of polarity is closely associated with advanced or metastatic tumors and epithelial-to-mesenchymal transition (EMT), a transcriptional program that downregulates the AJ protein, E-cadherin (305). To investigate E-cadherin protein expression and localization in G1 and G2 ECs lacking apicobasal polarity, we stained normal endometrium and ECs for E-cadherin. Interestingly, although apicobasal polarity was disrupted, E-cadherin remained present and localized to the basolateral membranes of glandular epithelial cells in G1 and G2 EC (Figure 13a-c, e). Subsequently in more advanced G3 EC, we see loss of E-cadherin expression indicating loss of E-cadherin is a late event in EC (Figure 13d). Overall, these data demonstrate that loss of apicobasal polarity, but not the AJ marker E-cadherin, corresponds with decreased cellular differentiation in low-grade endometrial tumors.



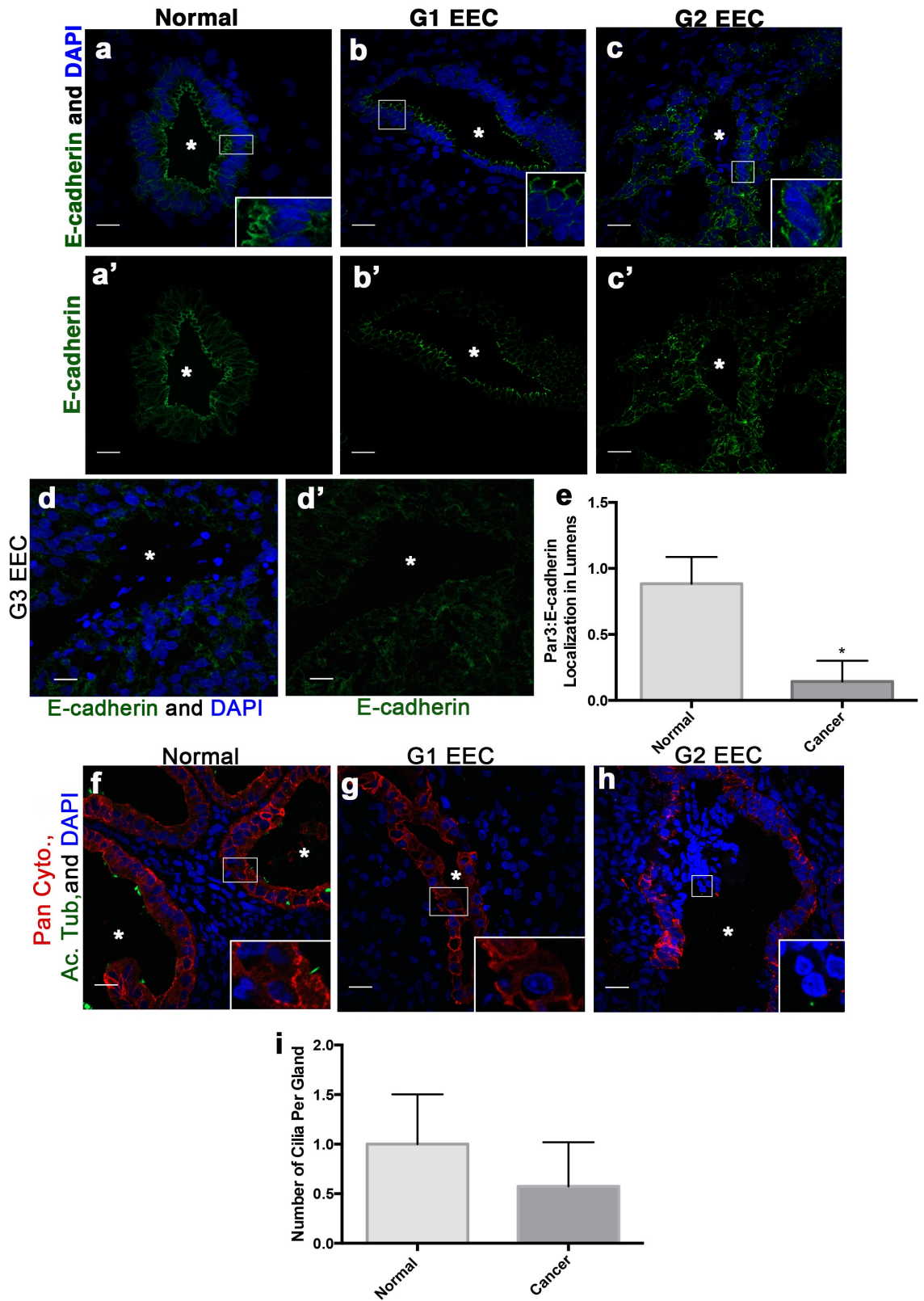


**Figure 13 E-cadherin localization and cilia presence in endometrial cancer with disrupted polarity.**

Normal endometrium (**a, a'**), G1 EEC (**b, b'**) and G2 EEC (**c, c'**) stained with an antibody against E-cadherin and DAPI. Images of (a-c) E-cadherin staining showing localization to the apical junctions and lateral border in normal endometrium, G1 EEC, and G2 EEC (**a'-c'**). Asterisks indicate glandular lumen. G3 EEC stained with antibodies against E-cadherin (green) with DAPI (**d**) or with E-cadherin staining only (**d'**) showing loss of localization to the apical junctions and lateral borders. Ratio of the apical localization of Par3 to the basolateral localization of E-cadherin (**e**). Localization of Par3 or E-cadherin was determined from 10 lumens of each sample (n = 3 normal, n = 4 EEC). Staining with antibodies against acetylated tubulin (Ac. Tub), a maker of cilia, pan cytokeratin (Pan Cyto.), an epithelial maker, and DAPI in normal endometrium (**f**), G1 EEC (**g**), and G2 EEC (**h**) shows a decrease in cilia indicative of decreased differentiation. Quantification of the number of cilia found per gland determined from 10 lumens of each sample (**i**, n=3 normal, n=5 EEC). Error bars represent SEM. \* <0.05. Scale bar, 20  $\mu$ m

## **5.22 Disruption of polarity in a 3D cell model phenocopies changes in cellular differentiation observed in low-grade endometrial tumors.**

To understand how apicobasal polarity was regulating differentiation we utilized a commonly used polarized epithelial cell model, Madin-Darby Canine Kidney (MDCK) cells, as we were unable to obtain normal endometrial epithelial cells. Apicobasal polarity was disrupted through shRNA-mediated knockdown of Par3, Ezrin or Merlin (Figure 14a-c). To better recapitulate the 3D organization of the endometrium, we cultured Scramble-shRNA (Scr-shRNA), Par3-shRNA (Par3 kd) and Ezrin-shRNA (Ezrin kd) cells in a 3D matrix and stained the cells for acetylated tubulin, a marker of cilia and Phalloidin or E-cadherin and ZO-1 (Figure 14d-f, k-m). Scr-shRNA cells formed single lumen structures with numerous cells extending cilia into the luminal space (Figure 14d, g-h). Confirming previous studies, we observed Par3 kd, Ezrin kd, and Merlin-shRNA (Nf2 kd) cells formed multi-lumen structures(134, 306) similar to what was observed in human ECs (Figure 14e-h, not shown)(307). Additionally, we observed an overall decrease in the presence of cilia in Par3 kd and Ezrin kd analogous to our observations in endometrial cancer (Figure 14h). Both the multi-lumen phenotype and the loss of cilia are indicative of a less differentiated state in epithelial cells (302–304, 307–309), implying that disruption of apicobasal polarity in the cell-based model caused a less differentiated state similar to ECs.

To provide additional evidence for altered differentiation in our Par3 kd and Ezrin kd cell model, we examined the localization of the polarized tight junction (TJ) marker ZO-1 and the formation of functional TJs, a known sign of

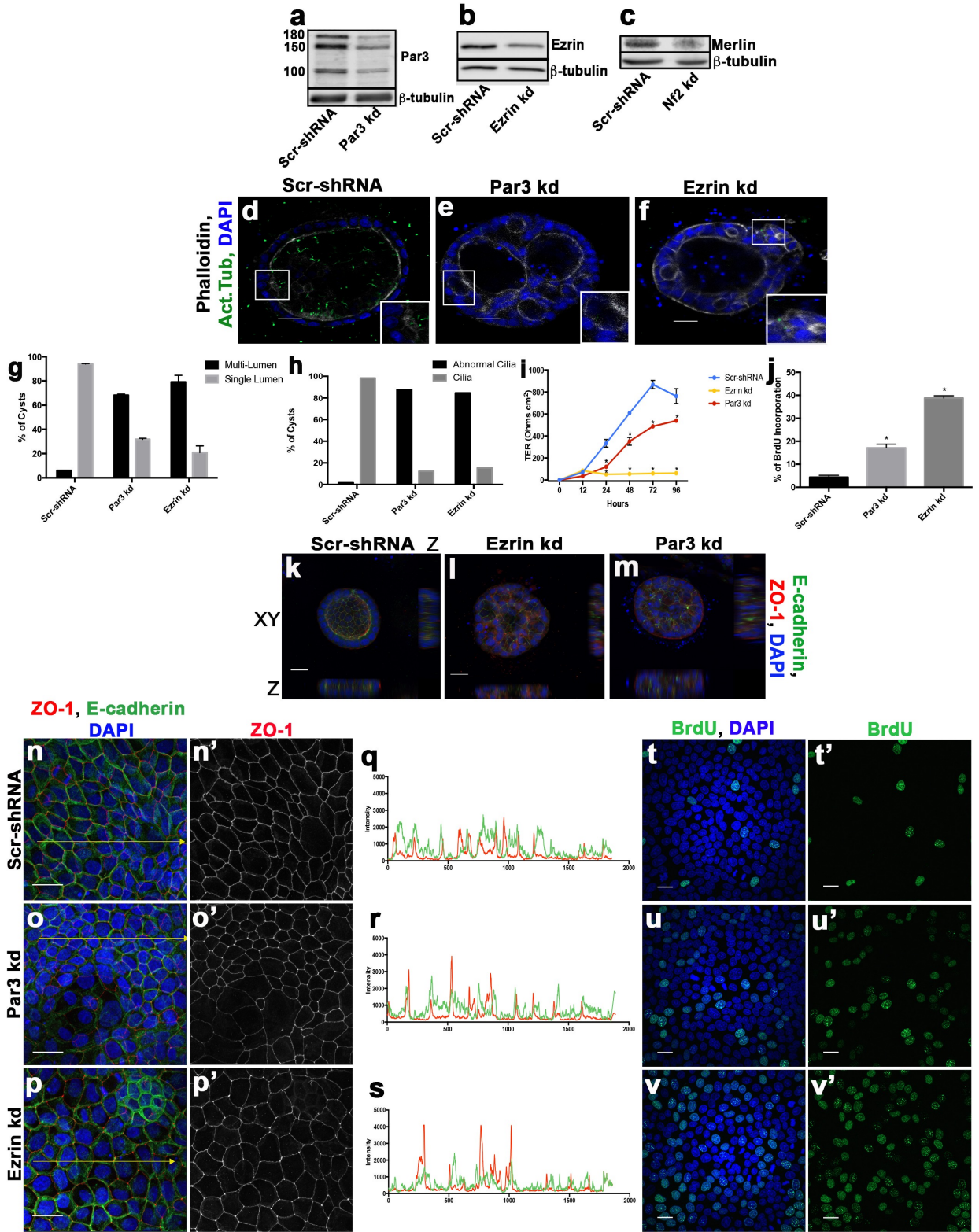


**Figure 14 Depletion of apical polarity proteins cause an increase in multiple lumen structures and a decrease in differentiation markers in epithelial 3D cell culture.**

Western blot analysis of (a) Par3, (b) Ezrin, and (c) Merlin knockdown in the MDCK cells compared to a scramble control (a-c). Immunofluorescence staining on (d) Scramble-shRNA (Scr-shRNA), (e) Par3-shRNA (Par3 kd), and (f) Ezrin-shRNA (Ezrin kd) 3D cysts for primary cilia by acetylated tubulin (ac. tub) and actin by Phalloidin (d-f). Scale bar, 20  $\mu\text{m}$ . Quantification of the (g) number of lumens ( $n = 2$ ) and (h) cilia ( $n = 1$ ) present within all 3D cysts compared to scramble control cells. Par3 kd, Ezrin kd, and Scr-shRNA had at least 49 cysts, 13 cysts, or 70 cysts examined per independent experiment (g, h). Abnormal cilia include cysts without cilia present or cilia that appears abnormal (h). Error bars represent SEM. Transepithelial resistance demonstrates loss of functional TJ in Par3 kd and Ezrin kd cells compared to Scr-shRNA cells calculated by Ohms per  $\text{cm}^2$  (i). Quantification of the number of BrdU positive cells in Scr-shRNA, Par3 kd, and Ezrin kd cells (j). Orthogonal view of (k) scr-shRNA, (l) Ezrin kd, or (m) Par3 kd with E-cadherin (green), ZO-1 (red), and DAPI showing multiple lumens in cysts depleted of apical polarity proteins (k-m). Immunofluorescence staining for ZO-1 shows altered TJ protein localization in Par3 kd and Ezrin kd cells indicative of decrease in differentiation by loss of epithelial cell junctions (n-p). E-cadherin is also stained to label junctional complexes. Scale bar, 20  $\mu\text{m}$ . ZO-1 only staining to show the aggregation of ZO-1 at tricellular junctions in white (n'-p'). Line plots of (n-p) showing intensity of E-cadherin (green line) and ZO-1 (red line) on the yellow line in the respective image, Scr-shRNA (q), Par3 kd (r), and Ezrin kd (s). Note the overlap in E-cadherin and ZO-1 intensities in Scr-shRNA compared to distinct peaks of ZO-1 intensity in Par3 kd and Ezrin kd indicative of mislocalized ZO-1 (q-s). Increased BrdU incorporation observed in Par3 kd and Ezrin kd cell lines compared to the Scr-shRNA cells (j, t-v). BrdU only staining (t'-v'). Scale bar, 20  $\mu\text{m}$ . \* $P < 0.05$

differentiation in MDCK cells(303). The Par3 kd and Ezrin kd cells displayed high concentrations of ZO-1 at tricellular contacts; however, ZO-1 levels were low or absent at other apical contact points (Figure 14n-p). Similarly, in 3D cultures ZO-1 had a disorganized staining pattern in the Par3 kd and Ezrin kd cells compared to control cells where it localized to the apical junctional border (Figure 14k-m). Additionally, the Scr-shRNA cells show an increase in TER over time; by contrast, the Par3 kd, as previously described (256), and Ezrin kd cell lines do not increase TER to the same degree, that these cells are less differentiated and cannot form a functional polarized TJ (Figure 14i). We also sought to determine whether disruption of apicobasal polarity increased cell proliferation, another marker of decreased cell differentiation. Cells depleted of either Par3 or Ezrin displayed increased BrdU incorporation compared to the control cells (Figure 14j, t-v). In concordance with our observations in low-grade endometrial cancer, these data demonstrate that disruption of apicobasal polarity decreases differentiation and increases proliferation of epithelial cells.

### **5.23 Disruption of apicobasal polarity decreases Notch signaling in epithelial cells and in low-grade endometrial cancer.**

To examine the underlying signaling pathways that could regulate differentiation in cells with disrupted polarity we utilized our Scr-shRNA, Par3 kd, Ezrin kd, and Nf2 kd cells. We examined Notch signaling as it regulates proliferation and differentiation in a tissue-specific manner and in the normal endometrium(245,

310–313). Notch signaling is tightly regulated during the menstrual cycle to assist in increasing and decreasing proliferation and differentiation(245). Furthermore, in *Drosophila*, Notch receptor localization is affected by Merlin which is known to regulate polarity(80). Using qRT-PCR we found MDCK cells express Notch1 and Notch2, and the Notch ligands, Jag1 and Jag2, along with several Notch targets known to play a role in differentiation and proliferation including HEYL, HEY1, and p21 (Figure 15a-c)(310–313). We observed a significant decrease in the expression of Notch receptors, Notch ligands, and Notch downstream targets in Par3 kd, Ezrin kd, and Nf2 kd cells indicating that altered apicobasal polarity disrupts Notch signaling in this mammalian cell-based model (Figure 15d-x).

We next asked whether a similar change occurs in the Notch signaling pathway in low-grade ECs. We performed qRT-PCR with normal endometrium, G1, and G2 EC samples. We observed a significant decrease in the Notch downstream targets, HEYL and HES1 and the Notch ligand, Jag1, indicating that overall Notch signaling is decreased in low-grade EC (Figure 16d-f). Additionally, we detected a significant decrease in the transcript levels of the Notch receptor, Notch4 but no decrease in Notch1 or Notch2 (Figure 16a-c). Previous work has demonstrated that overall levels of active Notch intracellular domain is critical for downstream Notch signaling suggesting that Notch1 and/or Notch2 protein could be regulated in other manners in low-grade EC(78, 314).

Our observation that Notch1 and Notch2 mRNA expression levels were similar, but that downstream targets were significantly reduced, in EC compared to normal samples, prompted us to examine the Notch1 and Notch2 proteins.

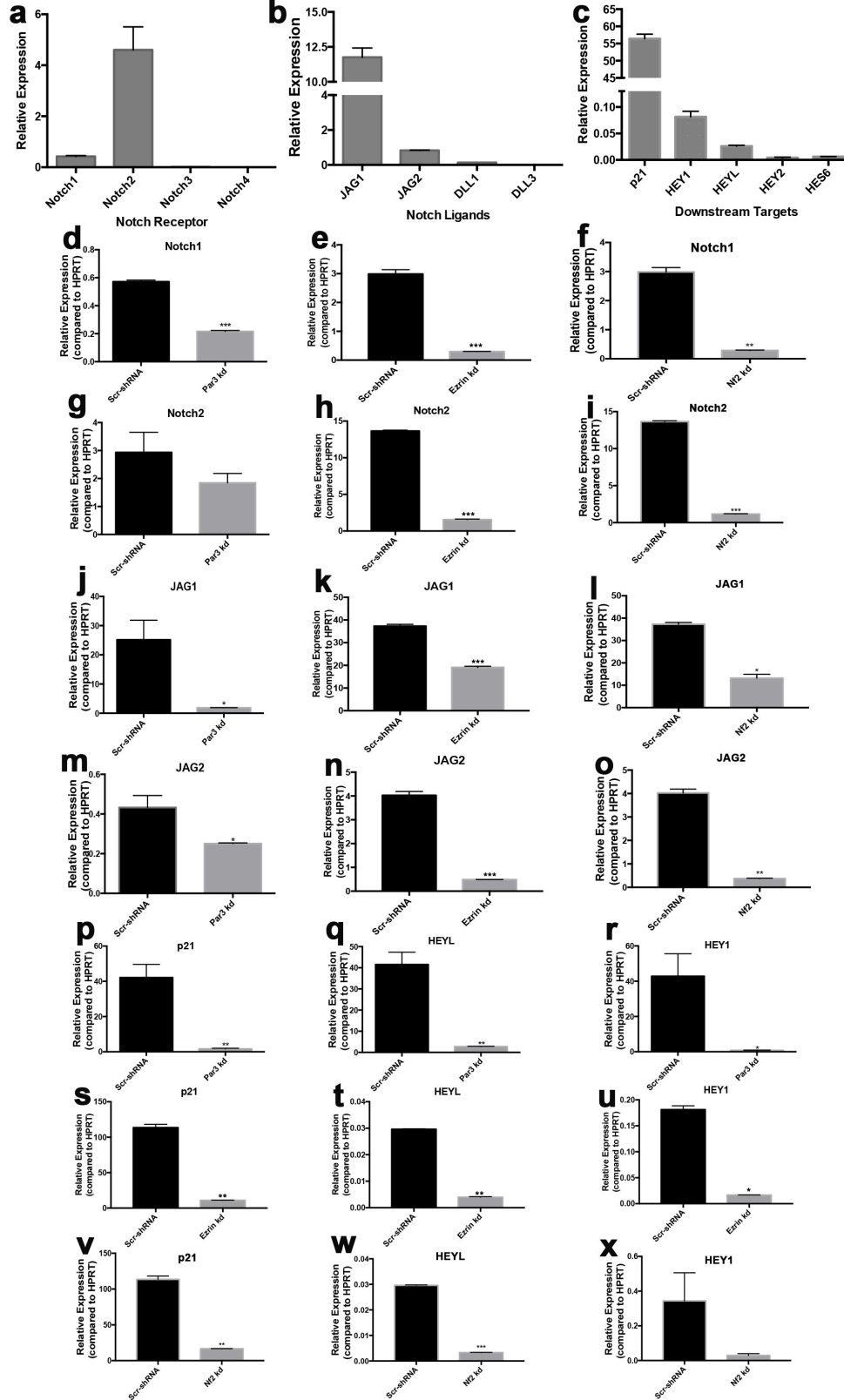




**Figure 15 Notch signaling decreases in Par3, Ezrin, and Merlin depleted epithelial cells.**

mRNA expression of Notch receptors (a), Notch ligands (b), and Notch downstream targets (c) expressed in wild-type MDCK cells (a-c). qRT-PCR analysis of Notch1 (d-f), Notch2 (g-i), JAG1 (j-l), JAG2 (m-o), p21 (p, s, v), HEYL (q, t, w), or HEY1 (r, u, x) expression in Scr-shRNA, Par3 kd (d, g, j, m, p-r), Ezrin kd (e, h, k, n, s-v), and Nf2 kd (f, i, l, o, v-x) cells. Samples were done in triplicate. Error bars signify SEM. \* <0.05, \*\* <0.001, \*\*\*<0.0001

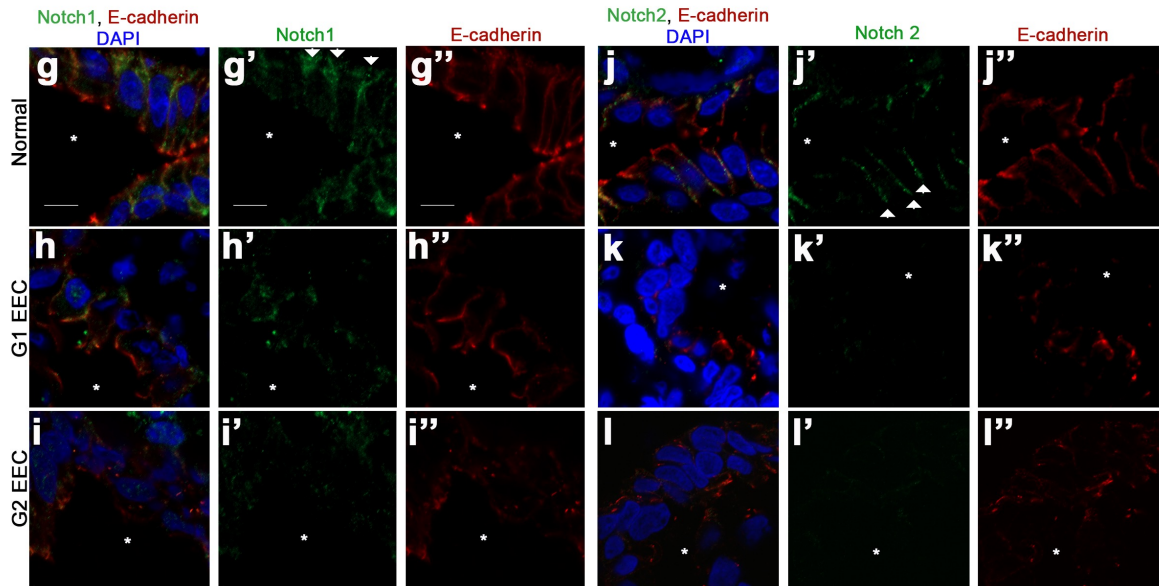
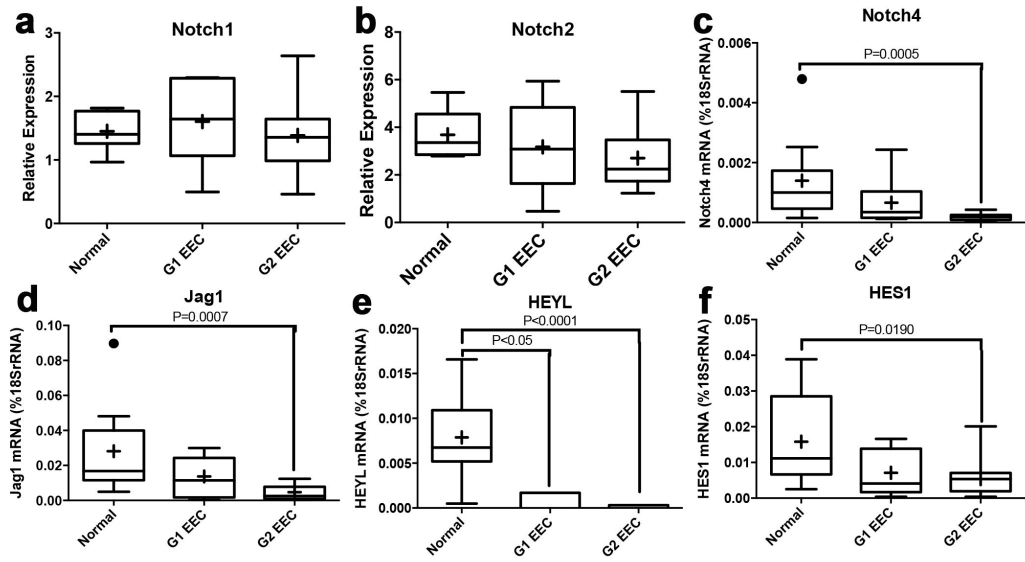


**Figure 16 Notch downstream signaling and receptor localization is disrupted in low-grade endometrial cancer.**

qRT-PCR of Notch receptors, ligands, and downstream targets in normal and in low-grade (G1 & G2 EEC) endometrial cancer (a-f). The Notch receptor, Notch1 (a) and Notch2 (b) show no change in expression while Notch4 (c) is decreased. Notch ligand Jag1 (d) and downstream targets HEYL (e) and HES1 (f) are down regulated in low-grade endometrial cancer. Notch1 (a) and Notch2 (b) data was analyzed using  $\Delta$ CT with the Tata box binding protein (DBP) as the reference gene with 7 samples for Normal, G1 EEC, and G2 EEC. Notch4 (c), Jag1 (d), HES1 (e), and HEYL (f) were analyzed by calculating the number of molecules of the gene of interest compared to 18SrRNA (c-f, %18SrRNA). Tukey box plots were used with SEM where + is the mean value and • are outliers. Normal (n = 10), G1 EEC (n = 9), and G2 EEC (n = 22). Immunofluorescence of Notch receptors showing localization of Notch1 (g-i, g'-i') and Notch2 (j-l, j'-l') in normal endometrium (g, j), G1 EEC (h, k), and G2 EEC (i, l). E-cadherin marks the basolateral cell:cell contacts (g-l). Asterisks signify the lumen. Scale bar, 20  $\mu$ m. Images of (g-l) with Notch1 or Notch2 respectively showing localization to the lumen (g'-l'). Arrows denote lateral localization of Notch1 or Notch2.

The Notch receptors are membrane-bound proteins whose activation may be affected by subcellular localization(315). In normal human endometrium Notch1 and Notch2 localize to the basolateral and lateral membranes of the glandular epithelial cells, respectively (Figure 16g, j). In low-grade ECs, by contrast, neither Notch1 nor Notch2 receptor proteins localize correctly to the lateral membrane of epithelial cells (Figure 16g-l). Moreover, Notch1 and Notch2 protein levels are decreased in the tumor. Collectively, these data show that low-grade ECs have disrupted apicobasal polarity and mislocalized and/or reduced protein levels of Notch1 and Notch2 receptors that may lead to the overall decrease observed in Notch downstream targets.

#### **5.24 Expression of Par3 in endometrial cancer cells promotes differentiation and decreased proliferation.**

To determine whether establishment of apicobasal polarity alters differentiation or proliferation in endometrial cancer, we assayed endometrial cancer cell lines for changes in apical polarity proteins. We examined Par3 expression in a panel of endometrial cancer cell lines from G1, G2, and G3 tumors(316). Western blot analysis revealed that Par3 was not readily detected in a majority of the endometrial cancer cell lines (Figure 17a). Not surprisingly since many of the cancer cell lines are well differentiated, detectable levels of E-cadherin were observed (Figure 17a). To determine how tumor cells would respond to Par3 expression, we overexpressed Par3 in Ishikawa and HEC-1-A cells (Figure 17b-c).

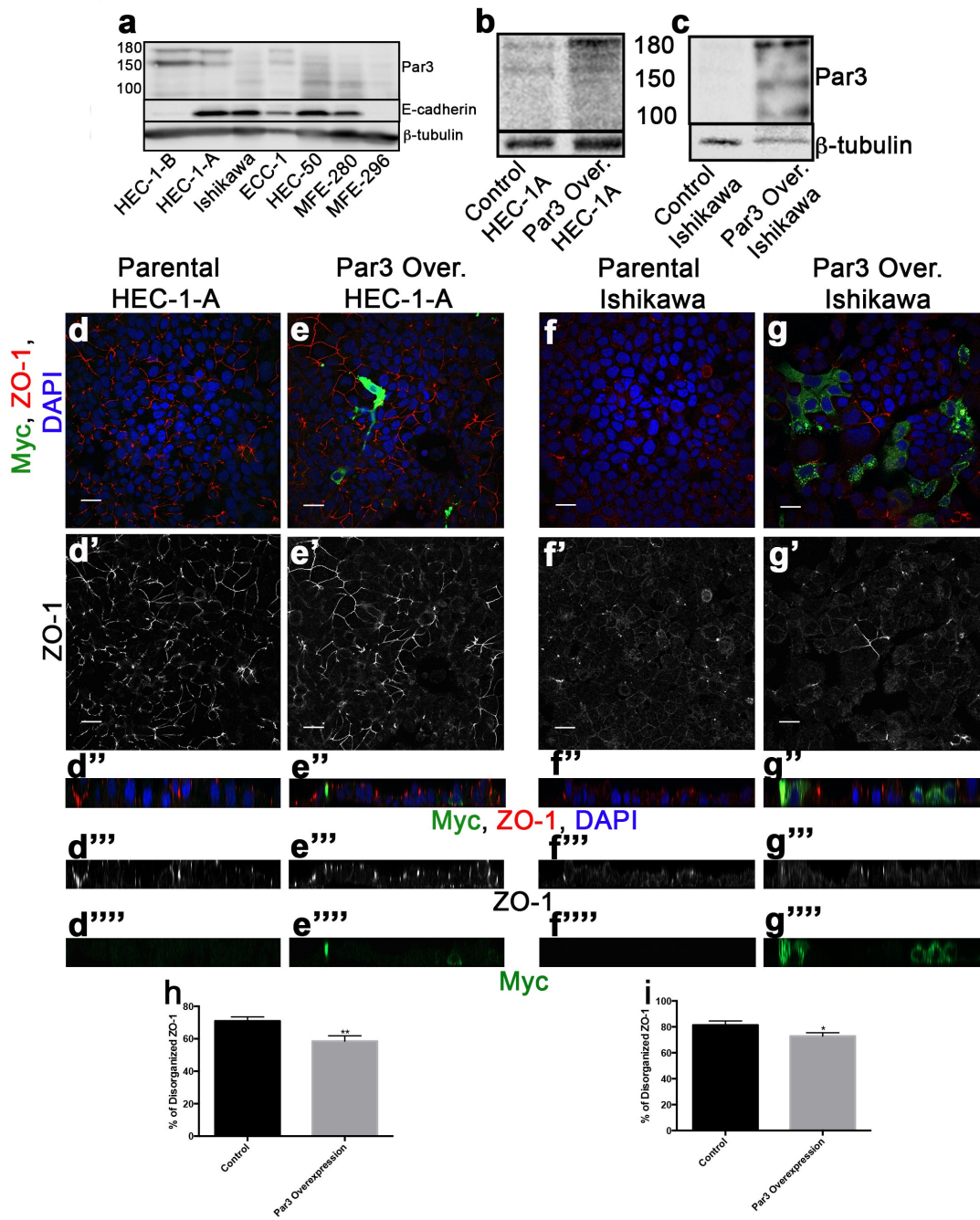


**Figure 17 Expressing Par3 in endometrial cancer cell lines cause differentiation phenotypes.**

Western blot analysis of a panel of endometrial cancer cell lines (HEC-1-B, HEC-1-A, Ishikawa, ECC-1, HEC-50, MFE-280, and MFE-296) for Par3 and E-cadherin (**a**). Ishikawa and ECC-1 are well-differentiated cell lines, HEC-1-A, HEC-1-B, MFE-296 are moderately differentiated cell lines, and HEC-50, MFE-280 are poorly differentiated cell lines (**a**). Western blot analysis of Par3 in control transfection (control) and Myc-Par3 overexpression in Hec-1-A (**b**) and Ishikawa (**c**) cells (**b-c**). Parental (**d, f**) or exogenous Par3 (**e, g**) in HEC-1-A (**d-e**) or Ishikawa (**f-g**) cells stained with ZO-1 (red), Myc (green), and DAPI (**d-g**). Scale bar, 20  $\mu$ M. ZO-1 only staining (**d'-g'**). Z-plane showing ZO-1, Myc and/or DAPI staining (**d''-g''**, **d'''-g'''**, **d''''-g''''**). Quantification of disorganized ZO-1 in the parental (n = 3) and Par3 overexpression HEC-1-A cells (n = 3) for at least three regions of interest (ROI) per experiment (**h**). Error bars represent. SEM \*\*<0.01. Quantification of disorganized ZO-1 in the parental (n = 3) and Par3 overexpression Ishikawa cells (n = 3) for at least three regions of interest (ROI) per experiment (**i**). Error bars represent. SEM \*<0.05.

In contrast to parental cells lacking Par3, in which the TJ protein ZO-1 did not localize to apical cell contacts in an organized pattern, we observed a more fence-like organization of ZO-1 in cells overexpressing Par3 (Figure 17d-i). These data are concordant with our previous observations indicating Par3 loss causes decreased differentiation in MDCK cells (Figure 14n-s). In addition, cells ectopically expressing Par3 showed lower levels of proliferation than in the parental endometrial tumor cell lines lacking Par3, as visualized by BrdU incorporation (Figure 18a-f). Finally, cells expressing exogenous Par3 showed an increase in Notch1 localization to cell:cell contacts compared to cytoplasmic Notch1 localization in parental cells with reduced levels of Par3 (Figure 18g-h). Interestingly, HES-1 (a Notch downstream target) also trended toward an increase in both Par3 overexpression cell lines (Figure 19a,d). These data provide evidence that expression and apical localization of Par3 is critical for the proper differentiation of the endometrial epithelium cells, and that disruption of apicobasal polarity affects the ability of endometrial epithelium to regulate differentiation, proliferation, and Notch receptor localization (Figure 18i).

### **5.25 Decreases in proliferation and migration observed in Par3 overexpressing cells is due to Notch signaling.**

Increased migration is a hallmark of cancer cells in culture, we examined migration in the endometrial cancer cell lines in the presence or absence of Par3. Par3 overexpression was found to decrease the distance HEC-1-A cells moved (Figure 19b, g-j). In addition, a similar trend was observed in Ishikawa cells, where Par3 overexpression decreased the distance that cells traveled

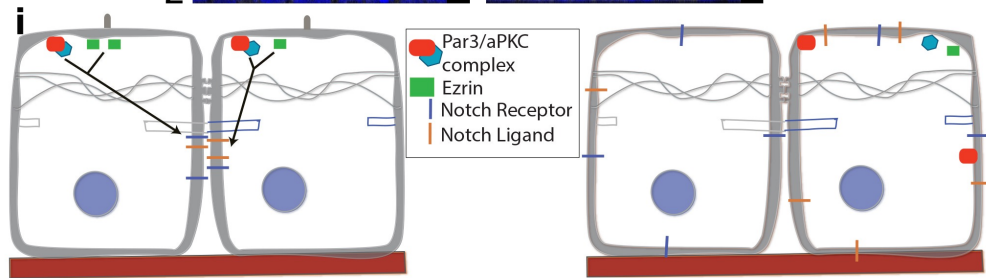
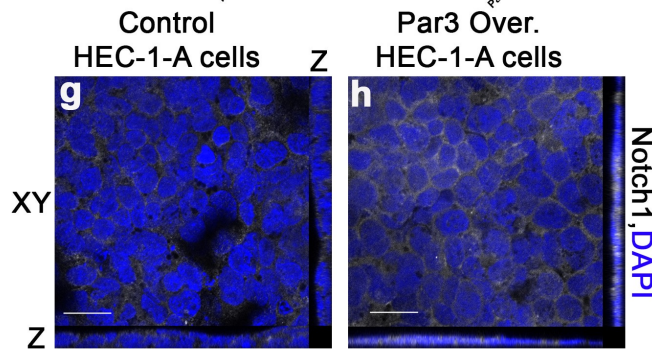
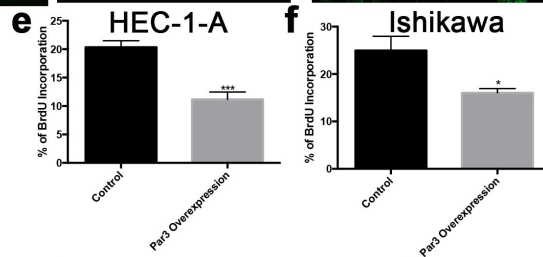
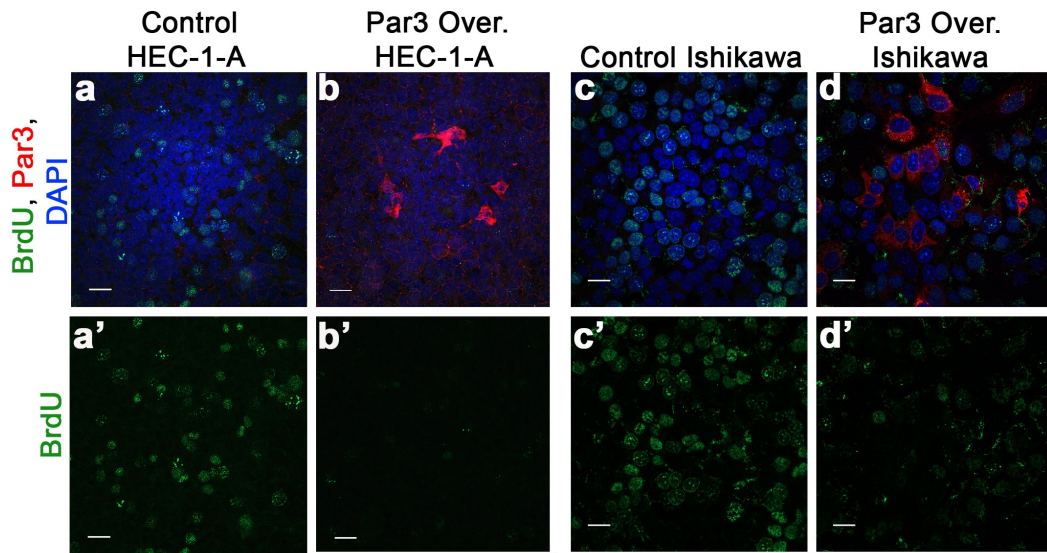




**Figure 18 Expressing Par3 in endometrial cancer cell lines blocks proliferation.**

Staining of parental (**a, c**) and Par3 overexpressing (**b, d**) Hec-1-A (**a-b**) and Ishikawa (**c-d**) cells for Par3, BrdU, and DAPI (**a-d**). Scale bar, 20  $\mu$ M. BrdU only staining (**a'-d'**). Quantification of BrdU incorporation in the parental (n = 3) and Par3 overexpression (n = 3) in HEC-1-A (**e**) and Ishikawa (**f**) cells for at least three ROI per experiment. Error bars represent. SEM \* $<0.05$ . \*\*\* $<0.001$ . Parental HEC-1-A (**g**) or HEC-1-A with exogenous Par3 (**h**) stained with DAPI and Notch1 (**g-h**). Schematic of proposed model for how apicobasal polarity controls differentiation of endometrial epithelial cells by regulating Notch receptor localization and, Notch downstream targets that modulate proliferation and differentiation (**i**).

(Figure 19e, k-n). To determine if the changes to proliferation and migration were related to Notch signaling, we utilized the  $\gamma$ -secretase inhibitor DAPT (N-[N-(3,5-Difluorophenacetyl)-L-alanyl]-S-phenylglycine t-butyl ester). Parental and Par3 overexpressing HEC-1-A and Ishikawa cells were treated with DAPT. HES-1 mRNA levels confirmed Notch signaling was inhibited when either parental or Par3 overexpression cells were treated (Figure 19a,d). The amount of distance traveled was measured and it was determined Par3 expressing cells treated with DAPT had similar amounts of migration as either HEC-1-A or Ishikawa parental cell lines respectively treated with DAPT (Figure 19b, e, g-n). Additionally, BrdU incorporation was shown to be similar between parental cell lines and Par3 overexpression cell lines when treated with DAPT (Figure 19c, f, o-r). These results demonstrate that Par3 expression increases Notch signaling in endometrial cancer cell lines resulting in decreased proliferation and migration.

### **5.26 PTEN loss decreases the effectiveness of Par3 expression in endometrial cancer cells**

PTEN (phosphatase and tensin homolog) is mutated in at least 50% of low-grade endometrial cancer cases, with 75% of cases showing protein loss(196). This indicates inactivation of PTEN can occur through either genomic mutation or post-translational mechanisms and deletion of PTEN can cause endometrial cancer *in vivo*(36, 196). PTEN is known as a negative regulator of the PI3K (Phosphoinositide 3-kinase) signaling pathway by converting the membrane lipid PIP<sub>3</sub> (phosphatidylinositol (3,4,5)-triphosphate) to PIP<sub>2</sub> (phosphatidylinositol (3,4,5)-biphosphate as previously discussed in Chapter 1

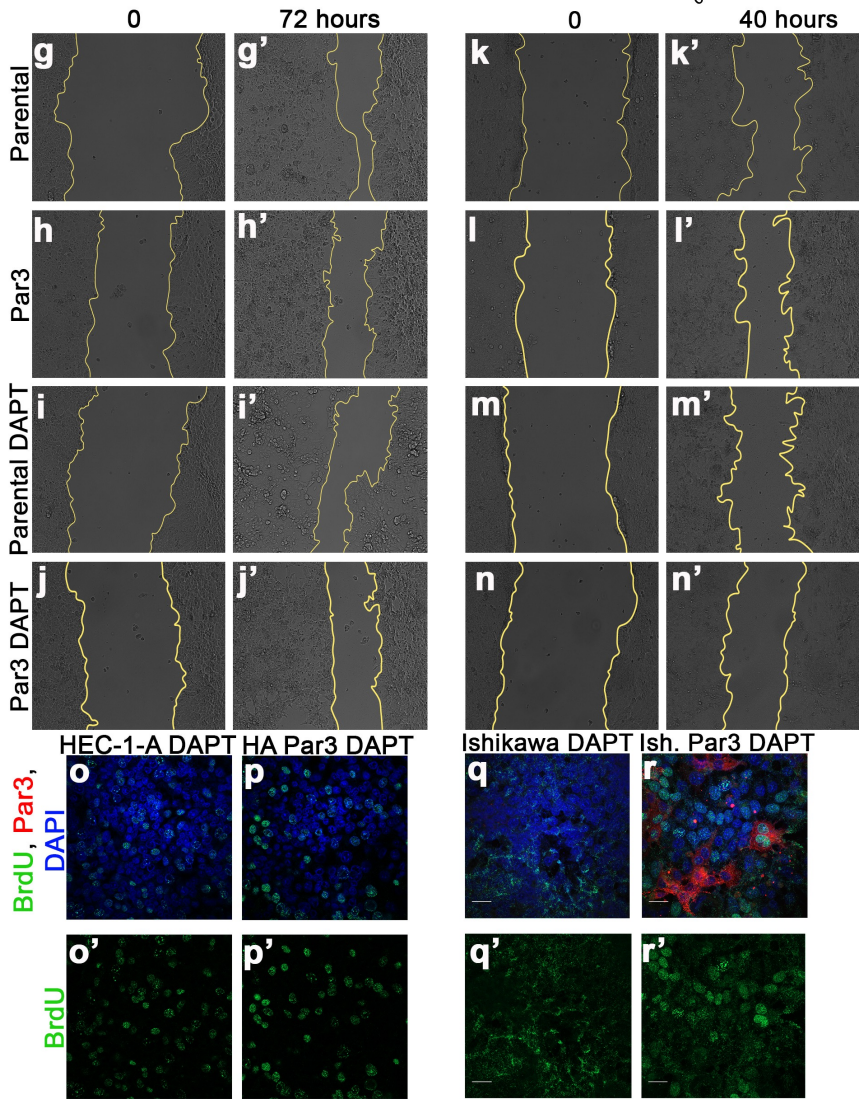
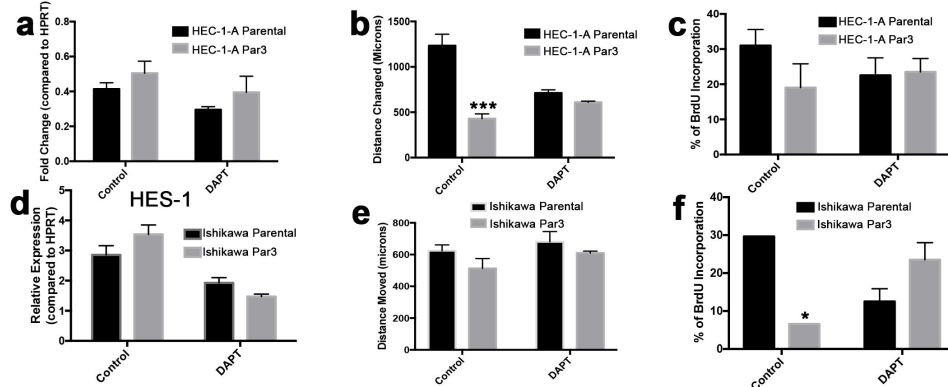


**Figure 19 Inhibiting Notch signaling rescues Par3 mediated changes in migration and proliferation.**

qRT-PCR analysis of the Notch target HES-1 in parental, Par3 overexpression and DAPT treated HEC-1-A (a) and Ishikawa (d) cells (a, d). Quantification of cell migration for HEC-1-A (b) and Ishikawa (e) parental, Par3 overexpression, and cells treated with the  $\gamma$ -secretase inhibitor (DAPT) to block Notch signaling (b, e). Quantification of BrdU incorporation in the parental, Par3 overexpression, and DAPT treated HEC-1-A (c) and Ishikawa (f) cells (c-f). Images showing the start and end of migration assays performed to examine rate of migration for HEC-1-A (g-j, g'-j') and Ishikawa (k-n, k'-n') parental cells (g, k), Par3 expression cells (h, l), and cells treated with DAPT (i-j, m-n). Immunofluorescent analysis of BrdU incorporation in HEC-1-A or Ishikawa parental cells treated with DAPT (o, q, o', q') or Par3 expressing cells treated with DAPT (p, r, p', r'). Top panels (o-r) show BrdU (green) with DAPI (blue) staining and panels (o'-r') show BrdU staining alone. Scale bar, 20  $\mu$ M. \*P<0.05, \*\*\*P<0.0001.

(Figure 20a)(317). PIP<sub>3</sub> is necessary for proper formation of the basal membrane and PIP<sub>2</sub> is found at the apical membrane in epithelium (Figure 20a)(193, 318). PTEN is also important for proper apical protein localization and is necessary for the formation of the apical membrane in epithelial cells(132). In fact, PTEN binds Par3 on the third PDZ binding domain (Figure 20b)(127, 131). It has been hypothesized that PTEN is able to assist in apicobasal polarity establishment through actin organization or apical protein localization(127, 131).

Since PTEN is inactivated in a majority of low-grade endometrial cancers, we examined PTEN protein in the panel of seven endometrial cancer cell lines previously examined for Par3 (Figure 17a, Figure 20c). We observed that many of the cell lines had low levels of PTEN including Ishikawa cells. In order to understand what role PTEN plays, we compared the phenotypes between the Ishikawa Par3 expression cell line and two cell lines containing PTEN: HEC-1-A and MFE-280 Par3 expression cell lines (Figure 20a). Initial observations showed that HEC-1-A cells had a more pronounced decrease in proliferation and the MFE-280 cells even showed a change from a multi-layer epithelial sheet to monolayer or bilayer epithelial sheet (Figure 18a-d, Figure 20d-e). Notch1 localization to the membrane increases in both Ishikawa and HEC-1-A cell lines when Par3 is expressed, however, it was more evident in the HEC-1-A Par3 expression cell lines (Figure 16g-h, Figure 20f-g). Ishikawa Par3 expressing cells reacted more to DAPT, the Notch signaling inhibitor, than HEC-1-A Par3 expressing cells in terms of proliferation and changes in HES-1 expression (Figure 19a, c-d, f, o-r).

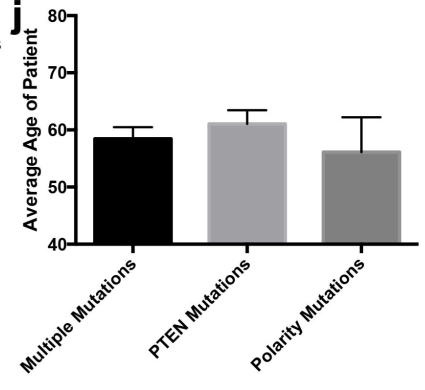
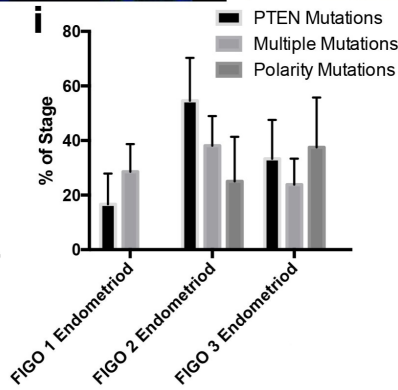
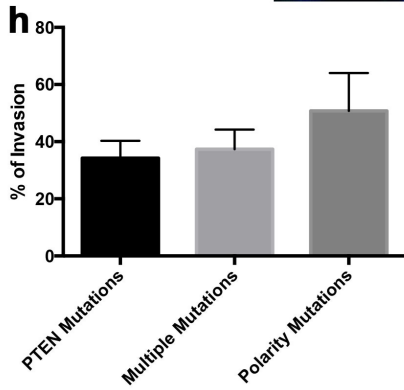
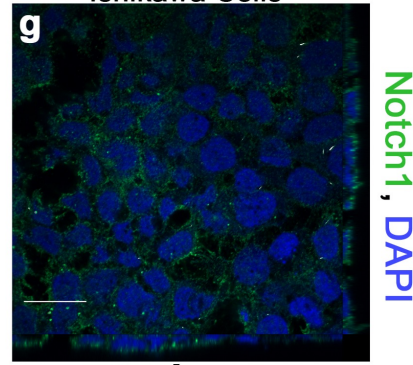
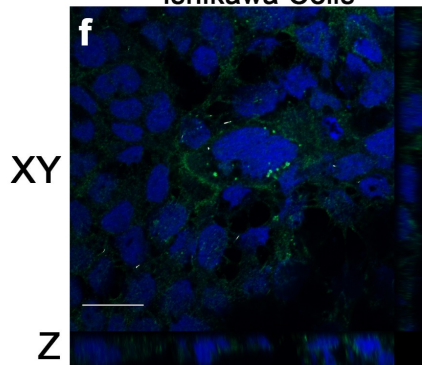
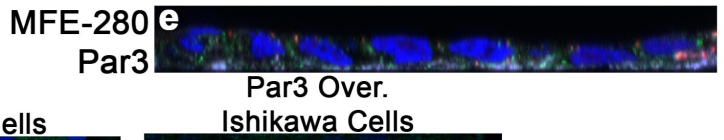
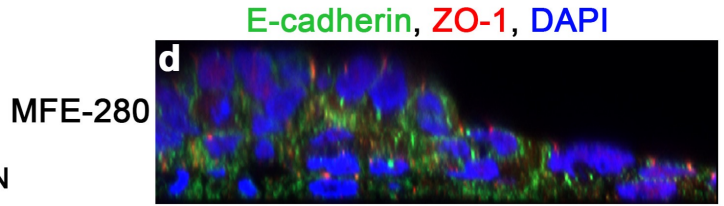
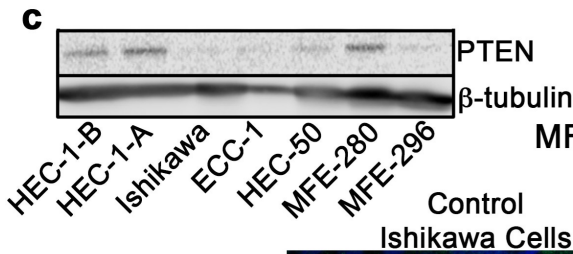
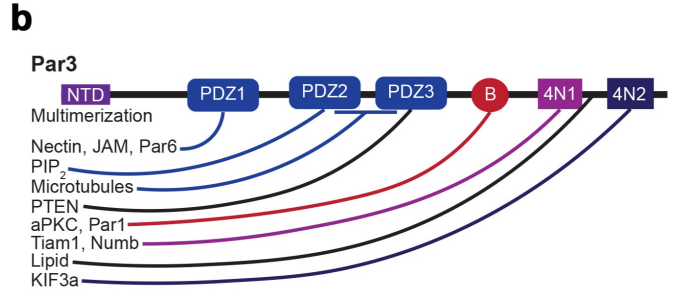
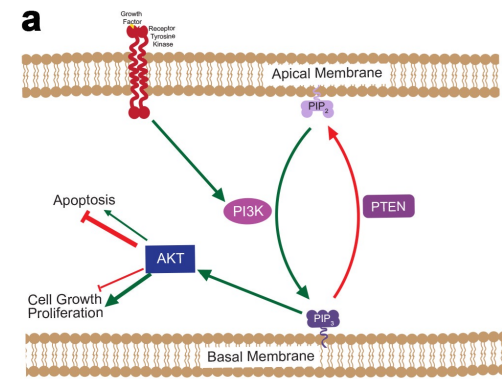


## Figure 20 The role of tumor suppressor PTEN in Par3-depletion phenotypes.

PI3K (Phosphoinositide 3-kinase) signaling consists of PTEN converting PIP<sub>3</sub> to PIP<sub>2</sub> and PI3K converting PIP<sub>2</sub> to PIP<sub>3</sub>(a)(317). PIP<sub>3</sub> causes activation of AKT (protein kinase B) which leads to inhibition of apoptosis and increases in cell growth (a). PIP<sub>2</sub> localizes to the apical membrane while PIP<sub>3</sub> is involved in basal membrane formation (a)(193, 318). Par3 binding partners include Par6, Numb, Kif3a, and PTEN (b). Western blot analysis of PTEN in seven endometrial cancer cell lines including HEC-1-B, HEC-1-A, Ishikawa, ECC-1, HEC-50, MFE-280, and MFE-296 (c). XZ-plane images of E-cadherin, ZO-1, and DAPI in MFE-280 parental (d) and Par3 overexpression (e) cells. Parental Ishikawa cells (f) or Ishikawa cells with exogenous Par3 (g) stained with DAPI and Notch1 (f-g). Quantification of invasion in ECs categorized by PTEN mutations, polarity mutations, or a combination of the two (h). Percentage of ECs by stage that have PTEN mutations, polarity mutations or a combination of the two (i). Quantification of the age of patients with PTEN mutations, polarity mutations, or a combination of the two (j).

Figure 20g)(164, 165). In addition, lower FIGO stage tumors have high amounts of polarity and PTEN mutations (Figure 20h)(164, 165). Finally, the age of patients diagnosed with endometrial cancer trended toward a decrease with polarity mutations with or without PTEN mutations in combination (Figure 20i)(164, 165). This points toward polarity potentially being involved in the low-grade or initial stages of endometrial cancer in addition to inactivation of PTEN.

### 5.3 Summary

From previous chapters, we found that Merlin regulates apicobasal polarity in the endometrium and is necessary for proper endometrial homeostasis. Polarity is frequently disrupted in epithelial cancers including endometrial cancer. We determined that similar to the Nf2eeKO mice, polarity was disrupted in early stage endometrial cancers, while E-cadherin exhibited relatively normal staining, demonstrating that cell polarity and cell adhesion can be exclusively affected. In order to understand how polarity was affecting the underlying biology of endometrial cancer, we utilized both canine kidney (MDCK) cells in three-dimensional cultures and endometrial cancer cell lines. Par3 loss in MDCK cells caused a multi-lumen phenotype similar to low-grade endometrial cancers. To understand what was causing an increase in proliferation in the MDCK cells without Par3, we examined a signaling pathway known to be affected by polarity proteins and regulated during menstruation, Notch signaling(81, 245). Par3, Ezrin, and Merlin knockdown in MDCK cells showed a decrease in Notch signaling downstream targets.



In addition, many endometrial cancer cell lines have low levels of Par3 protein. When Par3 is expressed in these cell lines, proliferation and migration decreases, potentially in a PTEN-dependent manner. Since Notch signaling was downregulated in the MDCK cells depleted of Par3, we examined Notch downstream targets in the endometrial cancer cell lines. We found there was a trend of HES-1 increasing in the Par3 expressing cells compared with the parental control cells. In order to confirm that Notch signaling played a role in proliferation and migration, we utilized a  $\gamma$ -secretase inhibitor and observed an increase in proliferation and migration, similar to parental cells treated with the inhibitor. This indicates that Notch signaling is involved in the changes in proliferation and migration. Interestingly, a Notch mutant mouse causes a similar phenotype as to what we observe in our Nf2seeKO and Nf2eeKO mice potentially showing that Notch is also important when polarity is disrupted in the endometrium(26). All together this data strongly suggests that polarity is necessary for proper membrane-bound Notch receptor signaling and tissue homeostasis in the endometrium; and the dysregulation of the Par complex early in endometrial cancers is involved in the progression of these tumors.

## Chapter 6: Conclusions, Discussion, and Future Directions

### 6.1 Conclusions and Discussion

Apicobasal polarity is known to be necessary for the asymmetric division of a one-cell embryo and proper development and homeostasis of epithelial tissues(72, 124, 139). Polarity has been noted to change during implantation of a blastocyst, but otherwise has not been examined within the endometrium. The endometrium is a complex organ that goes through two different types of tubulogenesis: Mullerian duct formation and endometrial gland development. Recognizing how polarity is involved in the endometrium can help us understand infertility, uterine diseases, and proper endometrial development. This dissertation delves into how the uterus utilizes apicobasal polarity and the polarity regulator, Merlin, to properly develop and function.

Merlin heterozygous female mice have a decreased litter size(219), however, before this dissertation it was not well understood why. We show that a conditional deletion of Merlin in the endometrium causes a loss of endometrial glands and disruption of apicobasal polarity on the luminal epithelium. The subfertility phenotype observed in *Nf2<sup>-/+</sup>* female mice may be caused by a loss of heterozygosity within some regions of the endometrium, affecting the number of endometrial glands. The affect that Merlin has on endometrial glands is not completely unexpected since Merlin has been shown previously to be involved in renal tubule proliferation and hair follicle formation(225, 238).

The loss of Merlin in the endometrium both embryonically (*Wnt7a-Cre*) and postnatally (*PR-Cre*) caused the loss of endometrial glands indicating the loss of glands is not due to defects in Mullerian duct formation. Additionally, through the two conditional Merlin knockouts, we have shown that Merlin deletion in the epithelium specifically causes the aglandular phenotype. Endometrial gland loss was accompanied by loss of FoxA2 and Sox9 nuclear expression in a majority of the endometrial epithelium. While most cells did lose FoxA2 and Sox9 there was a small subset of luminal epithelium that exhibited nuclear staining of these transcription factors. Muc1 staining also showed discrete areas that were similar in intensity to wild-type endometrial glands. *Nf2seeKO (Nf2<sup>lox/lox</sup>; PR-Cre)* mice are infertile, implying that the luminal epithelium that is positive for glandular markers may not fully function as glands. These results suggest that Merlin-deficient luminal epithelium is able to turn on some glandular transcription factors but is unable to properly form glandular architecture or function as glands.

If this is the case then we would expect proliferation, apoptosis, or cell movement/tension to change within the forming endometrial glands. Proliferation and apoptosis were examined to find minimal changes to the luminal epithelium at an early developmental stage suggesting that another area must be defective in gland formation. In order for the luminal epithelium to involute and form the glandular epithelium, changes in mechanical stress must occur allowing the initiation of the budding glandular structure. Tension markers were examined in Merlin-deficient tissue to show that an accumulation of Vinculin, Myosin IIB, and pMLC were observed at the basal membrane. Interestingly, the distribution of

cell:cell versus cell:extracellular matrix adhesion angles were also skewed between wild-type and Merlin-deficient tissue indicating disorganization of the luminal epithelium leading to stretching of the epithelial basal surface. We postulated that this change in basal membrane tension and angle distribution is related to the formation of a contractile actin ring at the apical lumen. When examined, we found a significant increase in intensity of the actin staining on the apical surface of the Merlin-deficient tissues. The increase in actin intensity was not only present at early stages like P7 but persisted and intensified by P21. Merlin is important in F-actin stabilization and loss of Merlin causes increased apical constriction in other epithelium(232, 319). This may indicate that the changes in transcription factors in the Merlin mutant could be caused by the increased apical constriction and changes in cellular tension.

A recent study demonstrated that the Hippo and Wnt pathway are involved in the response a cell has to tension(284). Nuclear  $\beta$ -catenin increased with strain in mammalian cells in a cadherin-dependent manner(284). Wnt signaling is also necessary in endometrial gland development(35, 46). Since  $\beta$ -catenin staining looked similar between wild-type and Merlin-deficient tissue, we utilized qRT-PCR to examine mRNA expression of Wnt downstream targets. We determined that Myc, a Wnt signaling downstream target, was significantly decreased. There was also a slight decrease in Sox9 mRNA expression. However, Wnt signaling downstream targets can be regulated in a tissue specific fashion and other Wnt downstream targets like Axin2 and Cyclin D1 were upregulated in P7 tissue. Conditional loss of Merlin in other epithelium causes

changes to EGFR (Epidermal Growth Factor Receptor) internalization increasing the amount of EGFR signaling(232). Potentially the increase observed in Cyclin D1 is related to EGFR signaling since Cyclin D1 has also been observed downstream of the EGFR pathway(320). Interestingly, Sox17, a Wnt signaling negative regulator, was significantly higher in Nf2eeKO (*Nf2<sup>lox/lox</sup>; Wnt7a-Cre*) mice than wild-type mice at P7. This could indicate that Merlin regulates Wnt signaling through Sox17. Since Merlin and ERM proteins are known to regulate the apical junctions and the actin cytoskeleton, potentially the increased P-cadherin levels in the mutant endometrium causes the increase in Sox17 because other cadherins have been shown to affect the amount of Sox17 in the endoderm(283). Whether the changes to Wnt signaling or the changes to tension cause the aglandular phenotype observed in both Nf2eeKO and Nf2seeKO mice are not understood. However, unlike most Wnt signaling mouse mutants(4, 25, 290), Nf2eeKO and Nf2seeKO have discrete patches of luminal epithelium that appear to function like wild-type glandular epithelium. This indicates that potentially Wnt signaling is secondary to the effects of tension and in fact the inability to form glandular architecture is due to changes in the cytoskeleton of the epithelium.

Loss of Merlin also causes a loss of polarized endometrial epithelium. This loss of polarity may be what promotes the tension-mediated aglandular phenotype. Polarity has previously been shown to be important in proper tubulogenesis(321). Even more importantly, loss of polarity, specifically the Par complex can cause apical constriction in epithelium(322). In *Drosophila*, dPar3

(Bazooka) deletion caused apical constriction pulses to persist longer than wild-type *Drosophila*(323). While in mammalian cell culture, loss of Par3 with mislocalization of aPKC caused an increase in ROCKs (Rho-associated kinases) mediated apical constriction(322). Thus the loss of Merlin causing mislocalization of Par3 and aPKC may cause the increased apical actin constriction and loss of gland formation(122).

Since polarity is necessary for the proper implantation of a blastocyst in the female uterus, we can postulate that even if endometrial glands were able to form, Merlin-deficient females would have decreased fertility. In addition, there is not a significant change to YAP nuclear localization between wild-type and mutant tissue, suggesting this aglandular phenotype could be independent of Hippo signaling. Since Wnt signaling is known to be involved in gland formation and is affected in our Merlin-deficient mice, Wnt signaling could be critical for the loss of glands.

The decrease in Wnt signaling in Nf2eeKO mice at P7 may be regulated by the role Merlin plays in cell junction maturation (Figure 3d). Since Merlin is necessary for the proper formation of adherens junctions, potentially the loss of Merlin causes an increase in the cytoplasmic pool of  $\alpha$ -catenin.  $\alpha$ -catenin has been shown to interact with APC and increase the propensity for  $\beta$ -catenin to be phosphorylated and degraded(51). With larger amounts of cytoplasmic  $\alpha$ -catenin, there would be potentially more of an opportunity for APC to phosphorylate  $\beta$ -catenin and in doing so decrease canonical Wnt signaling causing the downregulation of Myc and Sox9 observed.

While both Nf2eeKO and Nf2seeKO mice showed a similar phenotype, there were slight differences between Nf2eeKO and Nf2seeKO mice by P21. This could indicate that Merlin depletion in the stroma does cause an effect on the endometrium, however a stromal specific knockout of Merlin will better identify the individual roles of the epithelium and the stroma. One noted difference was that the myometrial density was more similar to wild-type mice in the Nf2seeKO mice than the Nf2eeKO mice (Figure 5o-p). In addition, Muc1 staining was more intense in the Nf2eeKO luminal epithelium compared to the Nf2seeKO epithelium (Figure 5d-f). Interestingly, a subset of the Nf2eeKO mice, but not the Nf2seeKO mice, exhibit a dual endometrium phenotype (Figure 21a-c). Since Wnt7a-Cre is expressed during Mullerian duct formation, this may be caused by a loss of polarized migration before PR-Cre is active, however this has not been examined in detail.

While the majority of Nf2eeKO mice were unable to survive past 2 months (Figure 10a), Nf2seeKO were viable and we were able to perform a fecundity study to examine if they were fertile. The fecundity study showed that Nf2seeKO mice are infertile. Since the phenotype in the early Nf2eeKO and Nf2seeKO mice are similar, we postulate that Nf2eeKO mice are also infertile. It should be noted that the death of Nf2eeKO mice is not thought to be related to loss of Merlin in the uterus but rather one of the other tissues (lung, neurons, etc) that Merlin is deleted in the Nf2eeKO mice.

Additionally, in the 4-month-old Nf2seeKO mice, we observed a gross morphology and histological change from wild-type mice. Some endometrial

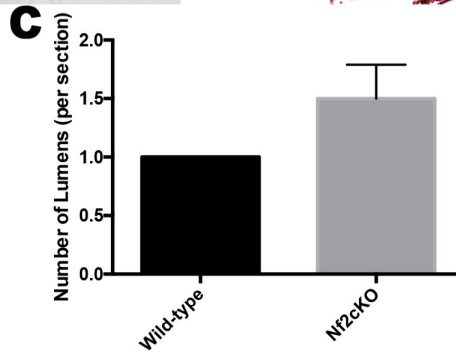
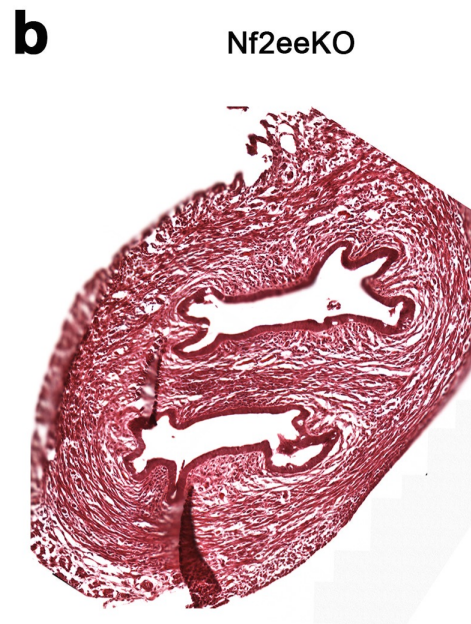
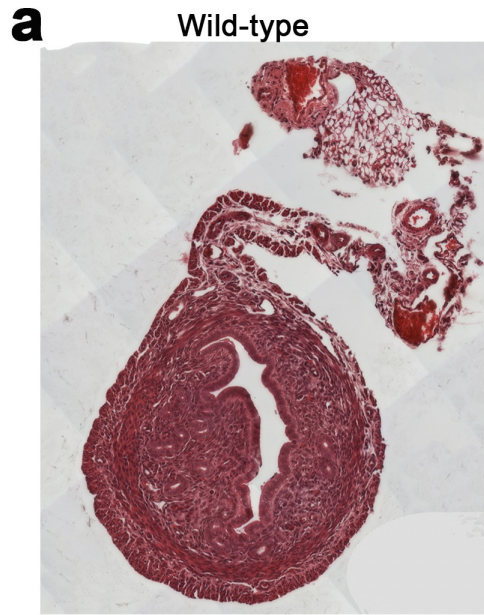




**Figure 21 Nf2eeKO mice has a double endometrium phenotype that Nf2seeKO mice do not.**

Wild-type (a) and Nf2eeKO (b) mice at P21 display a multi-lumen phenotype where 3 mice out of 10 mice have a double endometrium (c).

epithelium was found to have vaginal markers (K14<sup>+</sup>) and the luminal epithelium was condensed to a small ovular lumen. This change in the lumen may be related to the increase in F-actin at the apical surface observed in younger female mice (P7 and P21). Interestingly, the Nf2seeKO uteri look very similar to a wild-type decidualized uterus between E3.5-E5.5(288). The phenotype appeared to worsen over time where the gross morphology of the uterus was drastically more inflamed by 5 months of age. This change in gross morphology between the wild-type and Nf2seeKO uteri were not observed in the few Nf2seeKO uteri we were able to obtain. The phenotype was also exacerbated if the female was mated. This implies that hormonal signaling may be related to the change in the uterine tissue. However, more work is needed to confirm this. Most mouse models that affect decidualization, cause a lack of a decidual reaction or an inability to remodel the tissue after decidualization. Thus, if this tissue is confirmed to be decidua, this would be one of the first mutants that acquires a decidual response without a stimulus.

The 3-6 month old Nf2seeKO mouse also looks similar to a young female rat uterus in diestrus with a smaller ovular lumen(324). As female mice age, they eventually become acyclic(324, 325). One form of an acyclic uterus is persistent anestrus which also shows similarities to the small ovular luminal epithelium in 3-6 month old Nf2seeKO mutants, though it is normally only seen after 14 months of age in mice(324, 325). Thus, Merlin loss in the mouse endometrium may be an accelerated aging phenotype not previously described well in mice.

While we were surprised that the Nf2seeKO mouse model did not develop cancer at 6 months of age, the mouse model did have a cell fate change and abnormal gross morphology of the uterus suggesting it may still develop cancer. There are multiple endometrial hyperplasia and cancer mouse models that do not show malignancies until 10-12 months of age(22, 326). Thus, potentially the Nf2seeKO mice need to age to at least 10 months in order for hyperplasia to be visible. In the E-cadherin null uterus endometrial cancer is also not observed except when they mutate p53 in addition to deleting E-cadherin(45). This may also be an indication that Nf2seeKO mice must accrue other driver mutations with Merlin to drive tumorigenesis. A similar phenotype is observed in a Par3 skin knockout model where an increase in tumorigenesis is only observed when a carcinogen is applied(137).

Merlin is genetically altered in 5% of endometrial cancer cases(164, 165). Polarity genes including those regulated by Merlin are modified in 35% of endometrial cancer cases(164, 165). Interestingly, Par3, a protein directly regulated by Merlin is mislocalized in low-grade endometrial tumors. We found another apical protein, Ezrin, was disrupted in low-grade endometrial cancer. Controversially, one paper determined that Ezrin was not expressed in normal endometrial glands and increased in endometrial cancer, however our work and others work refutes this(200, 202). Since the formation of the apical junctions is necessary for proper apicobasal polarity establishment, we examined whether the apical junctions were also affected in low-grade endometrial cancer. Similar to the Nf2eeKO and Nf2seeKO mice, the adherens junction protein, E-cadherin,

still localizes properly in low-grade human endometrial cancer samples. This indicates adherens junctions are properly formed, however we were unable to tell whether the junctions are functional. Apicobasal polarity disruption without cell adhesion loss appears to be tissue specific, since it has been documented in many cancer cases that cell adhesion loss is linked to the disruption of apicobasal polarity. But our work and a few other labs have shown that cell adhesion may be maintained even when polarity is lost(72, 138, 327).

Previous studies have shown that disruption of polarity proteins like Par3 increase metastasis and late tumor progression(138), but our data indicates that polarity is lost in low-grade samples where metastasis is not common. This implies that polarity may be involved in tumor initiation or early tumor progression. In order to examine whether polarity actually contributes to early tumor formation or progression, we examined Par3 overexpression in endometrial cancer cells and Par3 knockdown in MDCK cells. We determined that Par3 regulates proliferation and migration in these cell lines through Notch signaling suggesting that Par3 is involved in tumor development.

Notch signaling is known to be tumor suppressive and oncogenic in different tissues. We confirm that Notch signaling is tumor suppressive within the endometrium(72, 73). Utilizing a Notch signaling inhibitor, we establish that Notch signaling plays a role in Par3-regulated cell proliferation and migration in endometrial cancer cells. Based on Notch receptor localization data, we postulate polarity is critical for proper membrane partitioning of Notch receptors in the endometrium. This suggests that when polarity is lost, Notch receptors

mislocalize causing aberrant Notch activation since both the Notch receptor and ligand are membrane bound proteins. It may be noted that HES-1 was not comparably increased in the Par3 overexpression endometrial cancer cell lines as the decrease observed in Par3 knockdown MDCK cell lines. Both HEC-1-A and Ishikawa cells are not only from individual tumors but also have been in culture for more than a decade, invariably causing new mutations and expression changes. Potentially these cell lines required more than just Par3 expression to increase Notch signaling. In addition, we are unclear whether polarity loss can only facilitate cancer progression, in the presence of another mutation.

PTEN is mutated in 50-80% of Type I ECs(71) and is known to be involved in cell polarity(130). In addition, PTEN has been shown to be lost in some tumors where it is not mutated(196). PTEN and AKT signaling are also linked to aberrant Notch signaling in prostate cancer(296, 328), so potentially there is a cooperation between PTEN, polarity and Notch signaling in EC. Moreover, when PTEN and polarity genes are genetically altered, there is a trend toward a decrease in cancer patients age and an increase in tumor invasion(164, 165). Thus, it is not unfeasible that PTEN may facilitate tumor progression and utilize polarity disruption to do so. Interestingly, in some endometrial cancer cell lines, those with PTEN and Par3 expression, caused the cells to form a bilayer or monolayer instead of a 4-5 multilayer cell sheet. These Par3 and PTEN expression cancer cell lines may be differentiating since in culture some differentiated mammalian epithelial cells form monolayers and localize ZO-1 to the apical junction.

Interestingly, PTEN, adhesion, and polarity proteins including Par3 have also been shown to have non-autonomous cell functions(246, 292, 329). This data along with the data from Chapter 5 implies that cell intrinsic changes in polarity, PTEN, and even adherens junction-mediated adhesion can be conveyed over a local area of the tissue (246, 292, 329). This is useful when looking at this research as a novel therapeutic approach. In fact, within the endometrial cancer cell line data, we noted that cells that had low to no Par3 present also exhibited decreases in proliferation and increases in tight junction protein localization. This indicates that if polarity is disrupted in a small subset of cells, there may be profound effect on the entire area, making it an interesting model for endometrial tumorigenesis. In addition, potentially finding a targeted approach to polarize a portion of the endometrial malignant epithelium may in fact help the entire endometrium, making this an ideal treatment strategy.

The Merlin-deficient mouse models and our endometrial cancer data both show a disruption of apicobasal polarity. In addition, Notch receptors increase membrane localization in Par3 expressing endometrial cancer cell lines. We postulated that the affect polarity has on Notch signaling is mediated through proper membrane compartmentalization of the Notch receptors. Notch mutant mice also cause an aglandular phenotype similar to the Merlin-deficient mice(26). In addition, both mice show increases in glandular marker, FoxA2, on the endometrial luminal epithelium(26). Merlin loss in the endometrium also causes downregulation of Wnt signaling. Wnt signaling has also been shown to be affected by the proper localization of the Wnt receptors (Frizzleds)(56).

Potentially, the conditional Merlin knockout mouse causes mislocalization of multiple membrane-bound receptors producing misregulation of different signaling pathways including Wnt and Notch leading to the aglandular phenotype observed.

### **6.11 Overall Conclusions**

This work highlights the dynamic nature of endometrial tissue both during development and homeostasis. Moreover, it implies that the proper regulation of apicobasal polarity is necessary for normal development of endometrial glands and for correct endometrial reorganization. This dissertation provides evidence that Merlin plays a role in female fertility and potentially that Neurofibromatosis Type 2 patients should work with genetic counselors for infertility, however in-human data is necessary to confirm this. In addition, this data alludes to a role for Merlin and apicobasal polarity within the aging of the endometrium and endometrial cancer (Figure 22). Figure 22 summarizes the findings of this dissertation. Overall this dissertation reveals novel results that may assist in future therapeutic approaches for female infertility and endometrial cancer.

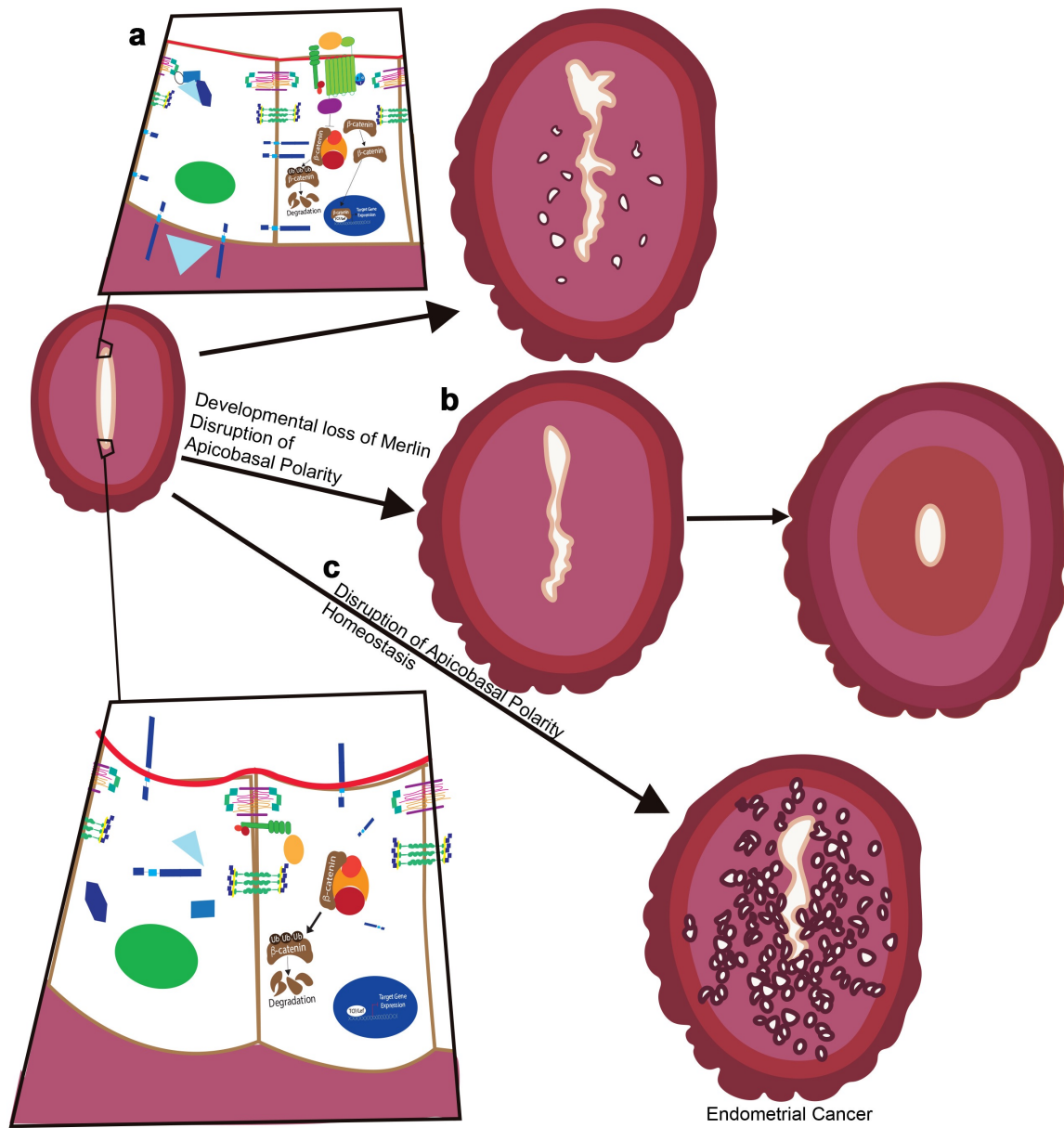




## Figure 22 Summary of Dissertation Findings

A wild-type endometrium forms glands around Postnatal day 5 (P5) that are fully formed by P21 (a). In a Merlin-deficient endometrium, apicobasal polarity is disrupted. In addition, basal membrane tension and apical contractile actin, may cause an increase in Wnt signaling since Wnt is known to react to changes in tension (b). Additionally, since Merlin is known to regulate apical junction maturation, the decrease in Wnt signaling may be related to a large cytoplasmic  $\alpha$ -catenin pool (b).  $\alpha$ -catenin group  $\beta$ -catenin in the presence of APC leading to  $\beta$ -catenin degradation(51). When polarity is lost during endometrial homeostasis this causes a mislocalization of Notch receptors which leads to decreases of Notch signaling and increases in epithelial proliferation and migration (c).

## 6.2 Future Directions

The endometrial cancer work within this dissertation found that apicobasal polarity affects cell migration and proliferation through Notch signaling. However, it would be interesting to examine how Notch receptor overexpression and knockdown cell lines differed or were similar to the Par3 overexpression cell lines. It would also solidify the data to examine how an extracellular membrane mutation that causes mislocalization on the Notch receptor genes affects cell migration and proliferation. In order to understand whether there is cooperation between polarity and PTEN in endometrial cancer, we would like to examine PTEN overexpression and knockdown in the Par3 overexpression cancer cell lines. This will help us determine whether PTEN loss increases cell proliferation, migration, and differentiation.

In addition, we would like to examine if Par3 affects the endometrial cancer cells, non-cell autonomously. In order to do this, we need to generate an inducible Par3 overexpression cell line and co-culture them with parental cells to determine if the parental cells also show a decrease in proliferation and migration. Ideally, utilizing endometrial cancer mouse models, Par3 expression or Notch expression can be examined as a potential endometrial cancer therapeutic. Future studies examining how apicobasal polarity and/or downstream signaling pathways can be manipulated in dynamic tissues such as the endometrium could lead to better therapeutic strategies for patients with endometrial cancer. This work can improve the overall health of endometrial cancer patients and help with quality of life issues that survivors experience(330).

The mouse studies performed in this dissertation showed that Merlin is necessary for proper gland formation. Immunofluorescent stainings show that while neither YAP nuclear staining nor E-cadherin localization differs between wild-type and Merlin-deficient endometrial samples, Par3 localization does. This suggests that loss of apicobasal polarity is necessary for proper endometrial gland formation. A conditional Par3 knockout within the endometrium would confirm this. In addition, we would like to manipulate Mullerian duct development culturing techniques to examine endometrial gland development in real-time. These techniques can also be utilized to understand the double endometrium phenotype found in a subset of the Nf2eeKO mice (Figure 21a-c). We hypothesize this phenotype is related to polarized migration of the Mullerian duct and we can visualize Mullerian duct formation in real-time to determine this.

We can utilize a canonical Wnt signaling reporter mouse (TCF/Lef:H2B-GFP) to determine where Wnt signaling is increased or decreased within the uterus of the Nf2eeKO and Nf2seeKO mice(331). Due to some early data on expression of Sox9 in the nuclei of Nf2eeKO and Nf2seeKO luminal epithelium, we are interested to also examine whether the tissue localization of active canonical Wnt signaling is affected in the early stages of endometrial gland development. Since it has been shown that Wnts are specifically active on the antimesometrial side of the uterus(24), we expect that Merlin may be important for correct localization of Wnt signaling.

In order to determine whether  $\alpha$ -catenin is involved in the decrease of Wnt signaling observed by qRT-PCR, we will examine  $\alpha$ -catenin *in vivo* for changes in localization. Furthermore, we would like to understand the degree to which actin is

affected in the Nf2eeKO and Nf2seeKO uteri through both cell culture and potentially *ex vivo* studies of endometrial tissue. If we are able to create an *ex vivo* technique to culture postnatal tissue, we would like to assess the role of tension in endometrial gland development as well. To investigate tension, we would utilize blebbistatin, a myosin II inhibitor, to manipulate actomyosin tension and observe whether glands are able to form.

In addition, the decidualization-like phenotype observed in Nf2seeKO mice needs to be further characterized and understood. First, to understand whether this is a decidualization phenotype, classification of the decidua is necessary. Confirmation that CD10 (membrane metalloendopeptidase), an endometrial stroma marker, is decreased and that BMP2 (Bone morphogenetic protein 2) increases will assist in this process(332). Furthermore, it has been shown that the makeup of immune cells present in decidua is different than endometrial stroma, specifically there is a decrease in T- and B-cells(333). Once we have confirmed this is in fact a spontaneous decidualization affect, we want to better understand the mechanism. We have hypothesized that since the mice do not begin to exhibit changes in the uteri until after puberty and it is exacerbated in multiparous females, hormones may be involved. In order to confirm this first, hormone levels need to be observed in wild-type versus Nf2seeKO mice. In addition, Nf2seeKO mice should have estradiol and/or progesterone injected to determine how that affects the uterine tissues. To determine whether this is a normal phenotype in aged female mice, we will examine older (1 year to 2 year) uteri for a similar uterus morphology. While we have time

points that span from day 7 to 6 months of age, potentially more time points between 1 month to 4 months are necessary to understand when the phenotype is initiated.

The question was broached of why we do not see tumor formation. To understand whether there will be a delayed tumor phenotype like other mutants, we should examine 12-month time points for potential malignant growths. In addition, PTEN and Merlin are genetically modified together in all except one EC case that Merlin is affected in(164, 165). Additionally, polarity and PTEN mutations together correlate with more invasive tumors than PTEN mutations alone(164, 165). In order to understand whether PTEN and Merlin work together in tumors, a *PTEN<sup>lox/lox</sup>*; *Nf2<sup>lox/lox</sup>*; *PR-Cre* mouse has been generated. Work needs to be done to characterize whether endometrial cancer is present and if it is more invasive than *PTEN<sup>lox/lox</sup>*; *PR-Cre* mice tumors. This dissertation brings to light a role of Merlin and apicobasal polarity in endometrial development and homeostasis that needs to be examined in more detail.

## Chapter 6: Appendix

Mouse Model/ Common Cre	Name used	Description	Reference
<i>PR-Cre</i>		Progesterone Receptor (PR)- Cre: PR knockin that appears to start expressing within the Mullerian duct around postnatal day 1-5. Expression observed in the uterus, ovary, oviduct, mammary gland, and thymus	(249)
<i>Wnt7a-Cre</i>		<i>Wnt7a-Cre</i> : A transgenic mouse line. A Wnt ligand expressed within the Mullerian duct epithelium at embryonic day 12.5. <i>Wnt7a</i> is also expressed within skin, lungs, limb bud formation, and neurogenesis.	(248)
<i>Ctnnb1<sup>lox/lox</sup>; PR-Cre</i>		<i>Ctnnb1<sup>lox/lox</sup></i> : <i>Lox/lox</i> targeting exons 2-6 of b-catenin gene. <i>PR-Cre</i> : previously described (pd)	(46, 334)
<i>Wnt7a<sup>lox/lox</sup>; PR-Cre</i>		<i>Wnt7a<sup>lox/lox</sup></i> : A Wnt ligand that in whole knockout mouse causes disruption of paramesonephric duct differentiation. <i>Lox/lox</i> targets exon 1 and 2 of the <i>Wnt7a</i> <i>PR-Cre</i> : pd	(290)
<i>Wnt5a<sup>lox/lox</sup>; PR-Cre</i>		<i>Wnt5a<sup>lox/lox</sup></i> : A Wnt ligand that is thought to be primarily utilized in the non-canonical planar cell polarity pathway. <i>Lox/lox</i> targeted exons 2 and 3 of <i>Wnt5a</i> . <i>PR-Cre</i> pd	(335, 336)
<i>Rosa26<sup>N1ICD/N1ICD</sup>; PR-Cre</i>		<i>Rosa26<sup>N1ICD/N1ICD</sup></i> : <i>Rosa26</i> promoter causes ubiquitous and constitute expression within mice. N1ICD amino acids 1749-2293 <i>PR-Cre</i> :pd	(26, 337)
<i>Rosa26<sup>N1ICD/N1ICD</sup>; Amhr2-Cre</i>		<i>Rosa26<sup>N1ICD/N1ICD</sup></i> : pd <i>Amhr2-Cre</i> : The Anti-Mullerian Hormone Receptor Type 2 is necessary for the differentiation of male reproductive organs. It is expressed in the ovarian granulosa cells and in the female reproductive tract from embryonic day 12.5. It is specifically expressed within the myometrium and endometrial stroma. Cre is knocked into the <i>Amhr2</i> locus.	(338)
<i>Ctnnb1<sup>lox/lox</sup>; PR-Cre</i>		<i>Ctnnb1<sup>lox/lox</sup></i> : <i>Lox/lox</i> targeting exons 2-6 of b-catenin gene. <i>PR-Cre</i> : previously described (pd)	(46, 334)

<i>Ctnnb1<sup>f(ex3)/+</sup>; PR-Cre</i>		<i>Ctnnb1<sup>f(ex3)</sup></i> : Lox/lox targeted the GSK-3 $\beta$ phosphorylation site in the 3rd exon of $\beta$ -catenin. This phosphorylation is necessary for degradation. PR-Cre:pd	(46)
<i>Vangl2<sup>Lp/wt</sup></i>		<i>Vangl2<sup>LP</sup></i> : Spontaneous point mutation in the <i>Vangl2</i> gene that causes an amino acid change. The heterozygous mice are called Looptail mice and exhibited "looped" tails, harelip, cleft palate, etc. Homozygous mutation causes the neural tube to be completely open.	(339, 340)
<i>Scrib<sup>Crc/wt</sup></i>		<i>Scrib<sup>Crc</sup></i> : Circletail mice have a spontaneous mutation in scribble that causes craniorachischisis in homozygous mice. Heterozygous mice exhibit a kinked tail.	(107)
<i>Dlg3<sup>Gt(P038A02)Wrst/Y</sup></i>		Gene trap vector utilized to mutate <i>Dlg3</i>	(341)
<i>Par3<sup><math>\Delta E3/\Delta E3</math></sup></i>		<i>Par3<sup><math>\Delta E3/\Delta E3</math></sup></i> : The exon 3 is deleted in the Partitioning defective 3 homolog ( <i>Par3</i> ) by flanking LoxP sites around exon 3 with a CAG-Cre.	(133)
<i>Par3<sup>lox/lox</sup>; K14-Cre</i>	Par3eKO	<i>Par3<sup>lox/lox</sup></i> : The <i>Par3<sup>lox/lox</sup></i> allele utilized in the <i>Par3<sup><math>\Delta E3/\Delta E3</math></sup></i> mouse model. K14-Cre: the neo version had weak expression in the basal epidermis and hair follicles. Expression was stronger after birth in the basal epidermis and the hair follicles.	(137, 342)
<i>aPkc<math>\lambda</math><sup>lox/lox</sup>; Nphs1-Cre</i>		<i>aPKC<math>\lambda</math><sup>lox/lox</sup></i> : Lox/lox sites surrounding exon 5 of <i>PKC<math>\lambda</math></i> . Nphs1-Cre: Nphs1 promoter in a Cre transgene that expresses in the podocytes.	(145, 343, 344)
<i>aPkc<math>\lambda</math><sup>lox/lox</sup>; K5-Cre</i>		<i>aPKC<math>\lambda</math><sup>lox/lox</sup></i> : pd. K5-Cre: A transgene containing the Keratin 5 promoter. K5 expression and deletion was observed in the basal epidermis and keratinocytes.	(345)
<i>Par6a<sup>tm1.1(KOMP)Vlcg/tm1.1(KOMP)Vlcg</sup></i>		<i>Pard6a<sup>tm1.1(KOMP)Vlcg</sup></i> : targeted mutation of <i>Pard6a</i> through a consortium	(148)
<i>APC<sup>Min/+</sup>; PKC<math>\zeta</math><sup>-/-</sup></i>		APC: a multiple intestinal neoplasia (Min) of the adenomatous polyposis coli (APC) gene. PKC $\zeta$ : deletion of PKC $\zeta$ by homologous recombination	(140, 346, 347)

<i>Cdh1<sup>lox/lox</sup>; PR-Cre</i>		<i>Cdh1<sup>lox/lox</sup></i> : E-cadherin gene with lox sites surrounding exons 6-10; PR-Cre: pd	(45, 348)
<i>Tjp1<sup>lox/lox</sup>; Nphs1-Cre</i>		<i>Tjp1<sup>lox/lox</sup></i> : Lox/lox sites flank exon 4 of the tight junction protein gene (ZO-1). Nphs-1-Cre: pd	(213)
<i>Cdh1<sup>tm1Cbm/tm1Cbm</sup></i>		<i>Cdh1<sup>tm1Cbm/tm1Cbm</sup></i> : E-cadherin gene with a portion of exon 7 and all of exon 8 replaced by a neomycin insert.	(218)
<i>Nf2<sup>lox/lox</sup>; Alb-Cre</i>	Nf2LKO	<i>Nf2<sup>lox/lox</sup></i> : Merlin gene with lox/lox sites flanking the 2nd exon. Alb-Cre: A transgenic mouse model with the liver-specific albumin promoter	(235, 255, 286)
<i>Nf2<sup>lox/lox</sup>; Vil-Cre</i>		<i>Nf2<sup>lox/lox</sup></i> :pd. Vil-Cre: Vilin promoter attached to a Cre showed expression of the Cre within the cortical renal tubule epithelia	(349)
<i>Nf2<sup>lox/lox</sup>; K14-Cre</i>	Nf2skinKO	<i>Nf2<sup>lox/lox</sup></i> :pd. K14-Cre:pd	
<i>Nf2<sup>lox/lox</sup>; Wnt7a-Cre</i>	Nf2eeKO	<i>Nf2<sup>lox/lox</sup></i> :pd. Wnt7a-Cre:pd	
<i>Nf2<sup>lox/lox</sup>; PR-Cre</i>	Nf2seeKO	<i>Nf2<sup>lox/lox</sup></i> : pd. PR-Cre:pd	
TCF/Lef:H2B-GFP		TCF/Lef:H2B-GFP: TA transgene containing the Wnt signaling responsive element, TCF/Lef was bound to H2B:GFP. Expression is observed when TCF/Lef are active (or Wnt signaling is on).	(331)
<i>PTEN<sup>lox/lox</sup>; PR-Cre</i>		<i>PTEN<sup>lox/lox</sup></i> : Lox/lox sites flanking PTEN gene exon 5. PR-Cre pd	(350)
<i>PTEN<sup>lox/lox</sup>; Nf2<sup>lox/lox</sup>; PR-Cre</i>		<i>PTEN<sup>lox/lox</sup></i> : pd. <i>Nf2<sup>lox/lox</sup></i> : pd. PR-Cre: pd	
<ul style="list-style-type: none"> <li>• <i>Nefh-Cre</i></li> <li>• <i>PO-Cre</i></li> <li>• <i>P0-Sch-Δ(39-121)</i></li> <li>• <i>Mx1-Cre</i></li> <li>• <i>Le-Cre</i></li> <li>• <i>Vil-CreER<sup>T2</sup></i></li> </ul>	Genes in Table 4 not described	Nefh-Cre: A transgenic Cre with the neurofilament-H gene promoter. Expression is observed primarily in the cortex and hippocampal neurons. PO-Cre:A transgenic Cre with the rat P0 gene. Expression is observed in Schwann cells. P0-Sch-Δ(39-121): A 62kD deletion mutant that is expressed in the peripheral nerves. Mx1-Cre: Mx1 promoter driving Cre-recombinase in collecting duct epithelial cells and a subset of nephrons. Induced by IFN-α	(225, 234, 235, 351, 352)



		<p>Le-Cre: The Le gene promoter is present on a transgene with Cre. Expression is initially observed at embryonic 9 in the lens placode and the eye lens.</p> <p>Vil-CreER<sup>T2</sup>: A tamoxifen inducible transgene with a Villin gene promoter bound to a Cre-Estrogen Receptor.</p>	
--	--	--	--

**Table 7 Mouse models discussed within the dissertation.**

## Chapter 7: References

1. Kobayashi, A., and R. R. Behringer. 2003. Developmental genetics of the female reproductive tract in mammals. *Nat. Rev. Genet.* 4: 969–980.
2. Jost, A., and S. Magre. 1984. Testicular development phases and dual hormonal control of sexual organogenesis. *Raven Press* .
3. Kispert, A., N. Chin, A. P. McMahon, S. Vainio, and M. Heikkila. 1999. Female development in mammals is regulated by Wnt-4 signalling. 397: 405–410.
4. Mericskay, M., J. Kitajewski, and D. Sassoon. 2004. Wnt5a is required for proper epithelial-mesenchymal interactions in the uterus. *Development* 131: 2061–2072.
5. Carroll, T. J., J. S. Park, S. Hayashi, A. Majumdar, and A. P. McMahon. 2005. Wnt9b plays a central role in the regulation of mesenchymal to epithelial transitions underlying organogenesis of the mammalian urogenital system. *Dev. Cell* 9: 283–292.
6. Spencer, T. E., K. Hayashi, J. Hu, and K. D. Carpenter. 2005. Comparative Developmental Biology of the Mammalian Uterus. *Curr. Top. Dev. Biol.* 68: 85–122.
7. Belle, M., D. Godefroy, G. Couly, S. A. Malone, F. Collier, P. Giacobini, and A. Chédotal. 2017. Tridimensional Visualization and Analysis of Early Human Development. *Cell* 169: 161–173.e12.
8. Zhao, F., H. L. Franco, K. F. Rodriguez, P. R. Brown, M. Tsai, S. Y. Tsai, and H. H. Yao. 2017. Elimination of the male reproductive tract in the female embryo is

promoted by COUP-TFII in mice. *720*: 717–720.

9. Taylor, H., G. Heuvel, and P. Igarashi. 1997. A conserved Hox axis in the mouse and human female reproductive system: late establishment and persistent adult expression of the Hoxa cluster genes. *Biol. Reprod.* 57: 1336–1345.

10. Branford, W. W., G. V Benson, L. Ma, R. L. Maas, and S. S. Potter. 2000. Characterization of Hoxa-10/Hoxa-11 transheterozygotes reveals functional redundancy and regulatory interactions. *Dev. Biol.* 224: 373–387.

11. Warot, X., C. Fromental-Ramain, V. Fraulob, P. Chambon, and P. Dollé. 1997. Gene dosage-dependent effects of the Hoxa-13 and Hoxd-13 mutations on morphogenesis of the terminal parts of the digestive and urogenital tracts. *Development* 124: 4781–91.

12. Miller, C., and D. A. Sassoon. 1998. Wnt-7a maintains appropriate uterine patterning during the development of the mouse female reproductive tract. *Development* 125: 3201–11.

13. Reed, B. G. 2015. The Normal Menstrual Cycle and the Control of Ovulation. In *EndoText* NCBI Bookshelf.

14. Bronson, F. H., C. P. Dagg, and G. D. Snell. 1968. Reproduction. In *Biology of the Laboratory Mouse* 187–204.

15. Nikolov, D., Hu, S., Lin, J., Gasch, A., Hoffmann, A., Horikoshi, M., Chua.N., Roeder, G., Burley, S. 1992. Blastocyst implantation depends on maternal

expression of leukaemia inhibitory factor. *Nature* 360: 40–46.

16. Chen, J. R., J. G. Cheng, T. Shatzer, L. Sewell, L. Hernandez, and C. L. Stewart. 2000. Leukemia inhibitory factor can substitute for nidatory estrogen and is essential to inducing a receptive uterus for implantation but is not essential for subsequent embryogenesis. *Endocrinology* 141: 4365–4372.

17. Boomsma, C. M., A. Kavelaars, M. J. C. Eijkemans, E. G. Lentjes, B. C. J. M. Fauser, C. J. Heijnen, and N. S. MacKlon. 2009. Endometrial secretion analysis identifies a cytokine profile predictive of pregnancy in IVF. *Hum. Reprod.* 24: 1427–1435.

18. Burton, G. J., A. L. Watson, J. Hempstock, J. N. Skepper, and E. Jauniaux. 2002. Uterine glands provide histiotrophic nutrition for the human fetus during the first trimester of pregnancy. *J. Clin. Endocrinol. Metab.* 87: 2954–2959.

19. Vue, Z., G. Gonzalez, C. A. Stewart, S. Mehra, and R. R. Behringer. 2018. Volumetric imaging of the developing prepubertal mouse uterine epithelium using light sheet microscopy. *Mol. Reprod. Dev.* Accepted: 1–6.

20. Arora, R., A. Fries, K. Oelerich, K. Marchuk, K. Sabeur, L. C. Giudice, and D. J. Laird. 2016. Insights from imaging the implanting embryo and the uterine environment in three dimensions. *Development* 143: 4749–4754.

21. Jeong, J.-W., I. Kwak, K. Y. Lee, T. H. Kim, M. J. Large, C. L. Stewart, K. H. Kaestner, J. P. Lydon, and F. J. DeMayo. 2010. Foxa2 is essential for mouse endometrial gland development and fertility. *Biol. Reprod.* 83: 396–403.

22. Gonzalez, G., S. Mehra, Y. Wang, H. Akiyama, and R. R. Behringer. 2016. Sox9 overexpression in uterine epithelia induces endometrial gland hyperplasia.

*Differentiation* 92: 204–215.

23. Franco, H. L., D. Dai, K. Y. Lee, C. a Rubel, D. Roop, D. Boerboom, J.-W.

Jeong, J. P. Lydon, I. C. Bagchi, M. K. Bagchi, and F. J. DeMayo. 2011. WNT4 is a key regulator of normal postnatal uterine development and progesterone signaling during embryo implantation and decidualization in the mouse. *FASEB J.* 25: 1176–1187.

24. Goad, J., Y. A. Ko, M. Kumar, S. M. Syed, and P. S. Tanwar. 2017. Differential Wnt signaling activity limits epithelial gland development to the anti-mesometrial side of the mouse uterus. *Dev. Biol.* 423: 138–151.

25. Guimarães-Young, A., T. Neff, A. J. Dupuy, and M. J. Goodheart. 2016.

Conditional deletion of Sox17 reveals complex effects on uterine adenogenesis and function. *Dev. Biol.* 414: 219–227.

26. Su, R.-W., M. R. Strug, J.-W. Jeong, L. Miele, and A. T. Fazleabas. 2016.

Aberrant activation of canonical Notch1 signaling in the mouse uterus decreases progesterone receptor by hypermethylation and leads to infertility. *Proc. Natl. Acad. Sci.* 113: 2300–2305.

27. Fisher, C. R., K. H. Graves, A. F. Parlow, and E. R. Simpson. 1998.

Characterization of mice deficient in aromatase (ArKO) because of targeted disruption of the cyp19 gene. *Proc. Natl. Acad. Sci.* 95: 6965–6970.

28. Vandenberg, A. L., and D. A. Sassoon. 2009. Non-canonical Wnt signaling regulates cell polarity in female reproductive tract development via van gogh-like 2. *Development* 136: 1559–1570.
29. Fullerton, P. T., D. Monsivais, R. Kommagani, and M. M. Matzuk. 2017. Follistatin is critical for mouse uterine receptivity and decidualization. *Proc. Natl. Acad. Sci.* 114: 4772–4781.
30. Clementi, C., S. K. Tripurani, M. J. Large, M. A. Edson, C. J. Creighton, S. M. Hawkins, E. Kovanci, V. Kaartinen, J. P. Lydon, S. A. Pangas, F. J. DeMayo, and M. M. Matzuk. 2013. Activin-Like Kinase 2 Functions in Peri-implantation Uterine Signaling in Mice and Humans. *PLoS Genet.* 9.
31. Dupont, S., A. Krust, A. Gansmuller, A. Dierich, P. Chambon, and M. Mark. 2000. Effect of single and compound knockouts of estrogen receptors alpha (ERalpha) and beta (ERbeta) on mouse reproductive phenotypes. *Development* 127: 4277–4291.
32. Post, L. C., and J. W. Innis. 1999. Infertility in adult hypodactyly mice is associated with hypoplasia of distal reproductive structures. *Biol. Reprod.* 61: 1402–1408.
33. Baker, J., M. P. Hardy, J. Zhou, C. Bondy, F. Lupu, A. R. Bellvé, and A. Efstratiadis. 1996. Effects of an Igf1 gene null mutation on mouse reproduction. *Mol. Endocrinol.* 10: 903–18.
34. Dai, X., C. Schonbaum, L. Degenstein, W. Bai, A. Mahowald, and E. Fuchs.

1998. The ovo gene required for cuticle formation and oogenesis in flies is involved in hair formation and spermatogenesis in mice. *Genes Dev.* 12: 3452–3463.

35. Dunlap, K. A., J. Filant, K. Hayashi, E. B. Rucker 3rd, G. Song, J. M. Deng, R. R. Behringer, F. J. DeMayo, J. Lydon, J. W. Jeong, and T. E. Spencer. 2011. Postnatal deletion of *Wnt7a* inhibits uterine gland morphogenesis and compromises adult fertility in mice. *Biol. Reprod.* 85: 386–396.

36. Daikoku, T., Y. Hirota, S. Tranguch, A. R. Joshi, F. J. DeMayo, J. P. Lydon, L. H. Ellenson, and S. K. Dey. 2008. Conditional loss of uterine *Pten* unfaillingly and rapidly induces endometrial cancer in mice. *Cancer Res.* 68: 5619–27.

37. Gonzalez, G., and R. R. Behringer. 2009. *Dicer* is required for female reproductive tract development and fertility in the mouse. *Mol. Reprod. Dev.* 76: 678–688.

38. Bellessort, B., M. Le Cardinal, A. Bachelot, N. Narboux-Nême, P. Garagnani, C. Pirazzini, O. Barbieri, L. Mastracci, V. Jonchere, E. Duvernois-Berthet, A. Fontaine, G. Alfama, and G. Levi. 2016. *Dlx5* and *Dlx6* control uterine adenogenesis during post-natal maturation: Possible consequences for endometriosis. *Hum. Mol. Genet.* 25: 97–108.

39. Shelton, D. N., H. Fornalik, T. Neff, S. Y. Park, D. Bender, K. DeGeest, X. Liu, W. Xie, D. K. Meyerholz, J. F. Engelhardt, and M. J. Goodheart. 2012. The role of *LEF1* in endometrial gland formation and carcinogenesis. *PLoS One* 7: 1–11.

40. Cui, T., B. He, S. Kong, C. Zhou, H. Zhang, Z. Ni, H. Bao, J. Qiu, Q. Xin, D.

Reinberg, J. P. Lydon, J. Lu, and H. Wang. 2017. PR-Set7 deficiency limits uterine epithelial population growth hampering postnatal gland formation in mice. *Cell Death Differ.* 24: 2013–2021.

41. Filant, J., and T. E. Spencer. 2013. Endometrial glands are essential for blastocyst implantation and decidualization in the mouse uterus. *Biol. Reprod.* 88: 93.

42. Zhang, X., E. Hoang, and W. B. Nothnick. 2009. Estrogen-induced uterine abnormalities in TIMP-1 deficient mice are associated with elevated plasmin activity and reduced expression of the novel uterine plasmin protease inhibitor serpinb7. *Mol. Reprod. Dev.* 76: 320–331.

43. Hayashi, K., S. Yoshioka, S. N. Reardon, E. B. Rucker, T. E. Spencer, F. J. DeMayo, J. P. Lydon, and J. A. MacLean. 2011. WNTs in the neonatal mouse uterus: potential regulation of endometrial gland development. *Biol. Reprod.* 84: 308–19.

44. Sone, M., K. Oyama, Y. Mohri, R. Hayashi, H. Clevers, and K. Nishimori. 2013. LGR4 expressed in uterine epithelium is necessary for uterine gland development and contributes to decidualization in mice. *FASEB J.* 27: 4917–4928.

45. Reardon, S. N., M. L. King, J. a. MacLean, J. L. Mann, F. J. DeMayo, J. P. Lydon, and K. Hayashi. 2012. Cdh1 Is Essential for Endometrial Differentiation, Gland Development, and Adult Function in the Mouse Uterus. *Biol. Reprod.* 86: 141–141.



46. Jeong, J.-W., H. S. Lee, H. L. Franco, R. R. Broaddus, M. M. Taketo, S. Y. Tsai, J. P. Lydon, and F. J. DeMayo. 2009. Beta-Catenin Mediates Glandular Formation and Dysregulation of Beta-Catenin Induces Hyperplasia Formation in the Murine Uterus. *Oncogene* 28: 31–40.
47. Franco, H. L., K. Y. Lee, C. a Rubel, C. J. Creighton, L. D. White, R. R. Broaddus, M. T. Lewis, J. P. Lydon, J.-W. Jeong, and F. J. DeMayo. 2010. Constitutive activation of smoothened leads to female infertility and altered uterine differentiation in the mouse. *Biol. Reprod.* 82: 991–999.
48. Krege, J. H., J. B. Hodgins, J. F. Couse, E. Enmark, M. Warner, J. F. Mahler, M. Sar, K. S. Korach, J.-A. Gustafsson, O. Smithies, K. S. Korach, J. a Gustafsson, and O. Smithies. 1998. Generation and reproductive phenotypes of mice lacking estrogen receptor beta. *Proc. Natl. Acad. Sci. U. S. A.* 95: 15677–15682.
49. Calder, M., Y. M. Chan, R. Raj, M. Pampillo, A. Elbert, M. Noonan, C. Gillio-Meina, C. Caligioni, N. G. Bérubé, M. Bhattacharya, A. J. Watson, S. B. Seminara, and A. V. Babwah. 2014. Implantation failure in female Kiss1<sup>-/-</sup> mice is independent of their hypogonadic state and can be partially rescued by leukemia inhibitory factor. *Endocrinology* 155: 3065–3078.
50. Afshar, Y., J.-W. Jeong, D. Roqueiro, F. DeMayo, J. Lydon, F. Radtke, R. Radnor, L. Miele, and a. Fazleabas. 2012. Notch1 mediates uterine stromal differentiation and is critical for complete decidualization in the mouse. *FASEB J.* 26: 282–294.

51. Choi, S. H., C. Estarás, J. J. Moresco, J. R. Yates, and K. A. Jones. 2013.  $\alpha$ -Catenin interacts with APC to regulate  $\beta$ -catenin proteolysis and transcriptional repression of Wnt target genes. *Genes Dev.* 27: 2473–2488.
52. Kim, S., and E. Jho. 2016. Merlin, a regulator of Hippo signaling, regulates Wnt/beta-catenin signaling. *BMB Rep.* 23: 1638–1647.
53. Quan, M., J. Cui, T. Xia, Z. Jia, D. Xie, D. Wei, S. Huang, Q. Huang, S. Zheng, and K. Xie. 2015. Merlin/NF2 Suppresses Pancreatic Tumor Growth and Metastasis by Attenuating the FOXM1-Mediated Wnt/beta-catenin Signaling. *Cancer Res.* 75: 4778–4790.
54. Konsavage, W. M., and G. S. Yochum. 2013. Intersection of Hippo / YAP and Wnt /  $\beta$ -catenin signaling pathways. *Acta Biochim. Biophysica Sin.* 45: 71–79.
55. Simmonds, A. J., G. DosSantos, I. Livne-Bar, and H. M. Krause. 2001. Apical localization of wingless Transcripts is Required for Wingless Signaling. *Cell* 105: 197–207.
56. Wu, J., T. J. Klein, and M. Mlodzik. 2004. Subcellular localization of frizzled receptors, mediated by their cytoplasmic tails, regulates signaling pathway specificity. *PLoS Biol.* 2: 1004–1014.
57. Kurnit, K. C., G. Kim, B. M. Fellman, D. Urbauer, G. B. Mills, W. Zhang, and R. R. Broaddus. 2017. Ctnnb1 mutation identifies low grade, early stage endometrial cancer patients at increased risk of recurrence. *Mod. Pathol.* 30: 1032–1041.

58. Maier, M. M., and M. Gessler. 2000. Comparative Analysis of the Human and Mouse Hey1 Promoter : Hey Genes Are New Notch Target Genes. *660*: 652–660.
59. Sasai, Y., R. Kageyama, Y. Tagawa, R. Shigemoto, and S. Nakanishi. 1992. Two mammalian helix-loop-helix factors structurally related to Drosophila hairy and Enhancer of split. 2620–2634.
60. Rangarajan, a, C. Talora, R. Okuyama, M. Nicolas, C. Mammucari, H. Oh, J. C. Aster, S. Krishna, D. Metzger, P. Chambon, L. Miele, M. Aguet, F. Radtke, and G. P. Dotto. 2001. Notch signaling is a direct determinant of keratinocyte growth arrest and entry into differentiation. *EMBO J.* 20: 3427–36.
61. Jho, E., T. Zhang, C. Domon, C. Joo, J. Freund, and F. Costantini. 2002. Wnt/ $\beta$ -Catenin/Tcf Signaling Induces the Transcription of Axin2 , a Negative Regulator of the Signaling Pathway. *Mol. Cell. Biol.* 22: 1172–1183.
62. He, T., A. B. Sparks, C. Rago, H. Hermeking, L. Zawel, L. T. Costa, P. J. Morin, B. Vogelstein, and K. W. Kinzler. 1998. Identification of c-MYC as a Target of the APC Pathway. *Science (80- )*. 281: 1509–1512.
63. Blache, P., M. Van De Wetering, I. Duluc, C. Domon, P. Berta, J. N. Freund, H. Clevers, and P. Jay. 2004. SOX9 is an intestine crypt transcription factor, is regulated by the Wnt pathway, and represses the CDX2 and MUC2 genes. *J. Cell Biol.* 166: 37–47.
64. Shtutman, M., J. Zhurinsky, I. Simcha, C. Albanese, M. D'Amico, R. Pestell, and a Ben-Ze'ev. 1999. The cyclin D1 gene is a target of the beta-catenin/LEF-1

pathway. *Proc. Natl. Acad. Sci. U. S. A.* 96: 5522–5527.

65. Torre, L. A., F. Bray, R. L. Siegel, J. Ferlay, J. Lortet-tieulent, and A. Jemal. 2015. Global Cancer Statistics, 2012. *CA a cancer J. Clin.* 65: 87–108.

66. Siegel, R. L., K. D. Miller, and A. Jemal. 2016. Cancer Statistics, 2016. 66: 7–30.

67. Sheikh, M. A., A. D. Althouse, K. E. Freese, S. Soisson, R. P. Edwards, S. Welburn, P. Sukumvanich, J. Comerci, J. Kelley, R. E. Laporte, and F. Linkov. 2014. USA Endometrial Cancer Projections to 2030: should we be concerned? *Futur. Oncol* 10: 2561–2568.

68. Kandoth, C., N. Schultz, A. D. Cherniack, R. Akbani, Y. Liu, H. Shen, A. G. Robertson, I. Pashtan, R. Shen, C. C. Benz, C. Yau, P. W. Laird, L. Ding, W. Zhang, G. B. Mills, R. Kucherlapati, E. R. Mardis, and D. A. Levine. 2013. Integrated genomic characterization of endometrial carcinoma. *Nature* 497: 67–73.

69. Westin, S. N., and R. R. Broaddus. 2012. Personalized therapy in endometrial cancer: challenges and opportunities. *Cancer Biol. Ther.* 13: 1–13.

70. Liu, Y., L. Patel, G. B. Mills, K. H. Lu, A. K. Sood, L. Ding, R. Kucherlapati, E. R. Mardis, D. A. Levine, I. Shmulevich, R. R. Broaddus, and W. Zhang. 2014. Clinical significance of CTNNB1 mutation and Wnt pathway activation in endometrioid endometrial carcinoma. *J. Natl. Cancer Inst.* 106: 1–8.

71. Liu, F. S. 2007. Molecular Carcinogenesis of Endometrial Cancer. *Taiwan. J. Obstet. Gynecol.* 46: 26–32.

72. Williams, E., A. Villar-Prados, J. Bowser, R. Broaddus, and A. B. Gladden. 2017. Loss of polarity alters proliferation and differentiation in low-grade endometrial cancers by disrupting Notch signaling. *PLoS One* 12: 1–20.
73. Jonusiene, V., A. Sasnauskiene, N. Lachej, D. Kanopiene, D. Dabkeviciene, S. Sasnauskiene, B. Kazbariene, and J. Didziapetriene. 2013. Down-regulated expression of Notch signaling molecules in human endometrial cancer. *Med. Oncol.* 30: 438.
74. Ferguson, L., E. M. Kaftanovskaya, C. Manresa, A. M. Barbara, R. J. Poppiti, Y. Tan, and A. I. Agoulnik. 2016. Constitutive Notch Signaling Causes Abnormal Development of the Oviducts, Abnormal Angiogenesis, and Cyst Formation in Mouse Female Reproductive Tract. *Biol. Reprod.* 94: 1–12.
75. Huenniger, K., A. Krämer, M. Soom, I. Chang, M. Köhler, R. Depping, R. H. Kehlenbach, and C. Kaether. 2010. Notch1 signaling is mediated by importins alpha 3, 4, and 7. *Cell. Mol. Life Sci.* 67: 3187–3196.
76. Schroeter, E. H., J. A. Kisslinger, and R. Kopan. 1998. Notch-1 signalling requires ligand-induced proteolytic release of intracellular domain. *Nature* 393: 382–386.
77. Liu, Z., S. Chen, S. C. Boyle, Y. Zhu, A. Zhang, D. Piwnica-Worms, M. X. G. Ilagan, and R. Kopan. 2014. The Extracellular Domain of Notch2 Increases its Cell-Surface Abundance and Ligand Responsiveness during Kidney Development. *Dev. Cell* 25: 585–598.

78. Guentchev, M., and R. D. McKay. 2006. Notch controls proliferation and differentiation of stem cells in a dose-dependent manner. *Eur. J. Neurosci.* 23: 2289–2296.
79. Matsuda, Y., Y. Wakamatsu, J. Kohyama, H. Okano, K. Fukuda, and S. Yasugi. 2005. Notch signaling functions as a binary switch for the determination of glandular and luminal fates of endodermal epithelium during chicken stomach development. *Development* 132: 2783–2793.
80. Maitra, S., R. M. Kulikauskas, H. Gavilan, and R. G. Fehon. 2006. The Tumor Suppressors Merlin and Expanded Function Cooperatively to Modulate Receptor Endocytosis and Signaling. *Curr. Biol.* 16: 702–709.
81. Bultje, R. S., D. R. Castaneda-Castellanos, L. Y. Jan, Y.-N. Jan, A. R. Kriegstein, and S.-H. Shi. 2009. Mammalian Par3 regulates progenitor cell asymmetric division via notch signaling in the developing neocortex. *Neuron* 63: 189–202.
82. Williams, S. E., S. Beronja, H. A. Pasolli, and E. Fuchs. 2011. Asymmetric cell divisions promote Notch-dependent epidermal differentiation. *Nature* 470: 353–8.
83. Rodriguez, J., F. Peglion, J. Martin, L. Hubatsch, J. Reich, N. Hirani, A. G. Gubieda, J. Roffey, A. R. Fernandes, D. St Johnston, J. Ahringer, and N. W. Goehring. 2017. aPKC Cycles between Functionally Distinct PAR Protein Assemblies to Drive Cell Polarity. *Dev. Cell* 42: 400–415.
84. Hurd, T. W., L. Gao, M. H. Roh, I. G. Macara, and B. Margolis. 2003. Direct interaction of two polarity complexes implicated in epithelial tight junction assembly.

*Nat. Cell Biol.* 5: 137–142.

85. Yamanaka, T., Y. Horikoshi, Y. Sugiyama, C. Ishiyama, A. Suzuki, T. Hirose, A. Iwamatsu, A. Shinohara, and S. Ohno. 2003. Mammalian Lgl Forms a Protein Complex with PAR-6 and aPKC Independently of PAR-3 to Regulate Epithelial Cell Polarity. *Curr. Biol.* 13: 734–743.

86. Goldstein, B., and I. G. Macara. 2007. The PAR Proteins: Fundamental Players in Animal Cell Polarization. *Dev. Cell* 13: 609–622.

87. Yamanaka, T., Y. Horikoshi, N. Izumi, A. Suzuki, K. Mizuno, and S. Ohno. 2006. Lgl mediates apical domain disassembly by suppressing the PAR-3 – aPKC – PAR-6 complex to orient apical membrane polarity. *J. Cell Sci.* 119: 2107–2118.

88. Tepass, U., C. Theres, and E. Knust. 1990. Crumbs encodes an EGF-like protein expressed on apical membranes of Drosophila epithelial cells and required for organization of epithelia. *Cell* 61: 787–799.

89. den Hollander, A. I., J. B. ten Brink, Y. J. de Kok, S. van Soest, L. I. van den Born, M. A. van Driel, D. J. van de Pol, A. M. Payne, S. S. Bhattacharya, U. Kellner, C. B. Hoyng, A. Westerveld, H. G. Brunner, E. M. Bleeker-Wagemakers, a F. Deutman, J. R. Heckenlively, F. P. Cremers, and A. A. Bergen. 1999. Mutations in a human homologue of Drosophila crumbs cause retinitis pigmentosa (RP12). *Nat. Genet.* 23: 217–221.

90. Makarova, O., M. H. Roh, C. Liu, S. Laurinec, and B. Margolis. 2003.

Mammalian Crumbs3 is a small transmembrane protein linked to protein associated

with Lin-7 ( Pals1 ) q. 302: 21–29.

91. Katoh, M., and M. Katoh. 2004. Identification and characterization of Crumbs homolog 2 gene at human chromosome 9q33.3. *Int. J. Oncol.* 24: 743–749.

92. Uhlén, M., L. Fagerberg, B. M. Hallström, C. Lindskog, P. Oksvold, A. Mardinoglu, Å. Sivertsson, C. Kampf, E. Sjöstedt, A. Asplund, I. Olsson, K. Edlund, E. Lundberg, S. Navani, C. A. Szigartyo, J. Odeberg, D. Djureinovic, J. O. Takanen, S. Hober, T. Alm, P. Edqvist, H. Berling, H. Tegel, J. Mulder, J. Rockberg, P. Nilsson, J. M. Schwenk, M. Hamsten, K. Von Feilitzen, M. Forsberg, L. Persson, F. Johansson, M. Zwahlen, G. Von Heijne, J. Nielsen, and F. Pontén. 2015. Tissue-based map of the human proteome. *Science (80-. )*. 347: 1–9.

93. Uhlen, M., P. Oksvold, L. Fagerberg, E. Lundberg, K. Jonasson, M. Forsberg, M. Zwahlen, C. Kampf, K. Wester, S. Hober, H. Wernerus, L. Björling, and F. Ponten. 2010. Towards a knowledge-based Human Protein Atlas. *Nat. Biotechnol.* 28: 1248–1250.

94. Whiteman, E. L., S. Fan, J. L. Harder, K. D. Walton, C. Liu, A. Soofi, V. C. Fogg, M. B. Hershenson, G. R. Dressler, G. H. Deutsch, and D. L. Gumucio. 2014. Crumbs3 Is Essential for Proper Epithelial Development and Viability. 34: 43–56.

95. Schluter, M. A., C. S. Pfarr, J. Pieczynski, E. L. Whiteman, T. W. Hurd, S. Fan, C. Liu, and B. Margolis. 2010. Trafficking of Crumbs3 during Cytokinesis is Crucial for Lumen Formation. *Mol. Biol. Cell* 21: 4042–4056.

96. Torkko, J. M., A. Manninen, S. Schuck, and K. Simons. 2008. Depletion of apical



transport proteins perturbs epithelial cyst formation and ciliogenesis. *J. Cell Sci.* 121: 1193–1203.

97. Roh, M. H., S. Fan, C. Liu, and B. Margolis. 2003. The Crumbs3-Pals1 complex participates in the establishment of polarity in mammalian epithelial cells. 3.

98. Lemmers, C., D. Michel, L. Lane-Guermonprez, M.-H. Delgrossi, E. Médina, J.-P. Arsanto, and A. Le Bivic. 2004. CRB3 Binds Directly to Par6 and Regulates the Morphogenesis of the Tight Junctions in Mammalian Epithelial Cells. *Mol. Biol. Cell* 15: 1324–1333.

99. Shin, K., S. Straight, and B. Margolis. 2005. PATJ regulates tight junction formation and polarity in mammalian epithelial cells. *J. Cell Biol.* 168: 705–711.

100. Michel, D. 2005. PATJ connects and stabilizes apical and lateral components of tight junctions in human intestinal cells. *J. Cell Sci.* 118: 4049–4057.

101. Adachi, M., Y. Hamazaki, Y. Kobayashi, M. Itoh, S. Tsukita, M. Furuse, and S. Tsukita. 2009. Similar and Distinct Properties of MUPP1 and Patj, Two Homologous PDZ Domain-Containing Tight-Junction Proteins. *Mol. Cell. Biol.* 29: 2372–2389.

102. Kim, S., M. K. Lehtinen, A. Sessa, M. W. Zappaterra, S. H. Cho, D. Gonzalez, B. Boggan, C. A. Austin, J. Wijnholds, M. J. Gambello, J. Malicki, A. S. LaMantia, V. Broccoli, and C. A. Walsh. 2010. The Apical Complex Couples Cell Fate and Cell Survival to Cerebral Cortical Development. *Neuron* 66: 69–84.

103. Bilder, D., and N. Perrimon. 2000. Localization of apical epithelial determinants

by the basolateral PDZ protein Scribble. *Nature* 403: 676–680.

104. Bilder, D., M. Li, and N. Perrimon. 2000. Cooperative regulation of cell polarity and growth by *Drosophila* tumor suppressors. *Science* 289: 113–116.

105. Zhan, L., A. Rosenberg, K. C. Bergami, M. Yu, Z. Xuan, B. Aron, C. Allred, and S. K. Muthuswamy. 2008. Deregulation of Scribble promotes mammary tumorigenesis and reveals a role for cell polarity in carcinoma. *Cell* 135: 865–878.

106. Montcouquiol, M., R. A. Rachel, P. J. Lanford, N. G. Copeland, N. A. Jenkins, and M. W. Kelley. 2003. Identification of Vangl2 and Scrb1 as planar polarity genes in mammals. *Nature* 423: 173–177.

107. Murdoch, J. N., D. J. Henderson, K. Doudney, C. Gaston-Massuet, H. M. Phillips, C. Paternotte, R. Arkell, P. Stanier, and A. J. Copp. 2003. Disruption of scribble (Scrb1) causes severe neural tube defects in the circletail mouse. *Hum. Mol. Genet.* 12: 87–98.

108. Woods, D. F., C. Hough, D. Peel, G. Callaini, and P. J. Bryant. 1996. Dlg Protein Is Required for Junction Structure, Cell Polarity, and Proliferation Control in *Drosophila* Epithelia. *J. Cell Biol.* 134: 1469–1482.

109. Van Campenhout, C. A., A. Eitelhuber, C. J. Gloeckner, P. Giallonardo, M. Gegg, H. Oller, S. G. N. Grant, D. Krappmann, M. Ueffing, and H. Lickert. 2011. Dlg3 Trafficking and apical tight junction formation is regulated by Nedd4 and Nedd4-2 E3 Ubiquitin ligases. *Dev. Cell* 21: 479–491.

110. McGee, a W., J. R. Topinka, K. Hashimoto, R. S. Petralia, S. Kakizawa, F. W. Kauer, a Aguilera-Moreno, R. J. Wenthold, M. Kano, D. S. Bredt, and F. Kauer. 2001. PSD-93 knock-out mice reveal that neuronal MAGUKs are not required for development or function of parallel fiber synapses in cerebellum. *J. Neurosci.* 21: 3085–91.

111. Cuthbert, P. C., L. E. Stanford, M. P. Coba, J. A. Ainge, A. E. Fink, P. Opazo, J. Y. Delgado, N. H. Komiyama, T. J. O'Dell, and S. G. N. Grant. 2007. Synapse-Associated Protein 102/dlg3 Couples the NMDA Receptor to Specific Plasticity Pathways and Learning Strategies. *J. Neurosci.* 27: 2673–2682.

112. Nagura, H., Y. Ishikawa, K. Kobayashi, K. Takao, T. Tanaka, K. Nishikawa, H. Tamura, S. Shiosaka, H. Suzuki, T. Miyakawa, Y. Fujiyoshi, and T. Doi. 2012. Impaired synaptic clustering of postsynaptic density proteins and altered signal transmission in hippocampal neurons, and disrupted learning behavior in PDZ1 and PDZ2 ligand binding-deficient PSD-95 knockin mice. *Mol. Brain* 5: 1–19.

113. Tarpey, P., J. Parnau, M. Blow, H. Woffendin, G. Bignell, C. Cox, J. Cox, H. Davies, S. Edkins, S. Holden, A. Kornly, U. Mallya, J. Moon, S. O'Meara, A. Parker, P. Stephens, C. Stevens, J. Teague, A. Donnelly, M. Mangelsdorf, J. Mulley, M. Partington, G. Turner, R. Stevenson, C. Schwartz, I. Young, D. Easton, M. Bobrow, P. A. Futreal, M. R. Stratton, J. Gecz, R. Wooster, and F. L. Raymond. 2004. Mutations in the DLG3 Gene Cause Nonsyndromic X-Linked Mental Retardation. *Am. J. Hum. Genet.* 75: 318–324.

114. Xing, J., H. Kimura, C. Wang, K. Ishizuka, I. Kushima, Y. Arioka, A. Yoshimi, Y.

- Nakamura, T. Shiino, T. Oya-Ito, Y. Takasaki, Y. Uno, T. Okada, T. Iidaka, B. Aleksic, D. Mori, and N. Ozaki. 2016. Resequencing and association analysis of Six PSD-95-related genes as possible susceptibility genes for schizophrenia and autism spectrum disorders. *Sci. Rep.* 6: 1–8.
115. Rivera, C., S. J. S. Simonson, I. F. Yamben, S. Shatadal, M. M. Nguyen, M. Beurg, P. F. Lambert, and A. E. Griep. 2013. Requirement for Dlg1 in Planar Cell Polarity and Skeletogenesis during Vertebrate Development. *PLoS One* 8.
116. Iizuka-Kogo, A., T. Ishida, T. Akiyama, and T. Senda. 2007. Abnormal development of urogenital organs in Dlg1-deficient mice. *Development* 134: 1799–1807.
117. Klezovitch, O., T. E. Fernandez, S. J. Tapscott, and V. Vasioukhin. 2004. Loss of cell polarity causes severe brain dysplasia in Lgl1 knockout mice. *Genes Dev.* 18: 559–571.
118. Sripathy, S., M. Lee, and V. Vasioukhin. 2011. Mammalian Lgl2 Is Necessary for Proper Branching Morphogenesis during Placental Development. *Mol. Cell. Biol.* 31: 2920–2933.
119. Parsons, L. M., M. Portela, N. A. Grzeschik, and H. E. Richardson. 2014. Lgl regulates notch signaling via endocytosis, independently of the apical aPKC-Par6-Baz polarity complex. *Curr. Biol.* 24: 2073–2084.
120. Clark, B. S., S. Cui, J. B. Miesfeld, O. Klezovitch, V. Vasioukhin, and B. A. Link. 2012. Loss of Lgl1 in retinal neuroepithelia reveals links between apical domain size, Notch activity and neurogenesis. *Development* 139: 1599–1610.

121. Hutterer, A., J. Betschinger, M. Petronczki, and J. A. Knoblich. 2004. Sequential roles of Cdc42, Par-6, aPKC, and Lgl in the establishment of epithelial polarity during *Drosophila* embryogenesis. *Dev. Cell* 6: 845–854.
122. Gladden, A. B., A. M. Hebert, E. E. Schneeberger, and A. I. McClatchey. 2010. The Nf2 Tumor Suppressor, Merlin, Regulates Epidermal Development Through the Establishment of a Junctional Polarity Complex. *Dev. Cell* 19: 727–739.
123. Ebnet, K., A. Suzuki, Y. Horikoshi, T. Hirose, M. K. Meyer Zu Brickwedde, S. Ohno, and D. Vestweber. 2001. The cell polarity protein ASIP/PAR-3 directly associates with junctional adhesion molecule (JAM). *EMBO J.* 20: 3738–3748.
124. Kemphues, K. J., J. R. Priess, D. G. Morton, and N. Cheng. 1988. Identification of Genes Required for Cytoplasmic Localization in Early C , *elegans* Embryos. 52: 311–320.
125. Gao, L., I. G. Macara, and G. Joberty. 2002. Multiple splice variants of Par3 and of a novel related gene, Par3L, produce proteins with different binding properties. *Gene* 294: 99–107.
126. Sfakianos, J., A. Togawa, S. Maday, M. Hull, M. Pypaert, L. Cantley, D. Toomre, and I. Mellman. 2007. Par3 functions in the biogenesis of the primary cilium in polarized epithelial cells. *J. Cell Biol.* 179: 1133–40.
127. von Stein, W., A. Ramrath, A. Grimm, M. Müller-Borg, and A. Wodarz. 2005. Direct association of Bazooka/PAR-3 with the lipid phosphatase PTEN reveals a link between the PAR/aPKC complex and phosphoinositide signaling. *Development* 132:

1675–1686.

128. Tabuse, Y., Y. Izumi, F. Piano, K. J. Kemphues, J. Miwa, and S. Ohno. 1998. Atypical protein kinase C cooperates with PAR-3 to establish embryonic polarity in *Caenorhabditis elegans*. *3614*: 3607–3614.

129. Lin, D., A. S. Edwards, J. P. Fawcett, G. Mbamalu, J. D. Scott, and T. Pawson. 2000. A mammalian PAR-3 – PAR-6 complex implicated in Cdc42 / Rac1 and aPKC signalling and cell polarity. *Nat. Cell Biol.* 2: 540–547.

130. von Stein, W. 2005. Direct association of Bazooka/PAR-3 with the lipid phosphatase PTEN reveals a link between the PAR/aPKC complex and phosphoinositide signaling. *Development* 132: 1675–1686.

131. Feng, W., H. Wu, L. N. Chan, and M. Zhang. 2008. Par-3-mediated junctional localization of the lipid phosphatase PTEN is required for cell polarity establishment. *J. Biol. Chem.* 283: 23440–23449.

132. Martin-Belmonte, F., A. Gassama, A. Datta, W. Yu, U. Rescher, V. Gerke, and K. Mostov. 2007. PTEN-Mediated Apical Segregation of Phosphoinositides Controls Epithelial Morphogenesis through Cdc42. *Cell* 128: 383–397.

133. Hirose, T., M. Karasawa, Y. Sugitani, M. Fujisawa, K. Akimoto, S. Ohno, and T. Noda. 2006. PAR3 is essential for cyst-mediated epicardial development by establishing apical cortical domains. *Development* 133: 1389–98.

134. Hao, Y., G. Du, X. Chen, Z. Zheng, J. L. Balsbaugh, S. Maitra, J. Shabanowitz,

D. F. Hunt, and I. G. Macara. 2010. Par3 Controls Spindle Pole Orientation in Epithelial cells by aPKC-mediated Phosphorylation of Pins at the Apical Cortex. *Curr. Biol.* 18: 1492–1501.

135. Ali, N. J. A., M. D. Gomes, R. Bauer, S. Brodesser, C. Niemann, and S. Iden. 2016. Essential Role of Polarity Protein Par3 for Epidermal Homeostasis through Regulation of Barrier Function , Keratinocyte Differentiation , and Stem Cell Maintenance. *J. Invest. Dermatol.* 136: 2406–2416.

136. Furuse, M., M. Hata, K. Furuse, Y. Yoshida, A. Haratake, Y. Sugitani, T. Noda, A. Kubo, and S. Tsukita. 2002. Claudin-based tight junctions are crucial for the mammalian epidermal barrier : a lesson from claudin-1-deficient mice. *J. Cell Biol.* 156: 1099–1111.

137. Iden, S., W. E. van Riel, R. Schäfer, J. Y. Song, T. Hirose, S. Ohno, and J. G. Collard. 2012. Tumor Type-Dependent Function of the Par3 Polarity Protein in Skin Tumorigenesis. *Cancer Cell* 22: 389–403.

138. McCaffrey, L. M., J. Montalbano, C. Mihai, and I. G. Macara. 2012. Loss of the Par3 Polarity Protein Promotes Breast Tumorigenesis and Metastasis. *Cancer Cell* 22: 601–614.

139. McCaffrey, L. M., and I. G. Macara. 2009. The Par3/aPKC interaction is essential for end bud remodeling and progenitor differentiation during mammary gland morphogenesis. *Genes Dev.* 23: 1450–1460.

140. Leitges, M., L. Sanz, P. Martin, A. Duran, U. Braun, J. F. Garcia, F. Camacho, T.

Diaz-meco, P. D. Rennert, and J. Moscat. 2001. Targeted Disruption of the zetaPKC Gene Results in the Impairment of the NF-KB Pathway. *Mol. Cell* 8: 771–780.

141. Metz, P. J., J. Arsenio, B. Kakaradov, S. H. Kim, K. A. Remedios, K. Oakley, K. Akimoto, S. Ohno, G. W. Yeo, and T. John. 2015. Regulation of Asymmetric Division and CD8+ T Lymphocyte Fate Specification by Protein Kinase C $\zeta$  and Protein Kinase C $\lambda$ . *J. Immunol.* 194: 2249–2259.

142. Sajan, M. P., R. A. Ivey, M. Lee, S. Mastorides, M. J. Jurczak, V. T. Samuels, G. I. Shulman, U. Braun, M. Leitges, and R. V Farese. 2014. PKC $\lambda$  Haploinsufficiency Prevents Diabetes by a Mechanism Involving Alterations in Hepatic Enzymes. *Mol. Endocrinol.* 28: 1097–1107.

143. Farese, R. V, M. P. Sajan, H. Yang, P. Li, S. Mastorides, W. R. G. Jr, S. Nimal, C. S. Choi, S. Kim, G. I. Shulman, C. R. Kahn, U. Braun, and M. Leitges. 2007. Muscle-specific knockout of PKC-  $\lambda$  impairs glucose transport and induces metabolic and diabetic syndromes. 117: 2289–2301.

144. Wald, F. A., A. S. Oriolo, A. Mashukova, N. L. Fregien, A. H. Langshaw, and P. J. I. Salas. 2008. Atypical protein kinase C (iota) activates ezrin in the apical domain of intestinal epithelial cells. *J. Cell Sci.* 121: 644–54.

145. Hirose, T., D. Satoh, H. Kurihara, C. Kusaka, H. Hirose, T. Matsusaka, I. Ichikawa, T. Noda, and S. Ohno. 2009. An Essential Role of the Universal Polarity Protein , aPKC I , on the Maintenance of Podocyte Slit Diaphragms. *PLoS One* 4: 1–9.



146. Yamanaka, T., A. Tosaki, M. Kurosawa, K. Akimoto, and T. Hirose. 2013. Loss of aPKC I in Differentiated Neurons Disrupts the Polarity Complex but Does Not Induce Obvious Neuronal Loss or Disorientation in Mouse Brains. *8*: 1–15.
147. Osada, S., N. Minematsu, F. Oda, K. Akimoto, S. Kawana, and S. Ohno. 2015. Atypical Protein Kinase C Isoform , aPKC  $\lambda$  , Is Essential for Maintaining Hair Follicle Stem Cell Quiescence. *J. Invest. Dermatol.* 135: 2584–2592.
148. Meehan, T. F., N. Conte, D. B. West, J. O. Jacobsen, J. Mason, J. Warren, C.-K. Chen, I. Tudose, M. Relac, P. Matthew, N. Karp, L. Santos, T. Fiegel, N. Ring, H. Westerberg, S. Greenaway, D. Sneddon, H. Morgan, G. F. Codner, M. E. Stewart, J. Brown, N. Horner, T. I. Mouse Phenotyping Consortium, M. Haendel, N. Washington, C. J. Mungall, C. L. Reynolds, J. Gallegos, V. Gailus-Durner, T. Sorg, G. Pavlovic, L. R. Bower, M. Moore, I. Morse, X. Gao, G. P. Tocchini-Valentini, Y. Obata, S. Y. Cho, J. K. Seong, J. Seavitt, A. L. Beaudet, M. E. Dickinson, Y. Herault, W. Wurst, M. H. de Angelis, K. C. K. Lloyd, A. M. Flenniken, L. M. Nutter, S. Newbigging, C. McKerlie, M. J. Justice, S. A. Murray, K. L. Svenson, R. E. Braun, J. K. White, A. Bradley, P. Flicek, S. Wells, W. C. Skarnes, D. J. Adams, H. Parkinson, A.-M. Mallon, S. D. M. Brown, and D. Smedley. 2017. Disease Model Discovery from 3,328 Gene Knockouts by The International Mouse Phenotyping Consortium. *Nat. Genet.* 49: 1231–1238.
149. Ozdamar, B., R. Bose, M. Barrios-Rodiles, H.-R. Wang, Y. Zhang, and J. L. Wrana. 2005. Regulation of the polarity protein Par6 by TGFbeta receptors controls epithelial cell plasticity. *Science* 307: 1603–1609.

150. Nolan, M. E., V. Aranda, S. Lee, B. Lakshmi, S. Basu, D. C. Allred, and S. K. Muthuswamy. 2008. The Polarity Protein Par6 induces Cell Proliferation and is Overexpressed in Breast Cancer. *Cancer Res.* 68: 8201–8209.
151. Hanahan, D., and R. A. Weinberg. 2011. Hallmarks of cancer: The next generation. *Cell* 144: 646–674.
152. Li, P., Y. Wang, X. Mao, Y. Jiang, J. Liu, J. Li, J. Wang, R. Wang, J. She, J. Zhang, J. Yang, Y. Liu, and P. Liu. 2017. CRB3 downregulation confers breast cancer stem cell traits through TAZ/ $\beta$ -catenin. *Oncogenesis* 6: 1–12.
153. Karp, C. M., T. T. Tan, R. Mathew, D. Nelson, K. Degenhardt, V. Karantzawadsworth, and E. White. 2008. Role of the Polarity Determinant Crumbs in Suppressing Mammalian Epithelial Tumor Progression. *Cancer Res.* 68: 4105–4115.
154. Nakagawa, S., and J. M. Huibregtse. 2000. Human scribble (Vartul) is targeted for ubiquitin-mediated degradation by the high-risk papillomavirus E6 proteins and the E6AP ubiquitin-protein ligase. *Mol. Cell. Biol.* 20: 8244–8253.
155. Gardiol, D., C. Kühne, B. Glaunsinger, S. S. Lee, R. Javier, and L. Banks. 1999. Oncogenic human papillomavirus E6 proteins target the discs large tumour suppressor for proteasome-mediated degradation. *Oncogene* 18: 5487–5496.
156. Watson, R. a, T. P. Rollason, G. M. Reynolds, P. G. Murray, L. Banks, and S. Roberts. 2002. Changes in expression of the human homologue of the Drosophila discs large tumour suppressor protein in high-grade premalignant cervical neoplasias. *Carcinogenesis* 23: 1791–6.

157. Pearson, H. B., P. a Perez-Mancera, L. E. Dow, A. Ryan, D. A. Tuveson, R. Simon, and P. O. Humbert. 2011. SCRIB expression is deregulated in human prostate cancer and its deficiency in mice promotes prostate neoplasia. *J. Clin. Invest.* 121: 4257–4267.
158. Feigin, M. E., S. D. Akshinthala, K. Araki, A. Z. Rosenberg, L. B. Muthuswamy, B. Martin, B. D. Lehmann, H. K. Berman, J. A. Pietenpol, R. D. Cardiff, and S. K. Muthuswamy. 2014. Mislocalization of the cell polarity protein scribble promotes mammary tumorigenesis and is associated with basal breast cancer. *Cancer Res.* 74: 3180–3194.
159. Humbert, P., S. Russell, and H. Richardson. 2003. Dlg, scribble and Lgl in cell polarity, cell proliferation and cancer. *BioEssays* 25: 542–553.
160. Li, P., X. Mao, Y. Ren, and P. Liu. 2015. Epithelial cell polarity determinant CRB3 in cancer development. *Int. J. Biol. Sci.* 11: 31–37.
161. Rejon, C., M. Al-Masri, and L. McCaffrey. 2016. Cell Polarity Proteins in Breast Cancer Progression. *J. Cell. Biochem.* 2223: 2215–2223.
162. Galvez, A. S., A. Duran, J. F. Linares, P. Pathrose, E. A. Castilla, S. Abu-Baker, M. Leitges, M. T. Diaz-Meco, and J. Moscat. 2009. Protein Kinase C Represses the Interleukin-6 Promoter and Impairs Tumorigenesis In Vivo. *Mol. Cell. Biol.* 29: 104–115.
163. Heikkilä, K., S. Ebrahim, and D. A. Lawlor. 2008. Systematic review of the association between circulating interleukin-6 (IL-6) and cancer. *Eur. J. Cancer* 44:

937–945.

164. Cerami, E., J. Gao, U. Dogrusoz, B. E. Gross, S. O. Sumer, B. A. Aksoy, A. Jacobsen, C. J. Byrne, M. L. Heuer, E. Larsson, Y. Antipin, B. Reva, A. P. Goldberg, C. Sander, and N. Schultz. 2012. The cBio Cancer Genomics Portal: An open platform for exploring multidimensional cancer genomics data. *Cancer Discov.* 2: 401–404.

165. Gao, J., B. A. Aksoy, U. Dogrusoz, G. Dresdner, B. Gross, S. O. Sumer, Y. Sun, A. Jacobsen, R. Sinha, E. Larsson, E. Cerami, C. Sander, and N. Schultz. 2013. Integrative analysis of complex cancer genomics and clinical profiles using the cBioPortal. *Sci. Signal.* 6: 1–34.

166. Ebnet, K., M. Mikl, C. R. Cowan, O. Bossinger, T. Wiesenfahrt, M. Hoffman, A. Navis, M. Bagnat, A. Wodarz, M. D. Tiwari, L.-E. Fielmich, S. van den Heuvel, M. Mescher, S. Iden, Y. Wang, X. Lu, C. Rejon, L. M. McCaffrey, G. Mikaty, X. Nassif, and M. Coureuil. 2015. *Cell Polarity 2 [Role in Development and Disease]*,.

167. Fuja, T. J., F. Lin, K. E. Osann, and P. J. Bryant. 2004. Somatic Mutations and Altered Expression of the Candidate Tumor Suppressors CSNK1  $\epsilon$  , DLG1 , and EDD / hHYD in Mammary Ductal Carcinoma. *Cancer Res.* 942–951.

168. Roberts, S., C. Delury, and E. Marsh. 2012. The PDZ protein discs-large (DLG): The “Jekyll and Hyde” of the epithelial polarity proteins. *FEBS J.* 279: 3549–3558.

169. Lin, W. H., Y. W. Asmann, and P. Z. Anastasiadis. 2015. Expression of polarity

genes in human cancer. *Cancer Inform.* 14: 15–28.

170. Makino, K., H. Kuwahara, N. Masuko, Y. Nishiyama, T. Morisaki, J. I. Sasaki, M. Nakao, A. Kuwano, M. Nakata, Y. Ushio, and H. Saya. 1997. Cloning and characterization of NE-dlg: a novel human homolog of the Drosophila discs large (dlg) tumor suppressor protein interacts with the APC protein. *Oncogene* 14: 2425–2433.

171. Garcia-Mata, R., A. D. Dubash, L. Sharek, H. S. Carr, J. A. Frost, and K. Burrige. 2007. The Nuclear RhoA Exchange Factor Net1 Interacts with Proteins of the Dlg Family, Affects Their Localization, and Influences Their Tumor Suppressor Activity. *Mol. Cell. Biol.* 27: 8683–8697.

172. Handa, K., T. Yugawa, M. Narisawa-Saito, S.-I. Ohno, M. Fujita, and T. Kiyono. 2007. E6AP-dependent degradation of DLG4/PSD95 by high-risk human papillomavirus type 18 E6 protein. *J. Virol.* 81: 1379–1389.

173. Smolen, G. a, J. Zhang, M. J. Zubrowski, E. J. Edelman, B. Luo, M. Yu, L. W. Ng, C. M. Scherber, B. J. Schott, S. Ramaswamy, D. Irimia, D. E. Root, and D. a Haber. 2010. A genome-wide RNAi screen identifies multiple RSK-dependent regulators of cell migration. 24: 2654–2665.

174. Daly, M. J., A. V. Pearce, L. Farwell, S. A. Fisher, A. Latiano, N. J. Prescott, A. Forbes, J. Mansfield, J. Sanderson, D. Langelier, A. Cohen, A. Bitton, G. Wild, C. M. Lewis, V. Annese, C. G. Mathew, and J. D. Rioux. 2005. Association of DLG5 R30Q variant with inflammatory bowel disease. *Eur. J. Hum. Genet.* 13: 835–839.

175. Liu, J., J. Li, P. Li, Y. Wang, Z. Liang, Y. Jiang, J. Li, C. Feng, R. Wang, H. Chen, C. Zhou, J. Zhang, J. Yang, and P. Liu. 2017. Loss of DLG5 promotes breast cancer malignancy by inhibiting the Hippo signaling pathway. *Sci. Rep.* 7: 42125.
176. Nam, K. H., M. A. Kim, G. Choe, W. H. Kim, and H. S. Lee. 2014. Deregulation of the cell polarity protein Lethal giant larvae 2 (Lgl2) correlates with gastric cancer progression. *Gastric Cancer* 17: 610–620.
177. Webb, A. E., W. Driever, and D. Kimelman. 2008. Psoriasis Regulates Epidermal Development in Zebrafish. *Dev. Dyn.* 237: 1153–1164.
178. Park, J. Y., L. J. Hughes, U. Y. Moon, R. Park, S.-B. Kim, K. Tran, J.-S. Lee, S.-H. Cho, and S. Kim. 2016. The apical complex protein Pals1 is required to maintain cerebellar progenitor cells in a proliferative state. *Development* 143: 133–146.
179. Wang, Q., Xi.-W. Chen, and B. Margolis. 2007. PALS1 Regulates E-cadherin Trafficking in Mammalian Epithelial Cells. *Mol. Biol. Cell* 18: 874–885.
180. Rothenberg, S. M., G. Mohapatra, M. N. Rivera, D. Winokur, P. Greninger, M. Nitta, P. M. Sadow, G. Sooriyakumar, B. W. Brannigan, M. J. Ulman, R. M. Perera, R. Wang, A. Tam, X.-J. Ma, M. Erlander, D. C. Sgroi, J. W. Rocco, M. W. Lingen, E. E. W. Cohen, D. N. Louis, J. Settleman, and D. a Haber. 2010. A genome-wide screen for microdeletions reveals disruption of polarity complex genes in diverse human cancers. *Cancer Res.* 70: 2158–64.
181. Zen, K., K. Yasui, Y. Gen, O. Dohi, N. Wakabayashi, S. Mitsufuji, Y. Itoh, Y. Zen, Y. Nakanuma, M. Taniwaki, T. Okanoue, and T. Yoshikawa. 2009. Defective

expression of polarity protein PAR-3 gene (PARD3) in esophageal squamous cell carcinoma. *Oncogene* 28: 2910–2918.

182. McCaffrey, L. M., J. Montalbano, C. Mihai, and I. G. Macara. 2012. Loss of the Par3 polarity protein promotes breast tumorigenesis and metastasis. *Cancer Cell* 22: 601–614.

183. Jan, Y., B. Ko, T. Liu, Y. Wu, and S. Liang. 2013. Expression of Partitioning Defective 3 ( Par-3 ) for Predicting Extrahepatic Metastasis and Survival with Hepatocellular Carcinoma. 111: 1684–1697.

184. Kojima, Y., K. Akimoto, Y. Nagashima, H. Ishiguro, S. Shirai, T. Chishima, Y. Ichikawa, T. Ishikawa, T. Sasaki, Y. Kubota, Y. Inayama, I. Aoki, S. Ohno, and H. Shimada. 2008. The overexpression and altered localization of the atypical protein kinase Clambda/iota in breast cancer correlates with the pathologic type of these tumors. *Hum. Pathol.* 39: 824–831.

185. Guyer, R. a., and I. G. Macara. 2015. Loss of the Polarity Protein PAR3 Activates STAT3 Signaling via an Atypical Protein Kinase C (aPKC)/NF- $\kappa$ B/Interleukin-6 (IL-6) Axis in Mouse Mammary Cells. *J. Biol. Chem.* 290: 8457–8468.

186. Paget, J. A., I. J. Restall, M. Daneshmand, J. A. Mersereau, M. A. Simard, D. A. E. Parolin, S. J. Lavictoire, M. S. Amin, S. Islam, and I. A. J. Lorimer. 2012. Repression of cancer cell senescence by PKCiota. *Oncogene* 31: 3584–3596.

187. Yang, Y., Y. Liu, J. He, J. Wang, P. Schemmer, C. Ma, Y. Qian, W. Yao, J.

Zhang, W. Qi, Y. Fu, W. Feng, and T. Yang. 2016. 14-3-3  $\zeta$  and aPKC- $\delta$  synergistically facilitate epithelial- mesenchymal transition of cholangiocarcinoma via GSK-3 $\beta$  / snail signaling pathway. *Oncotarget* 7: 55191–55210.

188. Felix, A. S., H. P. Yang, D. W. Bell, M. E. Sherman, D. Gupta, S. F. Lax, C. J. Walker, P. J. Goodfellow, M. Le Gallo, F. Lozy, D. W. Bell, N. Eritja, A. Yarmian, B.-J. Chen, D. Llobet-Navas, E. Ortega, E. Colas, M. Abal, X. Dolcet, J. Reventos, X. Matias-Guiu, C. G. Pena, D. H. Castrillon, T. H. Kim, J.-Y. Yoo, J.-W. Jeong, A. Joshi, and L. H. Ellenson. 2017. *Molecular Genetics of Endometrial Carcinoma*,.

189. Sherbet, G. V. 2013. The LKB1 (STK11) Suppressor Gene. In *Therapeutic Strategies in Cancer Biology and Pathology* 179–194.

190. Contreras, C. M., S. Gurumurthy, J. M. Haynie, L. J. Shirley, E. A. Akbay, S. N. Wingo, J. O. Schorge, R. R. Broaddus, K. K. Wong, N. Bardeesy, and D. H. Castrillon. 2008. Loss of Lkb1 provokes highly invasive endometrial adenocarcinomas. *Cancer Res.* 68: 759–766.

191. Dugay, F., X. Le Goff, N. Rioux-Leclercq, F. Chesnel, F. Jouan, C. Henry, F. Cabillic, G. Verhoest, C. Vigneau, Y. Arlot-Bonnemains, and M. a Belaud-Rotureau. 2014. Overexpression of the polarity protein PAR-3 in clear cell renal cell carcinoma is associated with poor prognosis. *Int. J. Cancer* 134: 2051–60.

192. Pickering, K., J. Alves-Silva, D. Goberdhan, and T. H. Millard. 2013. Par3/Bazooka and phosphoinositides regulate actin protrusion formation during *Drosophila* dorsal closure and wound healing. *Development* 140: 800–9.



193. Pinal, N., D. C. I. Goberdhan, L. Collinson, Y. Fujita, I. M. Cox, C. Wilson, and F. Pichaud. 2006. Regulated and polarized PtdIns(3,4,5)P3 accumulation is essential for apical membrane morphogenesis in photoreceptor epithelial cells. *Curr. Biol.* 16: 140–149.
194. Steck, P. a, M. a Pershouse, S. a Jasser, W. K. Yung, H. Lin, a H. Ligon, L. a Langford, M. L. Baumgard, T. Hattier, T. Davis, C. Frye, R. Hu, B. Swedlund, D. H. Teng, and S. V Tavtigian. 1997. Identification of a candidate tumour suppressor gene, MMAC1, at chromosome 10q23.3 that is mutated in multiple advanced cancers. *Nat. Genet.* 15: 356–362.
195. Li, J., C. Yen, D. Liaw, K. Podsypanina, S. Bose, S. I. Wang, J. Puc, C. Miliareis, L. Rodgers, R. McCombie, S. H. Bigner, B. C. Giovanella, M. Ittmann, B. Tycko, H. Hibshoosh, M. H. Wigler, and R. Parsons. 1997. PTEN , a Putative Protein Tyrosine Phosphatase Gene Mutated in Human Brain, Breast, and Prostate Cancer. *Science (80-. ).* 275: 1943–1947.
196. Djordjevic, B., B. T. Hennessy, J. Li, B. A. Barkoh, R. Luthra, G. B. Mills, and R. R. Broaddus. 2012. Clinical assessment of PTEN loss in endometrial carcinoma: immunohistochemistry outperforms gene sequencing. *Mod. Pathol.* 25: 699–708.
197. Braga, V. M., and S. J. Gendler. 1993. Modulation of Muc-1 mucin expression in the mouse uterus during the estrus cycle, early pregnancy and placentation. *J. Cell Sci.* 105: 397–405.
198. Allen, E. 1922. The oestrous cycle in the mouse. *Dev. Dyn.* 30: 297–371.

199. Murphy, C. R. 2004. Uterine receptivity and the plasma membrane transformation. *Cell Res.* 14: 259–267.
200. Ohtani, K., H. Sakamoto, T. Rutherford, Z. Chen, A. Kikuchi, T. Yamamoto, K. Satoh, and F. Naftolin. 2002. Ezrin, a membrane-cytoskeletal linking protein, is highly expressed in atypical endometrial hyperplasia and uterine endometrioid adenocarcinoma. *Cancer Lett.* 179: 79–86.
201. Sato, N., N. Funayama, A. Nagafuchi, S. Yonemura, S. Tsukita, and S. Tsukita. 1992. A gene family consisting of ezrin, radixin and moesin Its specific localization at actin filament/plasma membrane association sites. *J. Cell Sci.* 103: 131–143.
202. Ornek, T., a Fadiel, O. Tan, F. Naftolin, and a Arici. 2008. Regulation and activation of ezrin protein in endometriosis. *Hum. Reprod.* 23: 2104–12.
203. Bochner, B. S., F. W. Luscinckas, M. A. J. Gimbrone, W. Newman, S. Sterbinsky, C. Derse-Anthony, D. Klunk, and R. Schleimer. 1991. Adhesion of human basophils, eosinophils, and neutrophils to interleukin-1-activated human vascular endothelial cells: contribution of endothelial cell adhesion molecules. *J Exp Med* 173: 1553–1557.
204. Salzer, J. L. 2003. Polarized Domains of Myelinated Axons. *Neuron* 40: 297–318.
205. McCain, M. L., H. Lee, Y. Aratyn-Schaus, A. G. Kleber, and K. K. Parker. 2012. Cooperative coupling of cell-matrix and cell-cell adhesions in cardiac muscle. *Proc. Natl. Acad. Sci.* 109: 9881–9886.

206. Ridley, A. J., and A. Hall. 1992. The small GTP-binding protein rho regulates the assembly of focal adhesions and actin stress fibers in response to growth factors. *Cell* 70: 389–399.
207. Kornberg, L., H. S. Earp, J. T. Parsons, M. Schaller, and R. L. Juliano. 1992. Cell adhesion or integrin clustering increases phosphorylation of a focal adhesion-associated tyrosine kinase. *J. Biol. Chem.* 267: 23439–23442.
208. Green, K. J., and J. onathan C. R. Jones. 1996. Desmosomes and hemidesmosomes: structure and function of molecular components. *FASEB J.* 1: 871–81.
209. Karayiannakis, A. J., K. N. Syrigos, J. Efstathiou, A. Valizadeh, M. Noda, R. J. Playford, W. Kmiot, and M. Pignatelli. 1998. Expression of catenins and E-cadherin during epithelial restitution in inflammatory bowel disease. *J. Pathol.* 185: 413–418.
210. Peeters, M., Y. Ghoo, B. Maes, M. Hiele, K. Geboes, G. Vantrappen, and P. Rutgeerts. 1994. Increased permeability of macroscopically normal small bowel in Crohn's disease. *Dig. Dis. Sci.* 39: 2170–2176.
211. Meddings, J. B., L. R. Sutherland, and G. R. May. 1994. Intestinal permeability in patients with Crohn's disease. *Gut* 35: 1675.
212. Chen, D., C. R. M. Wilkinson, S. Watt, C. J. Penkett, W. M. Toone, N. Jones, and J. Bähler. 2007. High-Resolution Crystal Structure and In Vivo Function of a Kinesin-2 Homologue in *Giardia intestinalis*. *Mol. Biol. Cell* 19: 308–317.

213. Itoh, M., K. Nakadate, Y. Horibata, T. Matsusaka, J. Xu, W. Hunziker, and H. Sugimoto. 2014. The structural and functional organization of the podocyte filtration slits is regulated by Tjp1/ZO-1. *PLoS One* 9: 1–11.
214. Saitou, M., M. Furuse, H. Sasaki, J.-D. Schulzke, M. Fromm, H. Takano, T. Noda, and S. Tsukita. 2000. Complex Phenotype of Mice Lacking Occludin, a Component of Tight Junction Strands. *Mol. Biol. Cell* 11: 4131–4142.
215. Gow, A., C. M. Southwood, J. S. Li, M. Pariali, G. P. Riordan, S. E. Brodie, J. Danias, J. M. Bronstein, B. Kachar, R. A. Lazzarini, O. Gustave, L. L. Place, N. York, and N. York. 1999. CNS myelin and Sertoli cell tight junction strands are absent in *Osp/Claudin-11* null mice. *Cell* 99: 649–659.
216. Haegel, H., L. Larue, M. Ohsugi, L. Fedorov, K. Herrenknecht, and R. Kemler. 1995. Lack of  $\beta$ -catenin affects mouse development at gastrulation. *Development* 121: 3529–3537.
217. Larue, L., M. Ohsugi, J. Hirchenhain, and R. Kemler. 1994. E-cadherin null mutant embryos fail to form a trophectoderm epithelium. *Proc. Natl. Acad. Sci.* 91: 8263–8267.
218. Riethmacher, D., V. Brinkmann, and C. Birchmeier. 1995. A targeted mutation in the mouse E-cadherin gene results in defective preimplantation development. *Proc. Natl. Acad. Sci. U. S. A.* 92: 855–9.
219. McClatchey, A. I., I. Saotome, K. Mercer, D. Crowley, J. F. Gusella, R. T. Bronson, and T. Jacks. 1998. Mice heterozygous for a mutation at the *Nf2* tumor

suppressor locus develop a range of highly metastatic tumors. *Genes Dev.* 12: 1121–1133.

220. Trofatter, J. A., M. M. Maccoiin, J. L. Rutter, J. R. Murreil, M. P. Duyao, D. M. Parry, R. Eidridge, N. Kiey, A. G. Nlenon, K. Pulaski, V. H. Haase, C. M. Ambrose, D. Munroe, C. Bove, J. L. Haines, R. L. Martuza, M. E. Macdonald, B. R. Seizinger, M. P. Short, A. J. Buckler, and J. F. Gusella. 1993. A Novel Moesin- , Ezrin- , Radixin-like Gene Is a Candidate for the Neurofibromatosis Tumor Suppressor. 72.

221. Rouleau, G. A., P. Merel, M. Lutchman, M. Sanson, J. Zucman, C. Marineau, K. Hoang-Xuan, S. Demczuk, C. Desmaze, B. Plougastel, S. M. Pulst, G. Lenoir, E. Bijlsma, R. Fashold, J. Dumanski, P. de Jong, D. Parry, R. Eldrige, A. Aurias, O. Delattre, and G. Thomas. 1993. Alteration in a new gene encoding a putative membrane-organizing protein causes neuro-fibromatosis type 2. *Nature* 363: 515–521.

222. Lau, Y. K. I., L. B. Murray, S. S. Houshmandi, Y. Xu, D. H. Gutmann, and Q. Yu. 2008. Merlin is a potent inhibitor of glioma growth. *Cancer Res.* 68: 5733–5742.

223. Zhang, N., H. Bai, K. K. David, J. Dong, Y. Zheng, J. Cai, M. Giovannini, P. Liu, R. A. Anders, and D. Pan. 2010. The Merlin/NF2 Tumor Suppressor Functions through the YAP Oncoprotein to Regulate Tissue Homeostasis in Mammals. *Dev. Cell* 19: 27–38.

224. Benhamouche, S., M. Curto, I. Saotome, A. B. Gladden, C. H. Liu, M. Giovannini, and A. I. McClatchey. 2010. Nf2/Merlin controls progenitor homeostasis

and tumorigenesis in the liver. *Genes Dev.* 24: 1718–1730.

225. Morris, Z. S., and A. I. McClatchey. 2009. Aberrant epithelial morphology and persistent epidermal growth factor receptor signaling in a mouse model of renal carcinoma. *Proc. Natl. Acad. Sci. U. S. A.* 106: 9767–72.

226. McClatchey, A. I., I. Saotome, V. Ramesh, J. F. Gusella, and T. Jacks. 1997. The Nf2 tumor suppressor gene product is essential for extraembryonic development immediately prior to gastrulation. *Genes Dev.* 11: 1253–1265.

227. Lajeunesse, D. R., B. M. McCartney, and R. G. Fehon. 1998. Structural analysis of Drosophila Merlin Reveals Functional Domains Important for Growth Control and Subcellular Localization. *J. Cell Biol.* 141: 1589–1599.

228. Lallemand, D., M. Curto, I. Saotome, M. Giovannini, and A. I. McClatchey. 2003. NF2 deficiency promotes tumorigenesis and metastasis by destabilizing adherens junctions. *Genes Dev.* 17: 1090–1100.

229. Curto, M., B. K. Cole, D. Lallemand, C. H. Liu, and A. I. McClatchey. 2007. Contact-dependent inhibition of EGFR signaling by Nf2/Merlin. *J. Cell Biol.* 177: 893–903.

230. Zoch, A., S. Mayerl, A. Schulz, T. Greither, L. Frappart, J. Rüksam, H. Heuer, M. Giovannini, and H. Morrison. 2015. Merlin isoforms 1 and 2 both act as tumour suppressors and are required for optimal sperm maturation. *PLoS One* 10: 1–25.

231. Schulz, A., S. L. Baader, M. Niwa-Kawakita, M. J. Jung, R. Bauer, C. Garcia, A.

- Zoch, S. Schacke, C. Hagel, V.-F. Mautner, C. O. Hanemann, X.-P. Dun, D. B. Parkinson, J. Weis, J. M. Schröder, D. H. Gutmann, M. Giovannini, and H. Morrison. 2013. Merlin isoform 2 in neurofibromatosis type 2-associated polyneuropathy. *Nat. Neurosci.* 16: 426–436.
232. Mackenzie, C. C., Z. S. Morris, Q. Baca, B. Morris, J. K. Coker, R. Mirchev, A. E. Jensen, T. Carey, S. L. Stott, D. E. Golan, and A. I. Mcclatchey. 2015. NF2 / Merlin mediates contact-dependent inhibition of EGFR mobility and internalization via cortical actomyosin. *J. Cell Biol.* 211: 1–15.
233. Wiley, L. A., L. K. Dattilo, K. B. Kang, M. Giovannini, and D. C. Beebe. 2010. The tumor suppressor merlin is required for cell cycle exit, terminal differentiation, and cell polarity in the developing murine lens. *Investig. Ophthalmol. Vis. Sci.* 51: 3611–3618.
234. Schulz, A., R. Büttner, A. Toledo, S. L. Baader, J. von Maltzahn, A. Irintchev, R. Bauer, and H. Morrison. 2016. Neuron-Specific Deletion of the Nf2 Tumor Suppressor Impairs Functional Nerve Regeneration. *PLoS One* 11: e0159718.
235. Giovannini, M., E. Robanus-maandag, M. Van Der Valk, M. Niwa-kawakita, V. Abramowski, L. Goutebroze, J. M. Woodruff, A. Berns, and G. Thomas. 2000. Conditional biallelic Nf2 mutation in the mouse promotes manifestations of human neurofibromatosis type 2. *Genes Dev.* 14: 1617–1630.
236. Giovannini, M., E. Robanus-maandag, M. Niwa-kawakita, M. Van Der Valk, J. M. Woodruff, L. Goutebroze, P. Me, A. Berns, and G. Thomas. 1999. Schwann cell

hyperplasia and tumors in transgenic mice expressing a naturally occurring mutant NF2 protein. *Genes Dev.* 13: 978–986.

237. Hebert, A. M., B. Duboff, J. B. Casaletto, A. B. Gladden, and A. I. Mcclatchey. 2012. Merlin / ERM proteins establish cortical asymmetry and centrosome position. *Genes Dev.* 26: 2709–2723.

238. Fentress, M. K. 2015. MERLIN MEDIATED REGULATION OF HAIR FOLLICLE MORPHOGENESIS. *Masters Thesis* .

239. Evans, D. G. R. 2009. Neurofibromatosis type 2 (NF2): A clinical and molecular review. *Orphanet J. Rare Dis.* 4: 16.

240. Zhou, L., E. Ercolano, S. Ammoun, M. C. Schmid, M. a Barczyk, and C. O. Hanemann. 2011. Merlin-Deficient Human Tumors Show Loss of Contact Inhibition and Activation of Wnt /  $\beta$ -Catenin Signaling Linked to the PDGFR / Src and Rac/PAK Pathways. *Neoplasia* 13: 1101–1112.

241. Kim, M., S. Kim, S.-H. Lee, W. Kim, M.-J. Sohn, H.-S. Kim, J. Kim, and E.-H. Jho. 2016. Merlin inhibits Wnt/ $\beta$ -catenin signaling by blocking LRP6 phosphorylation. *Cell Death Differ.* 23: 1–10.

242. Morrow, K. A., S. Das, E. Meng, M. E. Menezes, K. Sarah, B. J. Metge, D. J. Buchsbaum, R. S. Samant, and A. Lalita. 2016. Loss of tumor suppressor Merlin results in aberrant activation of Wnt/ $\beta$ -catenin signaling in cancer. *Oncotarget* 7: 17991–18005.



243. Bosco, E. E., Y. Nakai, R. F. Hennigan, N. Ratner, and Y. Zheng. 2010. NF2-deficient cells depend on the Rac1-canonical Wnt signaling pathway to promote the loss of contact inhibition of proliferation. *Oncogene* 29: 2540–9.

244. Stemmer-Rachamimov, A. O., T. Wiederhold, G. P. Nielsen, M. James, D. Pinney-Michalowski, J. E. Roy, W. A. Cohen, V. Ramesh, and D. N. Louis. 2001. NHE-RF, a merlin-interacting protein, is primarily expressed in luminal epithelia, proliferative endometrium, and estrogen receptor-positive breast carcinomas. *Am. J. Pathol.* 158: 57–62.

245. Cobellis, L., F. Caprio, E. Trabucco, A. Mastrogiacomo, G. Coppola, L. Manente, N. Colacurci, M. De Falco, and A. De Luca. 2008. The pattern of expression of Notch protein members in normal and pathological endometrium. *J. Anat.* 213: 464–72.

246. Yang, C.-C., H. K. Graves, I. M. Moya, C. Tao, F. Hamaratoglu, A. B. Gladden, and G. Halder. 2015. Differential regulation of the Hippo pathway by adherens junctions and apical–basal cell polarity modules. *Proc. Natl. Acad. Sci.* 112: 1785–1790.

247. Kuwada, S. K., K. a Lund, X. F. Li, P. Cliften, K. Amsler, L. K. Opresko, and H. S. Wiley. 1998. Differential signaling and regulation of apical vs. basolateral EGFR in polarized epithelial cells. *Am. J. Physiol.* 275: 1419–1428.

248. Huang, C.-C., G. D. Orvis, Y. Wang, and R. R. Behringer. 2012. Stromal-to-epithelial transition during postpartum endometrial regeneration. *PLoS One* 7:

e44285.

249. Soyal, S. M., A. Mukherjee, K. Y. S. Lee, J. Li, H. Li, F. J. DeMayo, and J. P. Lydon. 2005. Cre-mediated recombination in cell lineages that express the progesterone receptor. *Genesis* 41: 58–66.

250. Giovannini, M., E. Robanus-Maandag, M. van der Valk, M. Niwa-Kawakita, V. Abramowski, L. Goutebroze, J. M. Woodruff, A. Berns, and G. Thomas. 2000. Conditional biallelic Nf2 mutation in the mouse promotes manifestations of human neurofibromatosis type 2. *Genes Dev.* 14: 1617–1630.

251. Jaffe, A. B., N. Kaji, J. Durgan, and A. Hall. 2008. Cdc42 controls spindle orientation to position the apical surface during epithelial morphogenesis. *J. Cell Biol.* 183: 625–633.

252. Pemberton, L., C. O. F., J. Julian, R. A. Pimental, C. Wegner, S. K. Dey, D. Carson, and S. K. Das. 1995. Expression and Steroid Hormonal Control of Muc-1 in the Mouse Uterus. *Society* 136: 3639–3647.

253. Eritja, N., D. Llobet, M. Domingo, M. Santacana, A. Yeramian, X. Matias-Guiu, and X. Dolcet. 2010. A novel three-dimensional culture system of polarized epithelial cells to study endometrial carcinogenesis. *Am. J. Pathol.* 176: 2722–31.

254. Elia, N., and J. Lippincott-schwartz. 209AD. Culturing Three Dimensional MDCK cells for Analyzing Intracellular Dynamics. *Curr. Protoc. Cell Biol.* .

255. Chiasson-MacKenzie, C., Z. S. Morris, Q. Baca, B. Morris, J. K. Coker, R.

- Mirchev, A. E. Jensen, T. Carey, S. L. Stott, D. E. Golan, and A. I. McClatchey. 2015. NF2/Merlin mediates contact-dependent inhibition of EGFR mobility and internalization via cortical actomyosin. *J. Cell Biol.* 211: 1–15.
256. Chen, X., and I. G. Macara. 2005. Par-3 controls tight junction assembly through the Rac exchange factor Tiam1. *Nat Cell Biol* 7: 262–269.
257. Schlumbrecht, M. P., S.-S. Xie, G. L. Shipley, D. L. Urbauer, and R. R. Broaddus. 2011. Molecular clustering based on ER $\alpha$  and EIG121 predicts survival in high-grade serous carcinoma of the ovary/peritoneum. *Mod. Pathol.* 24: 453–62.
258. Chandra, A., C. E. Copen, and E. H. Stephen. 2014. Infertility service use in the United States: data from the national survey of family growth, 1982-2010. *Natl. Health Stat. Report.* 1–21.
259. Chandra, A., C. E. Copen, and E. H. Stephen. 2013. Infertility and impaired fecundity in the United States, 1982-2010: data from the National Survey of Family Growth. *Natl. Health Stat. Report.* 1----18, 1 p following 19.
260. Filant, J., and T. E. Spencer. 2014. Uterine glands: biological roles in conceptus implantation, uterine receptivity and decidualization. *Int. J. Dev. Biol.* 58: 107–116.
261. Filant, J., and T. E. Spencer. 2013. Endometrial glands are essential for blastocyst implantation and decidualization in the mouse uterus. *Biol. Reprod.* 88: 93.
262. Karagouni, E. E., A. Chryssikopoulos, T. Mantzavinos, N. Kanakas, and E. N.

- Dotsika. 1998. Interleukin-1 $\beta$  and interleukin-1 $\alpha$  may affect the implantation rate of patients undergoing in vitro fertilization-embryo transfer. *Fertil. Steril.* 70: 553–559.
263. Vialard, F., M. El Sirkasi, V. Tronchon, R. Boudjenah, D. Molina-Gomes, M. Bergere, C. Mauduit, R. Wainer, J. Selva, and M. Benahmed. 2013. Tumor necrosis factor-308 polymorphism increases the embryo implantation rate in women undergoing in vitro fertilization. *Hum. Reprod.* 28: 2774–2783.
264. Hogan, B. L. M., and P. A. Kolodziej. 2002. Molecular Mechanisms of Tubulogenesis. *Nat. Rev. Genet.* 3: 513–523.
265. Gray, C. A., F. F. Bartol, B. J. Tarleton, A. A. Wiley, G. A. Johnson, F. W. Bazer, T. E. Spencer, and G. E. T. Al. 2001. Developmental Biology of Uterine Glands. *Biol. Reprod.* 65: 1311–1323.
266. Cunha, G. R., P. Young, and J. R. Brody. 1989. Role of Uterine Epithelium in the Development of Myometrial Smooth Muscle Cells. *Biol. Reprod.* 40: 861–871.
267. Kadokawa, Y., I. Fuketa, A. Nose, M. Takeichi, and N. Nakatsuji. 1989. Expression Pattern of E-Cadherin and P-Cadherin in Mouse Embryos and Uteri during the Periimplantation Period. *Dev. Growth Differ.* 31: 23–30.
268. Nose, A., and M. Takeichi. 1986. A novel cadherin cell adhesion molecule: Its expression patterns associated with implantation and organogenesis of mouse embryos. *J. Cell Biol.* 103: 2649–2658.
269. van der Linden, P. J., A. F. de Goeij, G. A. Dunselman, H. W. Erkens, and J. L.

- Evers. 1995. Expression of cadherins and integrins in human endometrium throughout the menstrual cycle. *Fertil. Steril.* 63: 1210–6.
270. Radice, G. L., M. C. Ferreira-Cornwell, S. D. Robinson, H. Rayburn, L. A. Chodosh, M. Takeichi, and R. O. Hynes. 1997. Precocious mammary gland development in P-cadherin-deficient mice. *J. Cell Biol.* 139: 1025–1032.
271. Bazellières, E., V. Conte, A. Elosegui-artola, X. Serra-picamal, M. Bintanel-morcillo, P. Roca-cusachs, J. J. Muñoz, M. Sales-pardo, R. Guimerà, and X. Trepap. 2015. Control of cell – cell forces and collective cell dynamics by the intercellular adhesome. 17.
272. Yonemura, S., Y. Wada, T. Watanabe, A. Nagafuchi, and M. Shibata. 2010. alpha-Catenin as a tension transducer that induces adherens junction development. *Nat. Cell Biol.* 12: 533–42.
273. Cohen, D. M., B. Kutscher, H. Chen, D. B. Murphy, and S. W. Craig. 2006. A conformational switch in vinculin drives formation and dynamics of a talin-vinculin complex at focal adhesions. *J. Biol. Chem.* 281: 16006–16015.
274. Dumbauld, D. W., H. Shin, N. D. Gallant, K. E. Michael, H. Radhakrishna, and A. J. Garcia. 2010. Contractility modulates cell adhesion strengthening through Focal Adhesion Kinase and assembly of Vinculin-Containing Focal Adhesions. *J. Cell Physiol.* 223: 746–756.
275. Amano, M., M. Ito, Y. Fukata, K. Chihara, T. Nakano, Y. Matsuura, and K. Kaibuchi. 1996. Phosphorylation and activation of Myosin by Rho-associated kinase

(Rho-kinase). *J. Biol. Chem.* 271: 20246–20249.

276. Brodland, G. W., J. H. Veldhuis, S. Kim, M. Perrone, D. Mashburn, and M. S. Hutson. 2014. CellFIT: A cellular force-inference toolkit using curvilinear cell boundaries. *PLoS One* 9.

277. Cerchiari, A. E., J. C. Garbe, N. Y. Jee, M. E. Todhunter, K. E. Broaders, D. M. Peehl, T. A. Desai, M. A. LaBarge, M. Thomson, and Z. J. Gartner. 2015. A strategy for tissue self-organization that is robust to cellular heterogeneity and plasticity. *Proc. Natl. Acad. Sci.* 112: 2287–2292.

278. Lavado, A., Y. He, J. Pare, G. Neale, E. N. Olson, M. Giovannini, and X. Cao. 2013. Tumor suppressor Nf2 limits expansion of the neural progenitor pool by inhibiting Yap/Taz transcriptional coactivators. *Development* 140: 3323–3334.

279. Dupont, S., L. Morsut, M. Aragona, E. Enzo, S. Giulitti, M. Cordenonsi, F. Zanconato, J. Le Digabel, M. Forcato, S. Bicciato, N. Elvassore, and S. Piccolo. 2011. Role of YAP/TAZ in mechanotransduction. *Nature* 474: 179–184.

280. Du, Y. C., H. Oshima, K. Oguma, T. Kitamura, H. Itadani, T. Fujimura, Y. S. Piao, T. Yoshimoto, T. Minamoto, H. Kotani, M. M. Taketo, and M. Oshima. 2009. Induction and Down-regulation of Sox17 and Its Possible Roles During the Course of Gastrointestinal Tumorigenesis. *Gastroenterology* 137: 1346–1357.

281. Chew, L.-J., W. Shen, X. Ming, V. V. Senatorov, H.-L. Chen, Y. Cheng, E. Hong, S. Knobloch, and V. Gallo. 2011. Sox17 Regulates the Wnt/beta-Catenin Signaling Pathway in Oligodendrocyte Progenitor Cells. *J. Neurosci.* 31: 13921–

13935.

282. McClatchey, A. I., I. Saotome, K. Mercer, D. Crowley, J. F. Gusella, R. T. Bronson, and T. Jacks. 1998. Mice heterozygous for a mutation at the. *Genes Dev.* 1121–1133.

283. Basilicata, M. F., M. Frank, D. Solter, T. Brabletz, and M. P. Stemmler. 2016. Inappropriate cadherin switching in the mouse epiblast compromises proper signaling between the epiblast and the extraembryonic ectoderm during gastrulation. *Sci. Rep.* 6: 1–15.

284. Benham-Pyle, B. W., B. L. Pruitt, and W. J. Nelson. 2015. Mechanical strain induces E-cadherin-dependent Yap1 and beta-catenin activation to drive cell cycle entry. *Science (80-. )*. 348: 1024–1027.

285. Morrow, K. A., S. Das, B. J. Metge, K. Ye, M. S. Mulekar, J. A. Tucker, R. S. Samant, and L. A. Shevde. 2011. Loss of tumor suppressor merlin in advanced breast cancer is due to post-translational regulation. *J. Biol. Chem.* 286: 40376–40385.

286. Curto, M., B. K. Cole, D. Lallemand, C. Liu, and A. I. McClatchey. 2007. Contact-dependent Inhibition of EGFR Signaling by Nf2/Merlin. *J. Cell Biol.* 177: 893–903.

287. Morrow, K. A., S. Das, E. Meng, M. E. Menezes, K. Sarah, B. J. Metge, D. J. Buchsbaum, R. S. Samant, and A. Lalita. 2016. Loss of tumor suppressor Merlin results in aberrant activation of Wnt /  $\beta$ -catenin signaling in cancer. *Oncotarget* 7:

17991–18005.

288. Edwards, A. K., J. Janzen-Pang, A. Peng, C. Tayade, A. Carniato, A. T.

Yamada, P. D. A. Lima, and D. Tse. 2014. *Microscopic Anatomy of the Pregnant Mouse Uterus Throughout Gestation*,. Elsevier.

289. Kurita, T., P. S. Cooke, and G. R. Cunha. 2001. Epithelial-stromal tissue interaction in paramesonephric (Müllerian) epithelial differentiation. *Dev. Biol.* 240: 194–211.

290. Dunlap, K. A., J. Filant, K. Hayashi, E. B. Rucker 3rd, G. Song, J. M. Deng, R. R. Behringer, F. J. DeMayo, J. Lydon, J. W. Jeong, and T. E. Spencer. 2011. Postnatal deletion of *Wnt7a* inhibits uterine gland morphogenesis and compromises adult fertility in mice. *Biol. Reprod.* 85: 386–396.

291. Regala, R. P., C. Weems, L. Jamieson, A. Khor, E. S. Edell, C. M. Lohse, and A. P. Fields. 2005. Atypical protein kinase Ci is an oncogene in human non-small cell lung cancer. *Cancer Res.* 65: 8905–8911.

292. Mescher, M., P. Jeong, S. K. Knapp, M. Rübsam, M. Saynisch, M. Kranen, J. Landsberg, M. Schlaak, C. Mauch, T. Tüting, C. M. Niessen, and S. Iden. 2017. The epidermal polarity protein Par3 is a non – cell autonomous suppressor of malignant melanoma. 1–21.

293. Kaech, S. M., C. W. Whitfield, and S. K. Kim. 1998. The LIN-2/LIN-7/LIN-10 complex mediates basolateral membrane localization of the C-elegans EGF receptor LET-23 in vulval epithelial cells. *Cell* 94: 761–771.



294. Johnston, C. L., H. C. Cox, J. J. Gomm, and R. C. Coombes. 1995. Fibroblast Growth Factor Receptors ( FGFRs ) Localize in Different Cellular Compartments. *J. Biol. Chem.* 270: 30643–30650.
295. Nicolas, M., A. Wolfer, K. Raj, J. A. Kummer, P. Mill, M. van Noort, C. C. Hui, H. Clevers, G. P. Dotto, and F. Radtke. 2003. Notch1 functions as a tumor suppressor in mouse skin. *Nat Genet* 33: 416–421.
296. Whelan, J. T., A. Kellogg, B. M. Shewchuk, K. Hewan-Lowe, and F. E. Bertrand. 2009. Notch-1 signaling is lost in prostate adenocarcinoma and promotes PTEN gene expression. *J. Cell. Biochem.* 107: 992–1001.
297. Pinnix, C. C., J. T. Lee, Z.-J. Liu, R. McDaid, K. Balint, L. J. Beverly, P. a Brafford, M. Xiao, B. Himes, S. E. Zabierowski, Y. Yashiro-Ohtani, K. L. Nathanson, A. Bengston, P. M. Pollock, A. T. Weeraratna, B. J. Nickoloff, W. S. Pear, A. J. Capobianco, and M. Herlyn. 2009. Active Notch1 confers a transformed phenotype to primary human melanocytes. *Cancer Res.* 69: 5312–20.
298. Sun, L., M. Liu, G.-C. Sun, X. Yang, Q. Qian, S. Feng, L. V. Mackey, and D. H. Coy. 2016. Notch Signaling Activation in Cervical Cancer Cells Induces Cell Growth Arrest with the Involvement of the Nuclear Receptor NR4A2. *J. Cancer* 7: 1388–1395.
299. Mitsuhashi, Y., A. Horiuchi, T. Miyamoto, H. Kashima, A. Suzuki, and T. Shiozawa. 2012. Prognostic significance of Notch signalling molecules and their involvement in the invasiveness of endometrial carcinoma cells. *Histopathology* 60:

826–37.

300. Lu, K. H., A. P. Patterson, L. Wang, R. T. Marquez, E. N. Atkinson, K. A. Baggerly, L. R. Ramoth, D. G. Rosen, J. Liu, I. Hellstrom, D. Smith, L. Hartmann, D. Fishman, A. Berchuck, R. Schmandt, R. Whitaker, D. M. Gershenson, G. B. Mills, R. C. Bast, and N. Carolina. 2004. Selection of Potential Markers for Epithelial Ovarian Cancer with Gene Expression Arrays and Recursive Descent Partition Analysis Selection of Potential Markers for Epithelial Ovarian Cancer with Gene Expression Arrays and Recursive Descent Partition Anal. *Clin. Cancer Res.* 10: 3291–3300.
301. Tan, O., T. Ornek, A. Fadiel, K. S. Carrick, A. Arici, K. Doody, B. R. Carr, and F. Naftolin. 2012. Expression and activation of the membrane-cytoskeleton protein ezrin during the normal endometrial cycle. *Fertil Steril* 97: 192–9 e2.
302. Masterton, R., E. . Armstrong, and I. A. . More. 1975. The Cyclical Variation in the Percentage of Ciliated Cells in the Normal Human Endometrium. *J. Reprod. Fertil.* 42: 537–540.
303. Karst, W., and H. M. 1988. The differentiation behaviour of MDCK cells grown on matrix components and in collagen gels. 22: 211–224.
304. McMurray, R. J., a. K. T. Wann, C. L. Thompson, J. T. Connelly, and M. M. Knight. 2013. Surface topography regulates wnt signaling through control of primary cilia structure in mesenchymal stem cells. *Sci. Rep.* 3: 25–28.
305. Thiery, J. P., H. Acloque, R. Y. J. Huang, and M. A. Nieto. 2009. Epithelial-mesenchymal transitions in development and disease. *Cell* 139: 871–90.

306. Bryant, D. M., J. Roignot, A. Datta, A. W. Overeem, M. Kim, W. Yu, X. Peng, D. J. Eastburn, A. J. Ewald, Z. Werb, and K. E. Mostov. 2014. A Molecular Switch for the Orientation of Epithelial Cell Polarization. *Dev. Cell* 31: 171–187.
307. Hendrickson, M. R., J. C. Ross, and R. L. Kempson. 1983. Toward the development of morphologic criteria for well-differentiated adenocarcinoma of the endometrium. *Am. J. Surg. Pathol.* 7: 819–838.
308. Pugacheva, E. N., S. A. Jablonski, T. R. Hartman, E. P. Henske, and E. A. Golemis. 2007. HEF1-dependent Aurora A activation induces disassembly of the primary cilium. *Cell* 129: 1351–63.
309. Hassounah, N. B., R. Nagle, K. Saboda, D. J. Roe, B. L. Dalkin, and K. M. McDermott. 2013. Primary cilia are lost in preinvasive and invasive prostate cancer. *PLoS One* 8: e68521.
310. Liu, M., M. H. Lee, M. Cohen, M. Bommakanti, and L. P. Freedman. 1996. Transcriptional activation of the Cdk inhibitor p21 by vitamin D3 leads to the induced differentiation of the myelomonocytic cell line U937. *Genes Dev.* 10: 142–153.
311. Tian, J. Q., A. Quaroni, and Q. Jean. 1999. Involvement of p21 (WAF1/Cip1) and p27 (Kip1) in intestinal epithelial cell differentiation. *Am. Physiol. Soc.* 21: 1245–1258.
312. Jalali, A., A. G. Bassuk, L. Kan, N. Israsena, A. Mukhopadhyay, T. McGuire, and J. a Kessler. 2011. HeyL promotes neuronal differentiation of neural progenitor cells. *J. Neurosci. Res.* 89: 299–309.

313. Sharff, K. a., W.-X. Song, X. Luo, N. Tang, J. Luo, J. Chen, Y. Bi, B.-C. He, J. Huang, X. Li, W. Jiang, G.-H. Zhu, Y. Su, Y. He, J. Shen, Y. Wang, L. Chen, G.-W. Zuo, B. Liu, X. Pan, R. R. Reid, H. H. Luu, R. C. Haydon, and T.-C. He. 2009. Hey1 Basic Helix-Loop-Helix Protein Plays an Important Role in Mediating BMP9-induced Osteogenic Differentiation of Mesenchymal Progenitor Cells. *J. Biol. Chem.* 284: 649–659.
314. Liu, Z., S. Chen, S. Boyle, Y. Zhu, A. Zhang, D. R. Piwnica-Worms, M. X. Ilagan, and R. Kopan. 2013. The extracellular domain of Notch2 increases its cell-surface abundance and ligand responsiveness during kidney development. *Dev Cell* 25: 585–598.
315. Yochem, J., K. Weson, and I. Greenwald. 1988. The *Caenorhabditis elegans* lin-12 gene encodes a transmembrane protein with overall similarity to *Drosophila* Notch. *Nature* 335: 547–550.
316. Clement, P. B., and R. H. Young. 2002. Endometrioid Carcinoma of the Uterine Corpus : A Review of Its Pathology With Emphasis on Recent Advances and Problematic Aspects. 9: 145–184.
317. Machama, T., and J. E. Dixon. 1998. The Tumor Suppressor , PTEN/MMAC1, Dephosphorylates the Lipid Second Messenger, Phosphatidylinositol 3,4,5-Triphosphate. *J. Biol. Chem.* 273: 13375–13379.
318. Gassama-Diagne, A., W. Yu, M. ter Beest, F. Martin-Belmonte, A. Kierbel, J. Engel, and K. Mostov. 2006. Phosphatidylinositol-3,4,5-trisphosphate regulates the

formation of the basolateral plasma membrane in epithelial cells. *Nat. Cell Biol.* 8: 963–970.

319. James, M. F., N. Manchanda, C. Gonzalez-Agosti, J. H. Hartwig, and V. Ramesh. 2001. The neurofibromatosis 2 protein product merlin selectively binds F-actin but not G-actin, and stabilizes the filaments through a lateral association.

*Biochem. J.* 356: 377–386.

320. Kobayashi, S., T. Shimamura, S. Monti, U. Steidl, C. J. Hetherington, A. M. Lowell, T. Golub, M. Meyerson, D. G. Tenen, G. L. Shapiro, and B. Halmos. 2006. Transcriptional profiling identifies cyclin D1 as a critical downstream effector of mutant epidermal growth factor receptor signaling. *Cancer Res.* 66: 11389–11398.

321. Zegers, M. M. P., L. E. O'Brien, W. Yu, A. Datta, and K. E. Mostov. 2003. Epithelial polarity and tubulogenesis in vitro. *Trends Cell Biol.* 13: 169–176.

322. Ishiuchi, T., and M. Takeichi. 2011. Willin and Par3 cooperatively regulate epithelial apical constriction through aPKC-mediated ROCK phosphorylation. *Nat. Cell Biol.* 13: 860–866.

323. David, D. J. V., A. Tishkina, and T. J. C. Harris. 2010. The PAR complex regulates pulsed actomyosin contractions during amnioserosa apical constriction in *Drosophila*. *Development* 137: 1645–1655.

324. Westwood, F. R. 2008. The Female Rat Reproductive Cycle: A Practical Histological Guide to Staging. *Toxicol. Pathol.* 36: 375–384.

325. Felicio, L. S., J. F. Nelson, and C. E. Finch. 1984. Longitudinal Studies of Estrous Cyclicity in Aging C57BL/6J Mice: II. Cessation of Cyclicity and the Duration of Persistent Vaginal Cornification. *Biol. Reprod.* 31: 446–453.
326. Podsypanina, K., L. H. Ellenson, A. Nemes, J. Gu, M. Tamura, K. M. Yamada, C. Cordon-Cardo, G. Catoretti, P. E. Fisher, and R. Parsons. 1999. Mutation of Pten/Mmac1 in mice causes neoplasia in multiple organ systems. *Proc. Natl. Acad. Sci.* 96: 1563–1568.
327. Thiery, J. P. 2002. Epithelial-mesenchymal transitions in tumour progression. *Nat. Rev. Cancer* 2: 442–454.
328. Wang, Z., Y. Li, S. Banerjee, D. Kong, A. Ahmad, V. Nogueira, N. Hay, and F. H. Sarkar. 2010. Down-regulation of Notch-1 and Jagged-1 inhibits prostate cancer cell growth, migration and invasion, and induces apoptosis via inactivation of Akt, mTOR, and NF- $\kappa$ B signaling pathways. *J. Cell. Biochem.* 736: n/a-n/a.
329. Hopkins, B. D., B. Fine, N. Steinbach, M. Dendy, J. Shaw, K. Pappas, J. S. Yu, C. Hodakoski, J. Klein, S. Pegno, M. Sulis, H. Goldstein, B. Amendolara, L. Lei, M. Maurer, J. Bruce, P. Canoll, H. Hibshoosh, and R. Parsons. 2013. A secreted PTEN phosphatase that enters cells to alter signaling and survival. *Science* (80-. ). 341: 399–402.
330. Tuyan İlhan, T., M. G. Uçar, A. Gül, T. Saymaz İlhan, G. Yavaş, and Ç. Çelik. 2017. Sleep quality of endometrial cancer survivors and the effect of treatments. *J. Turkish Soc. Obstet. Gynecol.* 14: 238–242.

331. Nowotschin, S., P. Xenopoulos, N. Schrode, and A. K. Hadjantonakis. 2013. A sensitive and bright single-cell resolution live imaging reporter of Wnt/beta-catenin signaling in the mouse. *BMC Dev. Biol.* 10.
332. Ramathal, C., I. Bagchi, R. Taylor, and M. K. Bagchi. 2010. Endometrial Decidualization: Of Mice and Men. *Semin. Reprod. Med.* 28: 17–26.
333. Bernard, B. Y. O., M. P. Scheid, M. Ripoche, and D. Bennett. 1978. Immunological studies of Mouse Decidual Cells I. Membrane Markers of Decidual Cells in the Days after Implantation. *J. Exp. Med.* 580–591.
334. Brault, V., R. Moore, S. Kutsch, M. Ishibashi, D. H. Rowitch, A. P. McMahon, L. Sommer, O. Boussadia, and R. Kemler. 2001. Inactivation of the  $\beta$ -catenin gene by Wnt1-Cre-mediated deletion results in dramatic brain malformation and failure of craniofacial development. *Development* 126: 1253–1264.
335. Miyoshi, H., R. Ajima, C. T. Luo, T. P. Yamaguchi, and T. S. Stappenbeck. 2012. Wnt5a Potentiates TGF- $\beta$  Signaling to Promote Colonic Crypt Regeneration After Tissue Injury. *Science* (80- ). 338: 108–114.
336. Cha, J., A. Bartos, C. Park, X. Sun, Y. Li, S. W. Cha, R. Ajima, H. Y. H. Ho, T. P. Yamaguchi, and S. K. Dey. 2014. Appropriate Crypt Formation in the Uterus for Embryo Homing and Implantation Requires Wnt5a-ROR Signaling. *Cell Rep.* 8: 382–392.
337. Murtaugh, L. C., B. Z. Stanger, K. M. Kwan, and D. A. Melton. 2003. Notch signaling controls multiple steps of pancreatic differentiation. *Proc. Natl. Acad. Sci.*

100: 14920–14925.

338. Ferguson, L., E. M. Kaftanovskaya, C. Manresa, A. M. Barbara, R. J. Poppiti, Y. Tan, and A. I. AgoulNIK. 2016. Constitutive Notch Signaling Causes Abnormal Development of the Oviducts, Abnormal Angiogenesis, and Cyst Formation in Mouse Female Reproductive Tract<sup>1</sup>. *Biol. Reprod.* 94: 1–12.

339. Strong, L. C., and W. F. Hollander. 1949. Hereditary Loop-Tail in the House Mouse. *J. Hered.* .

340. Kibar, Z., K. J. Vogan, N. Groulx, M. J. Justice, D. A. Underhill, and P. Gros. 2001. Ltap , a mammalian homolog of Drosophila Strabismus / Van Gogh , is altered in the mouse neural tube mutant Loop-tail. *Nat. Genet.* 28: 251–255.

341. Cox, B. J., M. Vollmer, O. Tamplin, M. Lu, S. Biechele, M. Gertsenstein, C. Van Campenhout, T. Floss, R. Ku, W. Wurst, H. Lickert, and J. Rossant. 2010. Phenotypic annotation of the mouse X chromosome. *Genome Res.* 1154–1164.

342. Huelsken, J., R. Vogel, B. Erdmann, G. Cotsarelis, and W. Birchmeier. 2001. Beta-Catenin Controls Hair Follicle Morphogenesis and Stem Cell Differentiation in the Skin. *Cell* 105: 533–545.

343. Imai, F., S. Hirai, K. Akimoto, H. Koyama, T. Miyata, M. Ogawa, S. Noguchi, T. Sasaoka, T. Noda, O. S. Development, F. Imai, S. Hirai, K. Akimoto, H. Koyama, T. Miyata, M. Ogawa, S. Noguchi, T. Sasaoka, T. Noda, and S. Ohno. 2006. Inactivation of aPKC  $\square$  results in the loss of adherens junctions in neuroepithelial cells without affecting neurogenesis in mouse neocortex. 1855: 1735–1744.



344. Asano, T., F. Niimura, I. Pastan, A. B. Fogo, and I. Ichikawa. 2005. Permanent Genetic Tagging of Podocytes : Fate of Injured Podocytes in a Mouse Model of Glomerular Sclerosis. 2257–2262.
345. Tarutani, M., S. Itami, M. Okabe, M. Ikawa, T. Tezuka, K. Yoshikawa, T. Kinoshita, and J. Takeda. 1997. Tissue-specific knockout of the mouse Pig-a gene reveals important roles for GPI-anchored proteins in skin development. *Proc Natl Acad Sci U S A* 94: 7400–7405.
346. Moser, A. R., H. C. Pitot, and W. F. Dove. 1990. A Dominant Mutation That Predisposes to Multiple Intestinal Neoplasia in the Mouse. *Science (80-. )*. 247: 322–324.
347. Ma, L., Y. Tao, A. Duran, V. Llado, A. Galvez, J. F. Barger, E. A. Castilla, J. Chen, T. Yajima, A. Porollo, M. Medvedovic, L. M. Brill, D. R. Plas, S. J. Riedl, M. Leitges, M. T. Diaz-Meco, A. D. Richardson, and J. Moscat. 2013. Control of nutrient stress-induced metabolic reprogramming by PKCzeta in tumorigenesis. *Cell* 152: 599–611.
348. Boussadia, O., S. Kutsch, A. Hierholzer, V. Delmas, and R. Kemler. 2002. E-cadherin is a survival factor for the lactating mouse mammary gland. *Mech. Dev.* 115: 53–62.
349. Morris, Z. S., and A. I. Mcclatchey. 2009. Aberrant epithelial morphology and persistent epidermal growth factor receptor signaling in a mouse model of renal carcinoma. 106.

350. Groszer, M., R. Erickson, D. D. Scripture-adams, R. Lesche, A. Trumpp, J. A. Zack, H. I. Kornblum, X. Liu, and H. Wu. 2001. Negative Regulation of Neural Stem/Progenitor Cell Proliferation by the Pten Tumor Suppressor Gene in Vivo. *Science* (80- ). 294: 2186–2189.

351. Giovannini, M., E. Robanus-maandag, M. Niwa-kawakita, M. Van Der Valk, J. M. Woodruff, L. Goutebroze, P. Me, A. Berns, and G. Thomas. 1999. Schwann cell hyperplasia and tumors in transgenic mice expressing a naturally occurring mutant NF2 protein. *Genes Dev.* 13: 978–986.

352. Marjou, F. El, K. Janssen, B. H. Chang, M. Li, L. Chan, D. Louvard, P. Chambon, D. Metzger, and S. Robine. 2004. Tissue-Specific and Inducible Cre-Mediated Recombination in the Gut Epithelium. *Genetics* 193: 186–193.

## **Vita**

Erin Williams Lopez was born in Auburn, Washington in 1990, the daughter of Matthew Warren Williams and Patricia Read-Williams. Erin completed Auburn High School in 2009. She attended University of San Diego in San Diego, California . She received the degree of Bachelor of Arts with a double major in biology and mathematics from University of San Diego in August 2013. In August of 2013 she entered The University of Texas MD Anderson Cancer Center UTHealth Graduate School of Biomedical Sciences. She carried out this dissertation work in the Department of Genetics at MD Anderson Cancer Center.

Permanent address:

5930 Kuldell Drive  
Houston, TX 77074